Supplementary Information

Stable Phenanthrene-Fused 1,2,4-Triazinyl Radicals with Ultra-narrow Electrochemical Gap Enabled by Attenuated Fusion-Ring Aromaticity

Weijie Guo,[a] Sijia Yue,[a] Ran Duan,[c] Zhibo Yuan,[a] Yuqing Yao,[a] Hua Jiang,*[a] Jing Guo,*[a] Andrzej Rajca,*[b] and Ying Wang*[a]

[a] College of Chemistry, Beijing Normal University, Beijing 100875, China

[b] Department of Chemistry, University of Nebraska, Lincoln, NE 68588–0304, USA

[c] Institute of Chemistry, Chinese Academy of Sciences, Beijing 100190, China

Email: jiangh@bnu.edu.cn, jguo1294@bnu.edu.cn, arajca1@unl.edu and ywang1@bnu.edu.cn

Table of Contents

1. Primary Strategies for Reducing the Electrochemical Gap

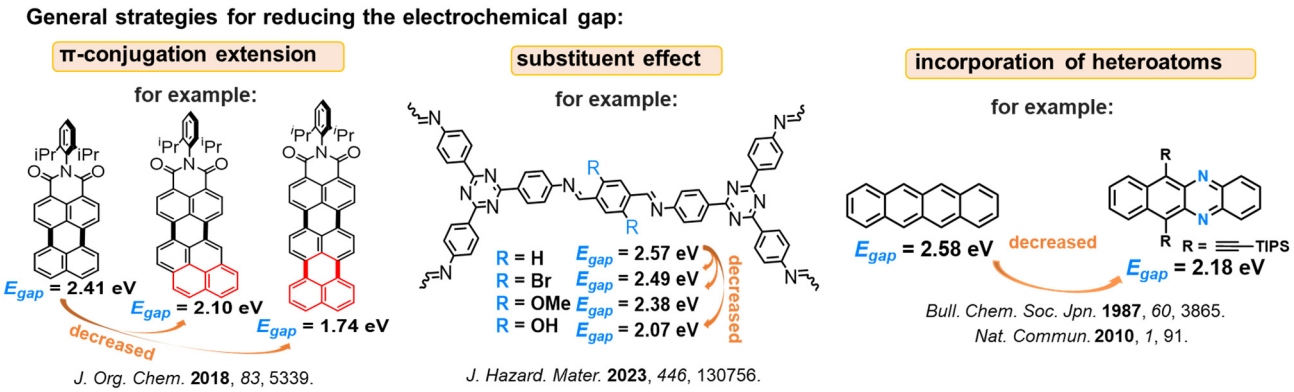

Fig. S1. General strategies for reducing the electrochemical gap, illustrated with selected closed-shell molecules.

2. Structures and Properties of Blatter and Its Representative Derivatives

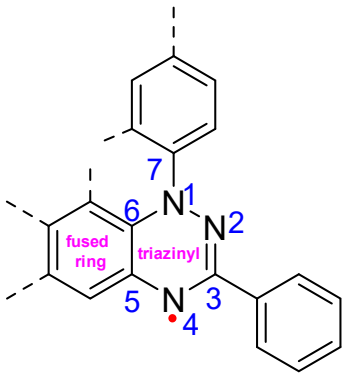

Fig. S2. General illustrations of the atomic labels and ring structures of the Blatter radical and its derivatives, showing only the common features. For the structure parameters related to the triazinyl and the triazinyl-fused six-membered rings as well as the experimental redox potentials and stabilities, see Table S1.

Table S1. Important structure parameters as well as the properties related to redox and stability of Blatter radical and its derivatives. For labels of the concerned atoms and rings, see Fig. S2.

Method of test	Items	Blatter[S1]	1	1-*t*Bu	2[S2]	3[S3]	4[S4,S8,S13]	5[S4]	6[S5,S9]	7[S6]	8[S7]
X-ray Structure	*CCDC #*	*264049*	*2488806*	/	*937185*	*913290*	*1483990*	*1483989*	*854300*	*2070220*	*1897729*
	$d_{N1–N2}$[a] (Å)	1.372(1)	1.375(5)	/	1.364(3)	1.355(3)	1.352(9)	1.368(3)	1.3635(19)	1.3639(13)	1.373(3)
	$d_{C3–N2}$[a] (Å)	1.336(2)	1.322(6)	/	1.337(4)	1.440(3)	1.325(10)	1.331(3)	1.336(2)	1.3412(14)	1.326(4)
	$d_{C3–N4}$[a] (Å)	1.333(2)	1.347(6)	/	1.337(4)	1.380(3)	1.362(9)	1.340(4)	1.338(2)	1.3371(14)	1.336(4)
	$d_{N4–C5}$[a] (Å)	1.369(2)	1.363(5)	/	1.357(4)	1.373(3)	1.381(10)	1.372(4)	1.368(2)	1.3760(15)	1.377(4)
	$d_{N1–C6}$[a] (Å)	1.392(2)	1.394(5)	/	1.390(4)	1.380(3)	1.407(9)	1.399(4)	1.391(2)	1.3977(14)	1.397(4)
	$\alpha_{C3–N2–N1}$[b] (°)	115.6(1)	115.8(4)	/	115.2(3)	115.2(2)	114.1(6)	116.3(2)	115.91(14)	116.24(9)	116.0(3)
	$\alpha_{N2–C3–N4}$[b] (°)	128.0(1)	127.1(4)	/	127.4(3)	127.3(2)	130.2(8)	128.1(3)	127.86(16)	128.76(11)	128.5(3)
	$\alpha_{C6–N1–C7}$[b] (°)	123.9(1)	124.4(3)	/	122.5(3)	122.6(2)	118.6(7)	123.2(2)	123.65(14)	119.38(10)	124.9(3)
	$\alpha_{C3–N4–C5}$[b] (°)	115.5(1)	115.2(3)	/	116.4(3)	116.7(2)	113.6(7)	115.3(2)	114.76(15)	114.64(10)	114.5(3)
	$\theta_{N1–N2–C3–N4}$[c] (°)	0.1(3)	2.5(6)	/	0.14	-1.61	1(1)	-0.8(4)	1.50	0.9	0.37
	$\theta_{C7–N1–N2–C3}$[c] (°)	–178.13	–149.88	/	–179.24	177.57	–179.70	170.14	–170.73	178.89	177.27
	$\theta_{C8–C7–N1–N2}$[c] (°)	50.6	-39.65	/	-60.22	-69.08	-2.92	-7.54	-37.66	-12.98	44.91
	$\delta_{triazinyl–(C3)Ph}$[d] (°)	9.1	12.71	/	1.61	2.80	2.9	30.2	17.14	6.58	15.10
	$\delta_{triazinyl–fused\ ring}$[d] (°)	5.44	15.98	/	1.58	7.20	1.17	3.08	13.42	8.12	5.38
	$\delta_{plan(N1, N2, C3)-plan(N4, C5, C6)}$[d] (°)	3.71	9.03	/ /	1.01	1.18	1.34	2.02	7.72	4.90	4.96
	$\delta_{(N1)Ph–fused\ ring}$	57.36	57.30	/	58.43	69.24	2.35	16.39	49.58	6.39	51.22
Voltammetry	$E_{1/2}^{0/+1}$ (V)	0.28	0.09	0.06	0.12[e]	0.20	0.31	0.33	0.42	0.41[e]	0.42[e]
	$E_{1/2}^{-1/0}$(V)	–0.92	–0.66	–0.72	–0.89[e]	–0.86	–0.87	–0.80	–0.77	–0.74[e]	–0.81[e]
	E_{gap}^{Expt} (V)	1.20	0.75	0.78	1.01[e]	1.06	1.18	1.13	1.19	1.15	1.23
	Solvent[f]	CH_2Cl_2	CH_2Cl_2	CH_2Cl_2	CH_2Cl_2	CH_2Cl_2	CH_2Cl_2	CH_2Cl_2	CH_2Cl_2	CH_2Cl_2	CH_2Cl_2
	Electrolyte[f]	*n*-Bu_4NPF_6	*n*-Bu_4NPF_6	*n*-Bu_4NPF_6	*n*-Bu_4NPF_6	*n*-Bu_4NPF_6	*n*-Bu_4NPF_6	*n*-Bu_4NPF_6	*n*-Bu_4NPF_6	*n*-Bu_4NPF_6	*n*-Bu_4NPF_6
Stability	TGA or DSC (°C)	269[S5] (DSC)	215[g] 314[h] (TGA)	217[g] 314[h] (TGA)	250[g, S8] (TGA)	/	/	/	288 (DSC)	/	/

[a] Bond distance. [b] Bond angle. [c] Twist angle. [d] The dihedral angle between the two planes. Plane of triazinyl is defined by N1, N2, N3. [e] Calculated from the literatures. [f] The solvent and supporting electrolyte used in the electrochemical measurements. [g] 1% Mass lost. [h] 5% Mass lost.

Table S2. The properties related to redox of Blatter radical and its derivatives. For labels of the concerned atoms and rings, see Fig. S2.

	Blatter				2	3	4			5	6		7	8
Ref	S9	S10	S11	S12	S2	S3	S4	S13	S14	S4	S5	S9	S6	S7
$E_{1/2}^{0/+1}$ (V)	*0.288*	0.28	0.28	0.103	0.12[a]	0.20	0.31	*0.31*	*0.31*	0.33	0.36	*0.476*	0.41[a]	0.42[a]
$E_{1/2}^{-1/0}$(V)	*-0.864*	–0.92	-0.92	-0.96	–0.89[a]	–0.86	–0.89	*-0.86*	*-0.87*	–0.80	–0.84	*-0.7*	–0.74[a]	–0.81[a]
E_{gap}^{Expt} (V)	*1.152*	1.20	1.20	1.06	1.01[a]	1.06	1.20	*1.16*	*1.18*	1.13	1.20	*1.176*	1.15	1.23
Solvent[b]	CH_2Cl_2	CH_2Cl_2	CH_2Cl_2	CH_2Cl_2	CH_2Cl_2	CH_2Cl_2	CH_2Cl_2	CH_2Cl_2	CH_2Cl_2	CH_2Cl_2	CH_2Cl_2	CH_2Cl_2	CH_2Cl_2	CH_2Cl_2
Electrolyte[b]	*Bu_4NPF_6*	Bu_4NPF_6	*Bu_4NPF_6*	*Bu_4NPF_6*	Bu_4NPF_6	Bu_4NPF_6	Bu_4NPF_6	Bu_4NPF_6	Bu_4NPF_6	Bu_4NPF_6	Bu_4NPF_6	Bu_4NPF_6	Bu_4NPF_6	Bu_4NPF_6

[a] Calculated from the literatures. [b] The solvent and supporting electrolyte used in the electrochemical measurements.

3. General Procedures and Materials

Anhydrous toluene and triethylamine were freshly distilled over sodium benzophenone and CaH_2, respectively, under argon. Anhydrous tetrahydrofuran (THF) was obtained from solvent purification system (Inert, PS-MD-5). Per-deuterated solvents for NMR spectroscopy were obtained from Cambridge Isotope Laboratories and used as received. All other commercially available chemicals were obtained from either Innochem, Bidepharmor or Energy Chemical and used without further purification, unless indicated otherwise.

Column chromatography (0–20 psig pressure) was performed by using silica gel. Analytical TLC plates were carried out on 0.25 mm MilliporeSigma silica plates (60F-254), using UV light as the visualizing agent. Deactivated analytical TLC plates as well as deactivated silica gel were obtained by treating with 3% triethylamine in hexane and then dried under vacuum before use. In some cases, recycle preparative HPLC was also tried for chemical purifications, in which the purifications were performed on a LaboACE LC-5060 Plus II (Japan Analytical Industry Co., Ltb., Japan) equipped with high-throughput separation GPC chromatographic column (JAIGEL-1HR and JAIGEL-2HR) and ultraviolet-visible detector (UV-VIS 4ch 800LA). UV–Vis–NIR spectra were recorded on a Shimadzu UV-3600 (Shimadzu,Japan) spectrophotometer. Cyclic voltammetry (CV) and differential pulse voltammetry (DPV) experiments were carried out using an electrochemical workstation from Chenhua Instruments Co. (Shanghai, China), employing a glass carbon electrode (4 mm in diameter) as the working electrode, a platinum wire as counter electrode and an Ag electrode as the reference electrode. X-band EPR spectra were recorded on a Bruker E500 spectrometer equipped with an Oxford ESR900 liquid helium cryostat and ITC-503 temperature controller. Thermal stabilities were tested using a STA 449 F5 Jupiter® (Netzsch, GER) TGA instrument under N_2 atmosphere. NMR spectra were recorded on JEOL Delta spectrometers (^{1}H, 400 and 600 MHz) using chloroform-*d* ($CDCl_3$) or dimethyl sulfoxide-d_6 ($(CD_3)_2SO$) as the solvent. The chemical shift references were as follows: (^{1}H) chloroform-*d*, 7.26 ppm (chloroform), (^{13}C) chloroform-*d*, 77.00 ppm (chloroform-*d*); (^{1}H) dimethyl sulfoxide-d_6, 2.50 ppm (dimethyl sulfoxide-d_5), (^{13}C) dimethyl sulfoxide-d_6, 39.52 ppm (dimethyl sulfoxide-d_5). Mass spectra (ESI-HRMS) were acquired on a GCT spectrometer (Bruker Daltonics Inc).

4. Synthesis of Radicals 1 and 1-*t*Bu

4.1 Synthesis of Radical 1

Scheme S1. Synthesis Route to **1**.

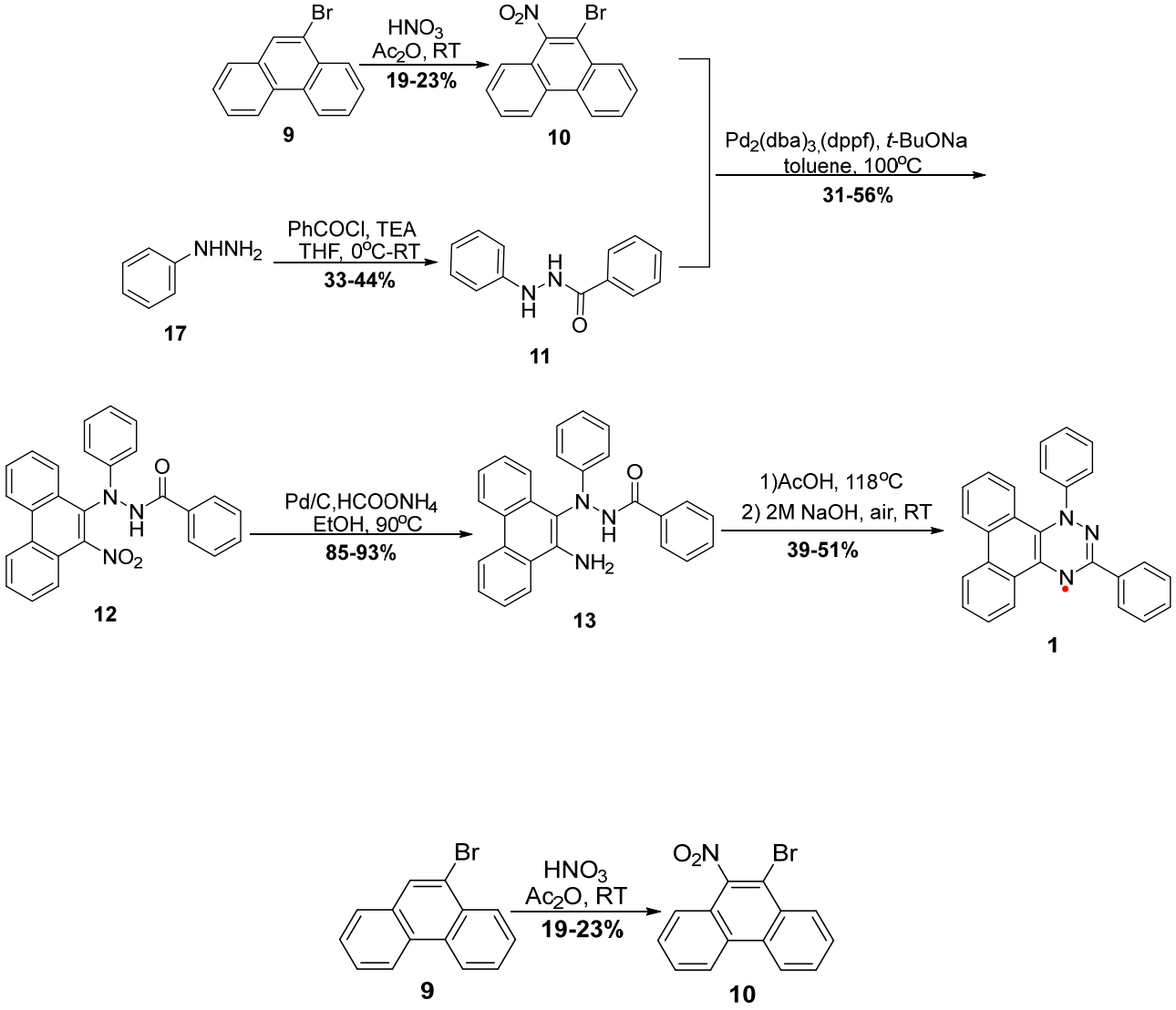

Table S3. Summary for preparation of **10**.

Run	ID	**9** (g/mmol/equiv)	68 % HNO_3 (mL/mmol/equiv)	Ac_2O mL	Product **10**	
					Amount/Yield (g/%)	TM Label
1	GWJ4–78	10.05/39.1/1.0	5.0/76.1/1.9	260.0	2.35/20	4–P120–U–2
2	GWJ4–97	25.01/97.3/1.0	9.5/144.6/1.5	650.0	6.76/23	4–P150–U–2
3	GWJ5–35	50.13/195.0/1.0	19.0/289.1/1.5	800.0	11.04/19	5–P138–U–2
4	GWJ6–13	100.05/389.1/1.0	40.0/608.6/1.6	600.0	23.30/20	6–P15–U–2

The compounds were prepared according to the procedure reported in the literature.[S15]

GWJ4–97: 9-Bromophenanthrene (25.01 g, 97.3 mmol, 1.0 equiv) was dissolved in acetic anhydride (500 mL). Concentrated nitric acid (68%, 9.5 mL, 144.6 mmol, 1.5 equiv) was diluted with acetic

anhydride (150 mL), and the resulting solution was added dropwise over 30 minutes to the solution of 9-bromophenanthrene under vigorous stirring. After complete addition, the mixture was stirred at room temperature for overnight. The mixture solvent was removed under reduced pressure. The residue was recrystallized from dichloromethane (300 mL) to afford compound **10** (3.57 g) as a yellow solid. The filtrate was then collected and the solvent was removed *in vacuo*. The resulting solid was further recrystallized from a mixture of chloroform and ethanol (128 mL, 1:1 v/v) to yield an additional amount of compound **10** (3.10 g). The total yield was 6.67 g, 23%.

10: R_f = 0.4 (PE/DCM, 4:1, v/v). ^{1}H NMR (600 MHz, 298 K, $CDCl_3$): δ = 8.71−8.73 (m, 2H), 8.46 (d, J = 9.4 Hz, 1H), 7.78−7.84 (m, 3H), 7.71 (t, J = 7.9 Hz, 1H), 7.66 (d, J = 8.2 Hz, 1H). *(Lit.[S15] ^{1}H NMR (400 MHz, $CDCl_3$) δ = 8.64−8.71 (m, 2H), 8.45−8.40 (m, 1H), 7.73−7.83 (m, 3H), 7.61−7.71 (m, 2H))*

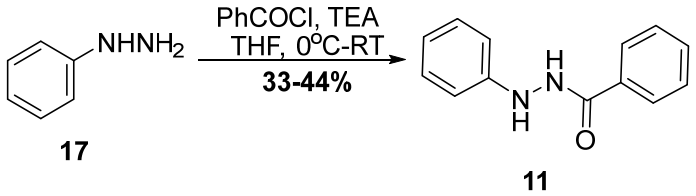

17 **11**

Table S4. Summary for preparation of **11**.

Run	ID	**17** (g/mmol/equiv)	PhCOCl (mL/mmol/equiv)	Anhydrous Et_3N (mL/mmol/equiv)	THF mL	Product	
						11	
						Amount/Yield (g/%)	TM Label
1	GWJ4–28	4.45/41.1/1.0	4.8/41.3/1.0	5.7/41.0/1.0	50.0	3.57/41	4–P37–U–4
2	GWJ4–105	5.01/46.3/1.0	5.4/46.5/1.0	7.3/52.5/1.1	50.0	3.21/33	3–P161–U-4
3	GWJ5–39	20.03/185.2/1.0	21.4/184.2/1.0	29.0/208.6/1.1	225.0	17.23/44	5–P42–U-4
4	GWJ–8–41	25.02/231.4/1.0	27.0/232.4/1.0	36.0/259.0/1.1	250.0	18.06/37	GWJ–8–57

The compounds were prepared according to the procedure reported in the literature.[S16]

GWJ4–28: Triethylamine (5.7 mL, 41.0 mmol, 1.0 equiv) was added to a solution of phenylhydrazine **17** (4.45 g, 41.1 mmol, 1.0 equiv) in anhydrous THF (50 ml) at 0 °C under Ar. The resulting mixture was stirred at 0 °C for 10 min and benzoyl chloride (4.8 mL, 41.3 mmol, 1.0 equiv) was added dropwise. The mixture was then left to stir for 18 hours while allowing the reaction mixture to slowly warm to rt. Water (20 ml) was added to quench the reaction followed by the addition of a saturated aqueous solution of sodium bicarbonate (20 ml). The phases were separated and the water phase was extracted with ethyl acetate (3 × 20 ml). The combined organic phase was washed with a saturated solution of sodium bicarbonate (2 × 20 ml), dried over sodium sulfate, filtered and the solvent was removed *in vacuo*. The resulting solid was recrystallized from ethanol (35 mL) to afford compound **11** (3.57 g, 41% yield) as a white solid.

11: R_f = 0.2 (DCM). ^{1}H NMR (400 MHz, 298 K, $(CD_3)_2SO$): δ = 10.34 (s, 1H), 7.91−7.92 (m, 3H), 7.58 (t, J = 6.8 Hz, 1H), 7.50 (t, J = 7.2 Hz, 2H), 7.15 (t, J = 7.2 Hz, 2H), 6.78 (d, J = 7.5 Hz, 2H), 6.72 (t, J = 6.8 Hz, 1H). *(Lit.[S16] ^{1}H NMR (400 MHz, $CDCl_3$) δ =7.85−7.87 (m, 3H), 7.57−7.60 (m, 1H), 7.48−7.52 (m, 2H), 7.25−7.29 (m, 3H), 6.92−6.96 (m, 3H))*

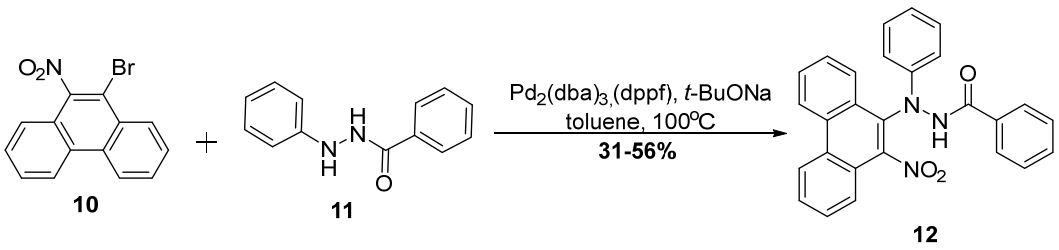

Table S5. Summary for preparation of **12**.

Run	ID	**10** (g/mmol/equiv)	**11** (g/mmol/equiv)	$Pd_2(dba)_3$ (g/mmol/equiv)	dppf (g/mmol/equiv)	*t*-BuONa (g/mmol/equiv)	Anhydrous toluene (mL)	Product **12**	
								Amount/Yield (g/%)	TM Label
1	GWJ4–92	1.02/3.4/1.0	1.41/6.6/1.9	0.85/0.9/0.3	0.71/1.3/0.4	0.48/5.0/1.5	3.0	0.46/31	4–P144–U–5
2	GWJ5–42	8.06/26.7/1.0	11.28/53.1/2.0	6.66/7.3/0.3	6.06/10.9/0.4	3.74/38.9/1.5	92.0	4.67/40	5–P45–U–5
3	GWJ5–147	4.04/13.4/1.0	5.64/26.6/2.0	3.33/3.6/0.3	3.03/5.5/0.4	1.87/19.5/1.5	46.0	2.64/45	5—P147–U-5
4	GWJ8-45	5.01/16.6/1.0	4.78/22.5/1.4	0.82/0.9/0.1	0.72/1.3/0.1	2.74/28.5/1.7	250.0	4.01/56	8—P59–U-5

GWJ5-42[S17]**:** $Pd_2(dba)_3$ (6.66 g, 0.3 mmol, 0.27 equiv), 1,1'-bis(diphenylphosphino)ferrocene (dppf) (6.06 g, 10.9 mmol, 0.4 equiv), compound **10** (8.06 g, 26.7 mmol, 1.0 equiv), compound **11** (11.28 g, 53.1 mmol, 2.0 equiv), and *t*-BuONa (3.74 g, 38.9 mmol, 1.5 equiv) were placed in a 250 mL two-necked round-bottom flask equipped a condenser tube. The flask was purged with argon, followed by the addition of freshly distilled anhydrous toluene (92 mL). The resulting mixture was degassed using the freeze–pump–thaw method for three cycles. It was then stirred at 100 °C for 12 hours. After completion of the reaction, the mixture was cooled to the room temperature and concentrated under reduced pressure. The crude residue was purified by flash column chromatography on silica gel, using petroleum ether/ethyl acetate (20:1, v/v) as the eluent, to afford compound **12** (4.67 g, 40%) as a brown solid.

12: R_f = 0.15 (PE/EA, 5:1, v/v). M.P.: 167.5−169.2 °C (under air). ^{1}H NMR (600 MHz, 298 K, $(CD_3)_2SO$): δ = 11.24 (s, 1H), 9.03 (d, J = 8.4 Hz, 1H), 8.99 (d, J = 8.4 Hz, 1H), 8.30 (d, J = 8.2 Hz, 1H), 7.81−7.89 (m, 5H), 7.71 (d, J = 8.2 Hz, 1H), 7.66 (t, J = 7.2 Hz, 1H), 7.58 (t, J = 6.9 Hz, 1H), 7.50 (t, J = 7.2 Hz, 2H), 7.23 (t, J = 7.3 Hz, 2H), 6.90 (t, J = 7.1 Hz, 1H), 6.72 (d, J = 5.8 Hz, 2H). ^{13}C NMR (150 MHz, 298 K, $(CD_3)_2SO$): δ = 116.4, 146.2, 132.2, 132.0, 131.3, 130.3, 129.6, 129.2, 129.1, 129.0, 128.9, 128.4, 127.9, 127.7, 127.5, 127.1, 123.7, 123.7, 122.9, 121.8, 120.7, 114.5. HRMS (ESI−TOF), $[M+H]^{1+}$: Calcd $C_{27}H_{20}N_3O_3$ 434.1505, found 434.1500 (-1.15 ppm).

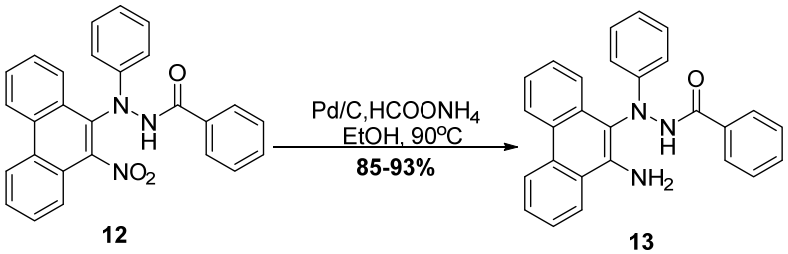

Table S6. Summary for preparation of **13**.

Run	ID	**12** (g/mmol/equiv)	10% Pd/C (g/mmol/equiv)	$HCOONH_4$ (g/mmol/equiv)	Anhydrous EtOH (mL)	Product **13**	
						Amount/Yield (g/%)	TM Label

1	GWJ4–95	0.33/0.8/1.0	0.30/0.3/0.4	2.81/44.6/55.8	25.0	0.30/93	4–P147–U-6
2	GWJ5–148	2.61/6.0/1.0	1.0/0.9/0.16	18.92/300.3/50.0	80.0	2.06/85	5–P148–U-6

GWJ4-95[S18]**:** Compound **12** (0.33 g, 0.8 mmol, 1.0 equiv), HCO_2NH_4 (2.81 g, 44.6 mmol, 55.8 equiv) and 10% Pd/C (0.30 g, 0.3 mmol, 0.4 equiv) were placed in a 50 mL two-necked round-bottom flask equipped a condenser tube. The flask was evacuated and backfilled with argon for three times, followed by the addition of degassed absolute EtOH (25 mL). The resulting mixture was stirred at 90 °C for 3 hours. When the starting material was completely consumed the reaction mixture was allowed to cool down to the room temperature and 100 mL of water was then added. The mixture was extracted three times with 50 mL of DCM, the organic phases were combined, dried over sodium sulfate, filtered and the solvent was removed under reduced pressure. The crude residue was purified by flash column chromatography on silica gel, using petroleum ether/ethyl acetate (5:1, v/v) as the eluent, to afford the compound **13** (0.30 g, 93%) as a white solid.

13: R_f = 0.5 (PE/DCM, 4:1, v/v). M.P.: 198.1−199.3 °C (under air). ^{1}H NMR (400 MHz, 298 K, $(CD_3)_2SO$): δ = 11.10 (s, 1H), 8.81 (d, J = 7.8 Hz, 1H), 8.67 (d, J = 8.0 Hz, 1H), 8.34 (d, J = 8.1 Hz, 1H), 7.96−7.98 (m, 2H), 7.71−7.75 (m, 2H), 7.67 (t, J = 7.2 Hz, 1H), 7.60 (t, J = 7.3 Hz, 1H), 7.51 (t, J = 7.2 Hz, 2H), 7.42 (t, J = 7.1 Hz, 1H), 7.34 (t, J = 7.7 Hz, 1H), 7.14 (t, J = 7.6 Hz, 2H), 6.72 (m, 3H), 6.54 (d, J = 7.9 Hz, 2H). ^{13}C NMR (100 MHz, 298 K, $(CD_3)_2SO$): δ = 146.9, 132.2, 132.1, 131.0, 130.5, 129.2, 128.5, 127.9, 127.5, 126.9, 126.3, 125.0, 123.7, 123.2, 123.0, 122.2, 118.2, 114.2, 111.6. HRMS (ESI−TOF), $[M + H]^{1+}$: Calcd $C_{27}H_{22}N_3O$ 404.1763, found 404.1762 (-0.25 ppm).

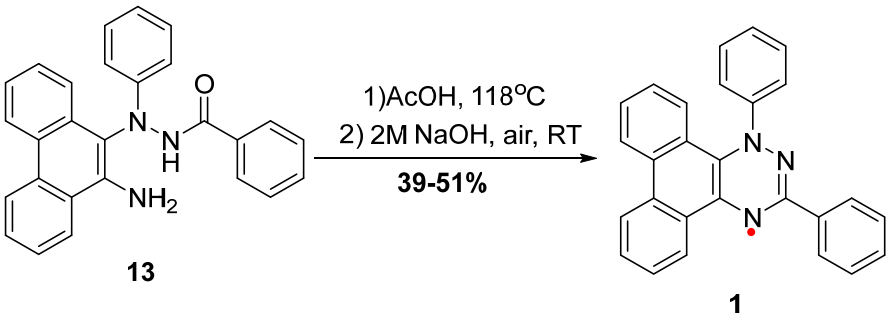

13 **1**

Table S7. Summary for preparation of **1**.

Run	ID	**13** (mg/mmol/equiv)	AcOH (mL)	Product **1**	
				Amount/Yield (mg/%)	TM Label
1	GWJ5–56	200.12/0.5/1.0	4.0	75.21/39	5–P61–U-7
2	GWJ5–P146	100.02/0.2/1.0	2.0	38.86/51	5–P146–U-7
3	GWJ8-51	1000.02/2.5/1.0	8.0	417.12/43	8-P66-U-7
4	GWJ9-44	200.01/0.5/1.0	4.0	84.58/44	9-P62-U-7

GWJ5–56[S19]**:** Compound **13** (200.12 mg, 0.5 mmol, 1.0 equiv) was dispersed in acetic acid (4.0 mL) under an argon atmosphere and heated to reflux (oil bath temperature: 118 °C) for 40 min, during which the mixture turned dark brown. After completion of the reaction, the mixture was allowed to cool down to room temperature. A solution of 2 M NaOH (150 mL) and ethanol (50 mL) was added directly. The resulting mixture was stirred under air for 4 h. The mixture was then extracted with

dichloromethane (3 ×50 mL). The combined organic layers were dried over sodium sulfate, filtered, and concentrated under reduced pressure. The residue was purified by the 3% Et_3N deactivated silica gel flash column chromatography with a mixture of petroleum ether/dichloromethane (8:1, v/v) as the eluent, to afford compound **1** (75.21 mg, 39%) as dark brown solids.

The free radical **1** used for all the characterizations was purified further by recrystallization from ethyl acetate. **1**: R_f = 0.4 (PE/DCM, 8:1, v/v, 3% deactivated silica plate). M.P.: 215.8 −216.2 °C (under Ar). HRMS (ESI−TOF), $[M]^{1+}$: Calcd: $C_{27}H_{18}N_3$ 384.1501, found 384.1491 (-2.60 ppm). EPR (X-band, 9.42 GHz, toluene, label:3-P61-U-7) spin concentration 100%.

4.2 Synthesis of Radical 1-*t*Bu

Scheme S2. Synthesis Route to **1-*t*Bu**.

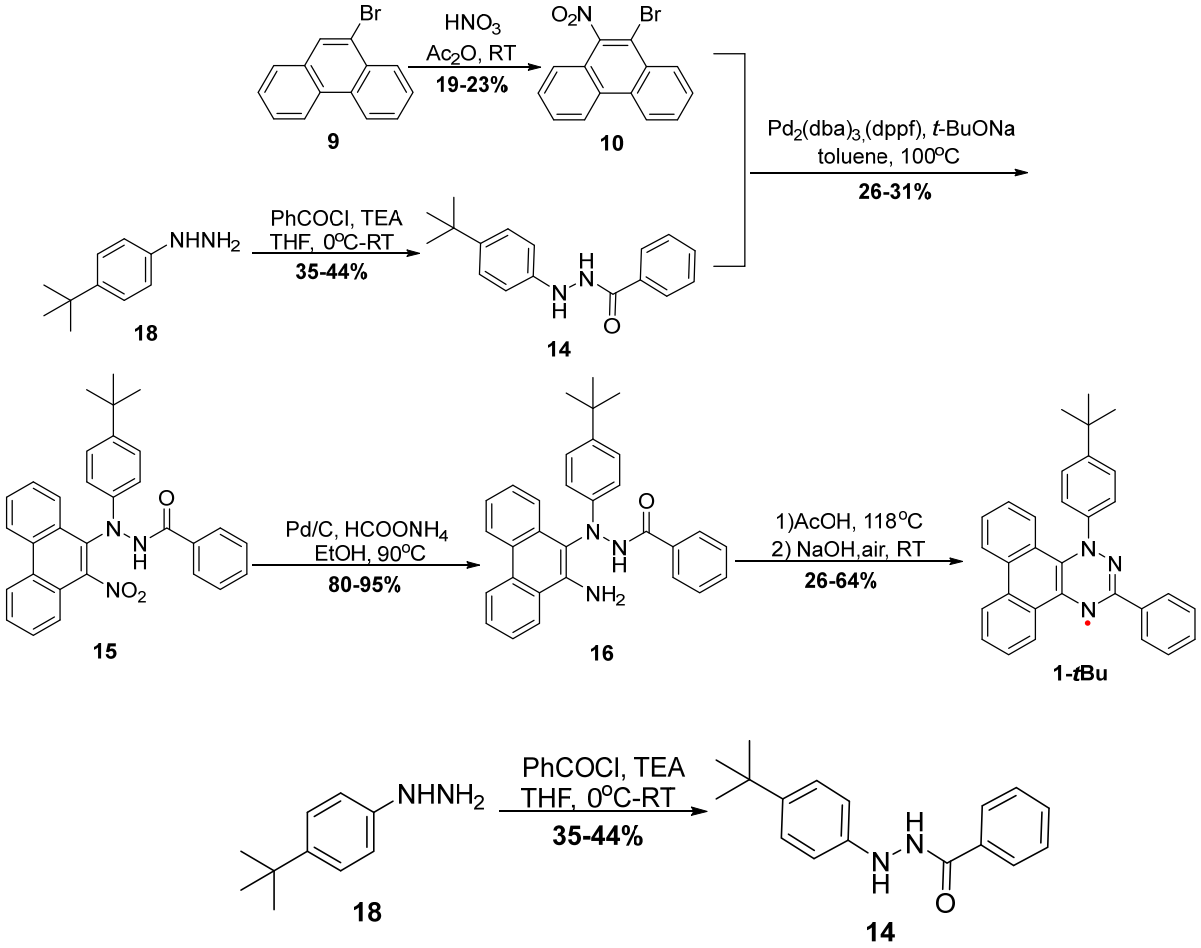

Table S8. Summary for preparation of **14**.

Run	ID	**18** (g/mmol/equiv)	PhCOCl (mL/mmol/equiv)	Anhydrous Et_3N (mL/mmol/equiv)	THF mL	Product **14**	
						Amount/Yield (g/%)	TM Label
1	GWJ5-73	0.1/0.6/1.0	0.07/0.6/1.0	0.24/1.72/2.9	5.0	0.067/42	5–P83–O–2
2	GWJ6–P90	5.02/30.6/1.0	3.6/30.6/1.0	10.4/74.6/2.4	50.0	3.59/44	4–P37–O–2
3	GWJ8–42	25.03/152.4/1.0	17.7/152.4/1.0	62.0/444.8/2.9	250.0	14.49/35	8–P56–O–2

The compounds were prepared according to the procedure reported in the literature.[S20]

GWJ6–P90: Triethylamine (10.4 mL, 74.6 mmol, 2.4 equiv) was added to a solution of compound **18** (5.02 g, 30.6 mmol, 1.0 equiv) in anhydrous THF (50 ml) at 0 °C under Ar. The resulting mixture was stirred at 0 °C for 10 min and benzoyl chloride (3.6 mL, 30.6 mmol, 1.0 equiv) was added dropwise. The mixture was stirred for 18 h while allowing the reaction mixture to slowly warm to the room temperature. Water (40 ml) was added to quench the reaction, followed by the addition of a saturated aqueous solution of sodium bicarbonate (40 ml). The phases were separated and the water phase was extracted with ethyl acetate (3 × 40 ml). The combined organic phase was washed with a saturated solution of sodium bicarbonate (2 × 40 ml), dried over sodium sulfate, filtered and the solvent was removed *in vacuo*. The crude residue was purified by flash column chromatography on silica gel, using petroleum dichloromethane/ethyl acetate (10:1, v/v) as the eluent, to afford compound **14** (3.59 g, 44% yield) as a white solid.

14: R_f = 0.4 (DCM). ^{1}H NMR (600 MHz, 298 K, $(CD_3)_2SO$): δ = 10.34 (s, 1H), 7.90 (d, J = 7.5 Hz, 2H), 7.73 (s, 1H), 7.57 (t, J = 7.4 Hz, 1H), 7.50 (t, J = 7.7 Hz, 2H), 7.17 (d, J = 8.5 Hz, 2H), 6.73 (d, J = 8.6 Hz, 2H), 1.23 (s, 9H). *(Lit.[S20] ^{1}H NMR (400 MHz, $CDCl_3$) δ = 10.36 (d, J = 3.0 Hz, 1H), 7.91 (d, J = 7.4 Hz, 2 H), 7.76 (d, J = 3.0 Hz, 1H), 7.57 (d, J = 7.2 Hz, 1H), 7.50 (t, J = 7.5 Hz, 2H), 7.17 (d, J = 8.5 Hz, 2H), 6.72 (d, J = 8.5 Hz, 2H), 1.23 (s, 9H).*

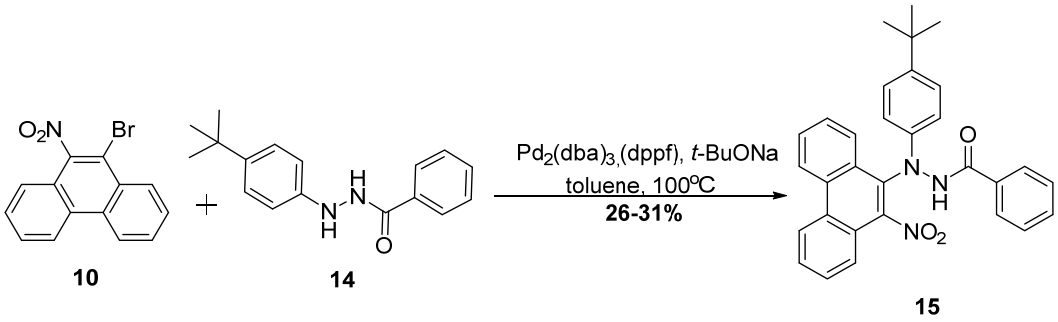

10 **14** **15**

Table S9. Summary for preparation of **15**.

Run	ID	**10** (g/mmol/equiv)	**14** (g/mmol/equiv)	$Pd_2(dba)_3$ (g/mmol/equiv)	dppf (g/mmol/equiv)	*t*-BuONa (g/mmol/equiv)	Anhydrous toluene (mL)	Product **15**	
								Amount/Yield (g/%)	TM Label
1	GWJ5-P114	0.50/1.7/1.0	0.89/3.3/1.9	0.42/0.5/0.3	0.39/0.7/0.4	0.24/2.5/1.5	5.0	0.26/31%	5–P114–O–5
2	GWJ5-P116	2.02/6.7/1.0	3.56/13.3/2.0	1.71/1.9/0.3	1.55/2.8/0.4	0.96/10.0/1.5	20.0	1.02/31	5–P116–O–5
3	GWJ6–P92	2.46/8.1/1.0	3.59/13.4/1.7	0.58/0.6/0.07	0.70/1.3/0.2	1.31/13.6/1.7	30.0	1.05/26	6–P92–O–5
4	GWJ8-P58	8.03/26.6/1.0	10.77/40.13/1.5	0.55/0.6/0.02	0.67/1.2/0.05	4.32/45.0/1.7	350.0	3.96/30	8–P58–O–5

GWJ5-P116[S17]**:** $Pd_2(dba)_3$ (1.71 g, 1.9 mmol, 0.3 equiv), 1,1'-bis(diphenylphosphino)ferrocene (dppf) (1.55 g, 2.8 mmol, 0.4 equiv), compound **10** (2.02 g, 6.7 mmol, 1.0 equiv), compound **14** (3.56 g, 13.3 mmol, 2.0 equiv), and *t*-BuONa (0.96 g, 10.0 mmol, 1.5 equiv) were placed in a 50 mL two-necked round-bottom flask equipped a condenser tube. The flask was purged with argon, followed by the addition of freshly distilled anhydrous toluene (20 mL). The resulting mixture was degassed using the freeze–pump–thaw method for three cycles. It was then stirred at 100 °C for 12 hours. After completion of the reaction, the mixture was cooled to room temperature and concentrated under reduced pressure. The crude residue was purified by flash column chromatography on silica gel, using petroleum ether/ethyl acetate (20:1, v/v) as the eluent, to afford compound **15** (1.02 g, 31%) as brown

solids.

15: R_f = 0.6 (PE/EA, 5:1, v/v). M.P.: 210.5−211.9 °C (under air). ^{1}H NMR (600 MHz, 298 K, $(CD_3)_2SO$): δ = 11.16 (s, 1H), 9.03 (d, J = 8.4 Hz, 1H), 8.99 (d, J = 8.5 Hz, 1H), 8.28 (d, J = 8.3 Hz, 1H), 7.81−7.89 (m, 5H), 7.67 (t, J = 8.5 Hz, 2H), 7.58 (t, J = 7.3 Hz, 1H), 7.49 (t, J = 7.8 Hz, 2H), 7.25 (d, J = 8.8 Hz, 2H), 6.63 (t, J = 8.2 Hz, 1H), 1.22 (s, 9H). ^{13}C NMR (150 MHz, 298 K, $(CD_3)_2SO$): δ =166.4, 143.9, 143.1, 132.3, 132.0, 131.3, 130.5, 129.6, 129.4, 129.1, 128.8, 128.5, 127.9, 127.8, 127.5, 127.3, 125.9, 123.8, 123.7, 122.9, 121.8, 114.5, 33.9, 31.3. HRMS (ESI−TOF), $[M + H]^{1+}$: Calcd $C_{31}H_{28}N_3O_3$ 490.2131, found 490.2130 (-0.20 ppm).

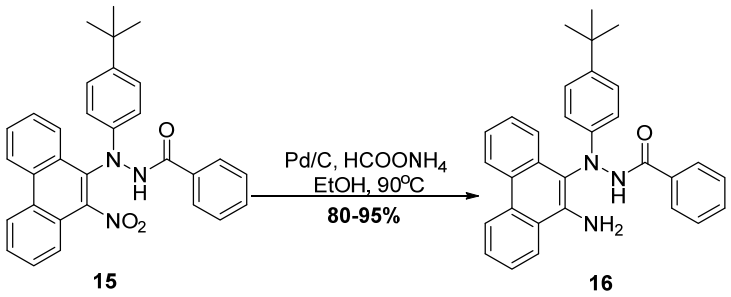

Table S10. Summary for preparation of **16**.

Run	ID	**15** (g/mmol/equiv)	10% Pd/C (g/mmol/equiv)	$HCOONH_4$ (g/mmol/equiv)	Anhydrous EtOH (mL)	Product **16**	
						Amount/Yield (g/%)	TM Label
1	GWJ5–P123	1.01/2.1/1.0	0.94/0.9/0.4	7.73/122.7/58.4	25.0	0.77/80	5–P123–O-6
2	GWJ6–93	0.92/1.9/1.0	0.66/0.6/0.3	7.76/123.2/64.8	25.0	0.76/87	6–P93–O-6
3	GWJ8-48	3.96/8.1/1.0	2.87/2.7/0.3	34.58/548.9/67.8	250.0	3.53/95	8–P63–O-6

GWJ6-93[S18]**:** Compound **15** (0.92 g, 1.9 mmol, 1.0 equiv), HCO_2NH_4 (7.76 g, 123.2 mmol, 64.8 equiv) and 10% Pd/C (0.66 g, 0.6 mmol, 0.3 equiv) were placed in a 50 mL two-necked round-bottom flask equipped a condenser tube. The flask was evacuated and backfilled with argon for three times, followed by the addition of degassed absolute EtOH (25 mL). The resulting mixture was stirred at 90 °C for 3 hours. When the starting material was completely consumed, the reaction mixture was allowed to cool down to the room temperature and 100 mL of water was then added. The mixture was extracted three times with 50 mL of dichloromethane. The organic phases were combined, dried over sodium sulfate, filtered and the solvent was removed under reduced pressure. The crude residue was purified by flash column chromatography on silica gel, using petroleum ether/ethyl acetate (5:1, v/v) as the eluent, to afford the compound **16** (0.76 g, 87%) as a white solid.

16: R_f = 0.2 (PE/EA, 5:1, v/v). M.P.: 148.3–150.1 °C (under air). ^{1}H NMR (600 MHz, 298 K, $(CD_3)_2SO$): δ = 11.06 (s, 1H), 8.80 (d, J = 8.3 Hz, 1H), 8.67 (d, J = 8.3 Hz, 1H), 8.34 (d, J = 8.2 Hz, 1H), 7.96 (d, J = 8.3 Hz, 1H), 7.79 (s, 1H), 7.72 (t, J = 7.1 Hz, 1H), 7.66 (t, J = 7.2 Hz, 1H), 7.60 (t, J = 7.5 Hz, 1H), 7.51 (t, J = 7.8 Hz, 2H), 7.43 (t, J = 7.02 Hz, 1H), 7.33 (t, J = 7.5 Hz, 1H), 7.16 (t, J = 10.1 Hz, 2H), 6.72 (s, 2H), 6.46 (d, J = 9.0 Hz, 2H), 1.20 (s, 9H). ^{13}C NMR (150 MHz, 298 K, $(CD_3)_2SO$): δ = 144.5, 140.2, 132.4, 132.1, 131.3, 130.5, 128.5, 127.9, 127.5, 127.0, 126.3, 125.8, 125.0, 124.9, 123.7, 123.2, 123.0, 122.2, 114.4, 111.3, 33.5, 31.4. HRMS (ESI−TOF), $[M + H]^{1+}$: Calcd $C_{31}H_{30}N_3O$ 460.2389, found 460.2389 (0.00 ppm).

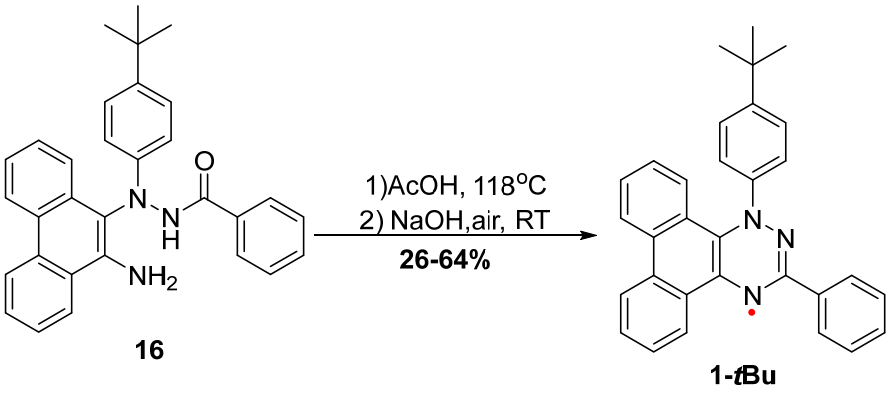

Table S11. Summary for preparation of **1-*t*Bu**.

Run	ID	**16** (mg/mmol/equiv)	AcOH (mL)	Product	
				1-*t*Bu	
				Amount/Yield (mg/%)	TM Label
1	GWJ6–91	175.11/0.4/1.0	5.0	46.07/26	6–P91–O-7
2	GWJ6–101	200.12/0.4/1.0	5.0	50.21/28	6–P101–O-7
3	GWJ8-54	1000.03/2.2/1.0	8.0	617.23/64	8-P69-O-7
4	GWJ9-44	200.37/0.44/1.0	4.0	60.32/31	9-P59-O-7

GWJ6–101[S19]**:** Compound **16** (200.12 mg, 0.4 mmol, 1.0 equiv) was dispersed in acetic acid (5.0 mL) under an argon atmosphere and heated to reflux (oil bath temperature: 118 °C) for 1 h, during which the mixture turned dark brown. After completion of the reaction, the mixture was allowed to cool down to room temperature. A solution of 2 M NaOH (100 mL) and ethanol (30 mL) was added. The resultant mixture was stirred under air for 10 minutes, then extracted with dichloromethane (3 × 50 mL). The combined organic layers were dried over sodium sulfate, filtered, and concentrated under reduced pressure. The residue was purified by the 3% Et_3N deactivated silica gel flash column chromatography with a mixture of petroleum ether/dichloromethane (8:1, v/v) as the eluent, to afford compound **1-*t*Bu** (50.21 mg, 28%) as dark brown solids.

The radical **1-*t*Bu** used for all the characterization was purified further by the recycling preparative GPC. **1-*t*Bu**: R_f = 0.7 (PE/DCM, 8:1, v/v, 3% deactivated silica plate). M.P.: 215 °C (DSC, under Ar). HRMS (ESI−TOF), $[M]^{1+}$: Calcd: $C_{31}H_{26}N_3$ 440.2127, found 440.2124 (-0.681 ppm). EPR (X-band, 9.42 GHz, toluene, label: 6-P101-O-7) spin concentration 99%.

5. X–ray Crystallography

Crystals of **1** suitable for X–ray diffraction analysis were obtained by slow diffusion of *n*-pentane into ethyl acetate solutions at –20 °C. Black, block-shaped crystals were obtained.

X–ray single crystal diffraction was performed on XtalLAB Synergy X–ray diffractometer equipped with Cu Kα radiation (λ = 1.54184 Å) source. The crystal was kept at 100.15 K during data collection. Using Olex2[S21], the structure was solved with the ShelXT [S22] structure solution program

using Direct Methods and refined with the ShelXL refinement package using Least Squares minimization. All non-hydrogen atoms were refined anisotropically. All hydrogen atoms were positioned by geometric idealization. The space group $P2_1$ was determined based on intensity statistics and the lack of systematic absences. The obtained X–ray molecular structure is shown in Fig. 3, Fig. S3 and Fig. S4; the short intermolecular contacts between C-N and N-N were listed in Table S13; additional crystal and refinement information is summarized in Table S12.

Table S12. Crystal data and structure refinement for compound **1**.

Identification code	**1**
Empirical formula	$C_{27}H_{18}N_3$
Formula weight	384.44
Temperature/K	100.15
Crystal system	monoclinic
Space group	$P2_1$
a/Å	12.5350(4)
b/Å	5.2858(2)
c/Å	14.2151(5)
α/°	90
β/°	96.963(3)
γ/°	90
Volume/Å^3	934.91(6)
Z	2
ρcalcg/cm^3	1.366
μ/mm^{-1}	0.633
F(000)	402.0
Crystal size/mm^3	0.5 × 0.3 × 0.15
Radiation	CuKα (λ = 1.54184)
2Θ range for data collection/°	7.104 to 152.768
Index ranges	$-15 \leq h \leq 15$, $-5 \leq k \leq 6$, $-12 \leq l \leq 17$
Reflections collected	6104
Independent reflections	2923 [R_{int} = 0.1154, R_{sigma} = 0.1054]
Data/restraints/parameters	2923/1/271
Goodness-of-fit on F^2	1.100
Final R indexes [I>=2σ (I)]	R_1 = 0.0546, wR_2 = 0.1386
Final R indexes [all data]	R_1 = 0.0834, wR_2 = 0.1495
Largest diff. peak/hole / e Å^{-3}	0.21/-0.27

(a)

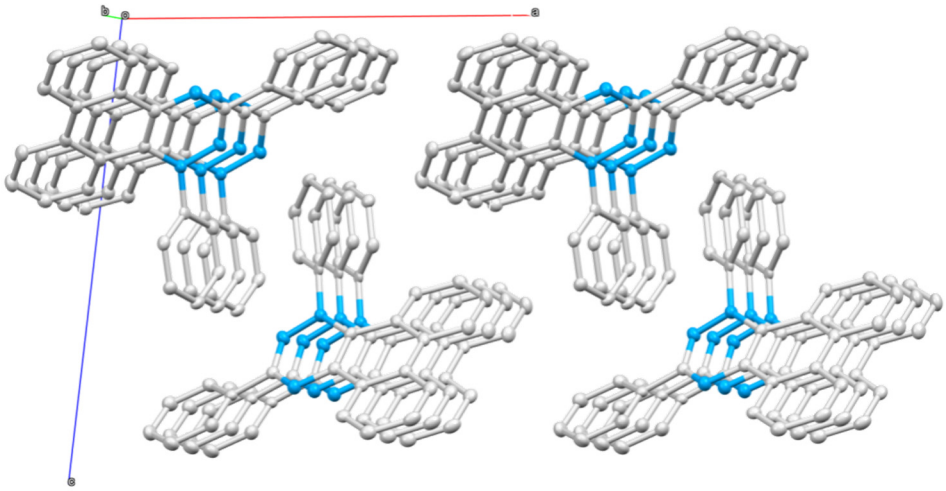

(b)

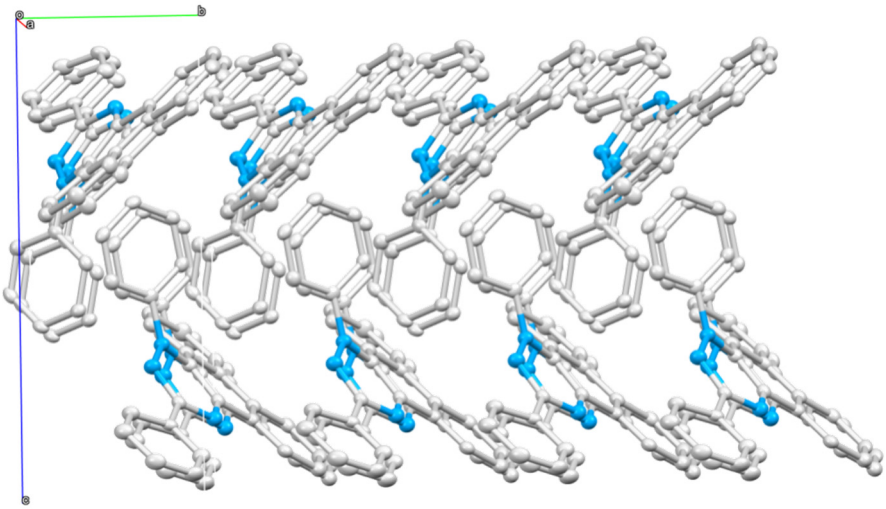

(c)

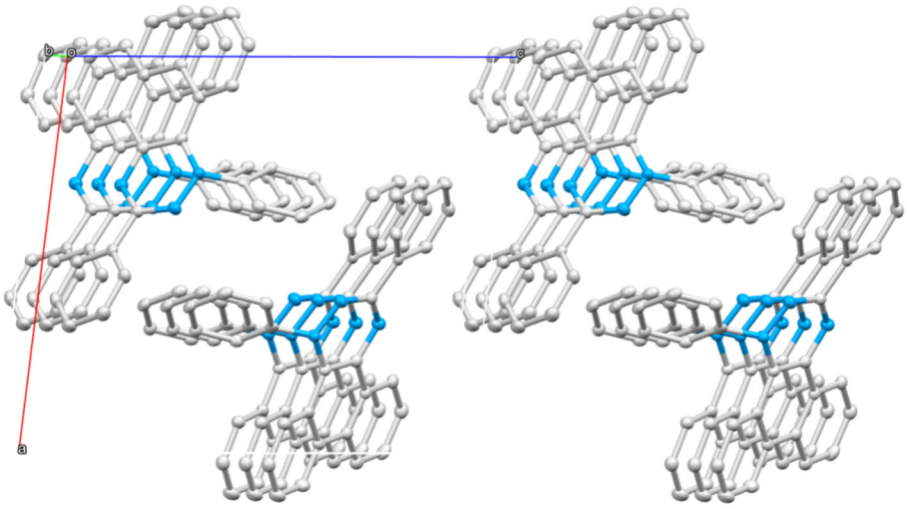

Fig. S3. X–ray crystallographic structure of **1**. (a) the crystal packing of **1** viewed along *a*-axis; (b) the crystal packing of **1** viewed along *b*-axis; (c) the crystal packing of **1** viewed along *c*-axis.

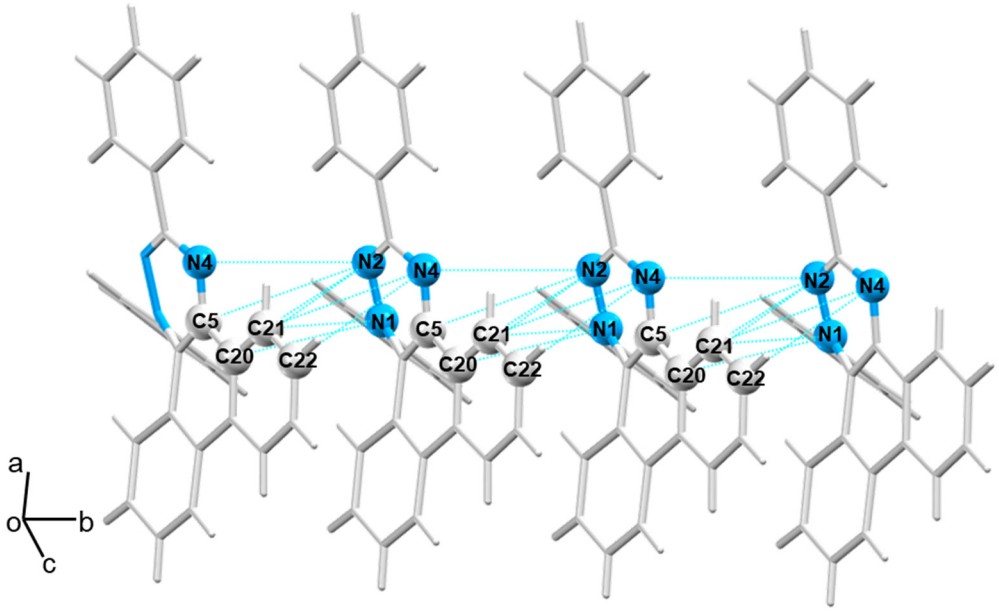

Fig. S4. Short intermolecular C···N and N···N contacts in the crystal structure of radical **1**.

Table S13. Intermolecular short contacts between C and N, and between N and N atoms, observed in the X-ray crystal structure of radical **1**.

	Short contact (Å)		Short contact (Å)		Short contact (Å)		Short contact (Å)
N4···N2	3.877	C20···N1	3.822	C21···N1	3.757	C21···N4	3.834
C5···N2	3.995	C20···N2	3.977	C21···N2	3.674	C22···N4	3.792

6. Thermogravimetric Analysis/ Differential Scanning Calorimetry (TGA/DSC)

Empty crucible was used as the reference. In the TGA measurements, **1** (3.7 mg) and **1-*t*Bu** (2.1 mg) was placed in a small sublimation chamber, respectively. Samples were measured in the temperature range of 50 ~ 550 °C with the scanning speed fixed at 10 °C min^{-1} and a nitrogen flowing of 100 mL min^{-1}. In DSC the measurements, **1** (3.2 mg) and **1-*t*Bu** (2.3 mg) was placed in a 40 μL flat-bottom aluminum crucible (6.0 mm × 1.7 mm), respectively. Samples were measured in the temperature range of 50 ~ 400 °C with the scanning speed fixed at 5 °C min^{-1} and a nitrogen flowing of 100 mL min^{-1}. The obtained TGA and DSC spectra are shown in Fig. S5 and S6.

Both compounds exhibited similar TGA profiles, with onset decomposition temperatures, corresponding to a 1% weight loss, at 215 °C and 217 °C for **1** and **1-*t*Bu**, respectively. A 5% weight

loss was observed at 314 °C for both radicals, and their maximum decomposition rates occurred at 395 °C. DSC data revealed a distinct endothermic peak at 215 °C for both compounds.

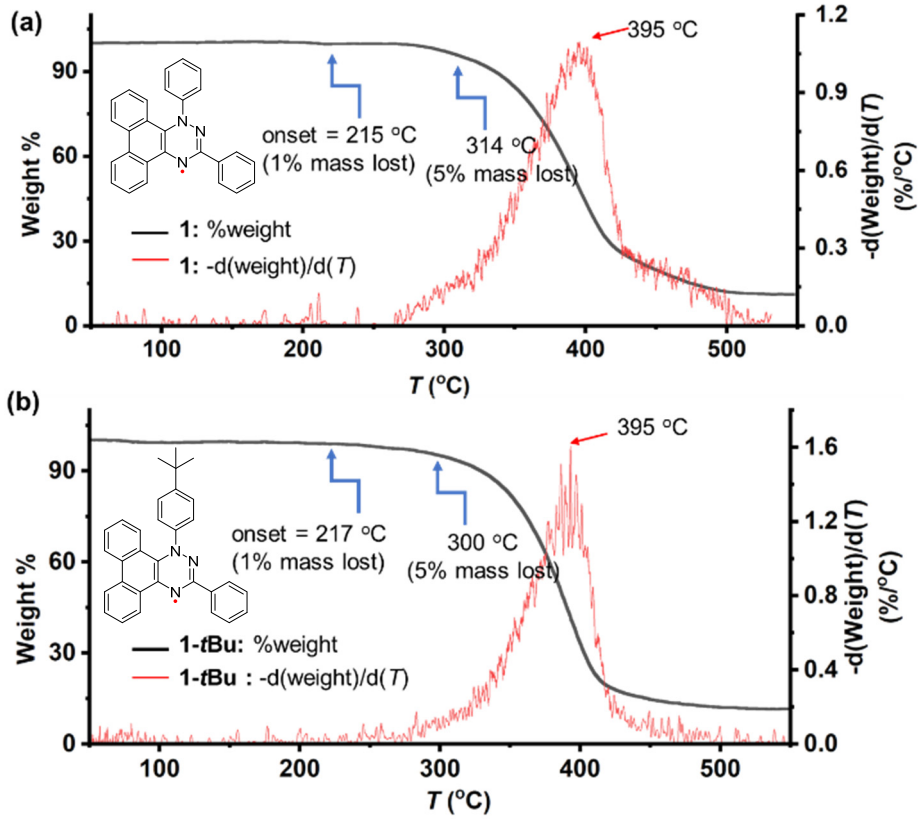

Fig. S5. Thermogravimetric analysis of radical **1** (label: 3-P61-U-7, spin concentration 100%) and **1-*t*Bu** (label: 6-P101-O-7, spin concentration 99%). The experiment was carried out under N_2 flow, with a heating rate of 10 ºC/min. Data were corrected by subtracting a baseline measured under identical conditions using an empty crucible.

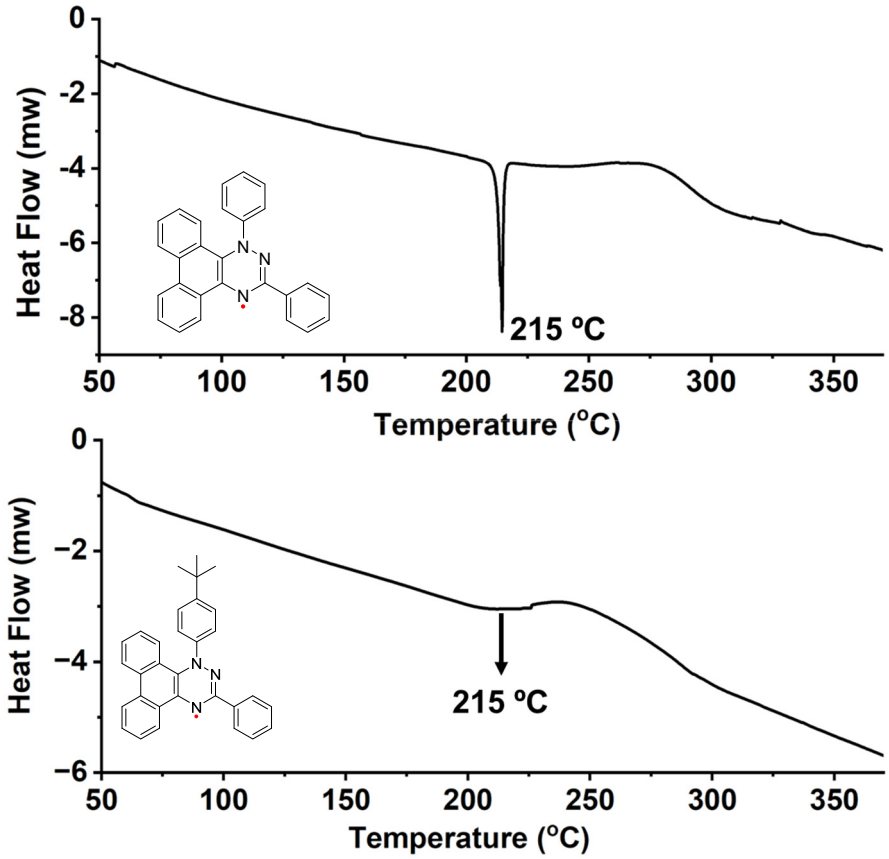

Fig. S6. Differential Scanning Calorimetry of radical **1** (label: 3-P61-U-7, spin concentration 100%); and **1-*t*Bu** (label: 6-P101-O-7, spin concentration 99%). The experiment was carried out under N_2 flow, with the heating rate of 5 °C/min. Data were corrected by subtracting a baseline measured under identical conditions using an empty crucible.

7. UV-Vis-NIR Spectroscopy

UV-vis-NIR measurements: Compound **1** (3.63 mg) and **1-*t*Bu** (4.24 mg) was dissolved in dichloromethane in a 2 mL volumetric flask to prepare a stock solution with concentration of 4.7×10^{-3} M for **1** and 4.8×10^{-3} M for **1-*t*Bu**, respectively. These stock solutions were then diluted to final concentrations of 2.8×10^{-5} M for **1** and 3.2×10^{-5} M for **1-*t*Bu**. The UV-vis-NIR spectra of both compounds in dichloromethane exhibit the longest-wavelength absorption bands at approximately 600–1000 nm, characterized by broad absorption envelopes. According to tauc plot method based on coefficient α[S23], the optical band gaps were determined to be E_g^{opt} = 1.35 eV for radical **1** and E_g^{opt} = 1.34 eV for radical **1-*t*Bu** (Fig. S8). [S24]

Beer-Lambert plots. Radical **1** (3.84 mg) in a 10 mL volumetric flask was dissolved using

dichloromethane (DCM) to give a stock solution with concentration of 1.00×10^{-3} M. A series of solutions with varying concentrations (from 1.00 mM to 0.008 mM) were prepared by diluting the stock solution using volumetric flasks. Absorbance measurements on the samples were conducted using 5-mm pathlength quartz cells. The resulting data were plotted as the derived intensity at 468 and 760 nm, respectively, versus concentration, yielding linear Beer-Lambert plots that spanned the 1.00 – 0.008 mM concentration range (Fig. S9).

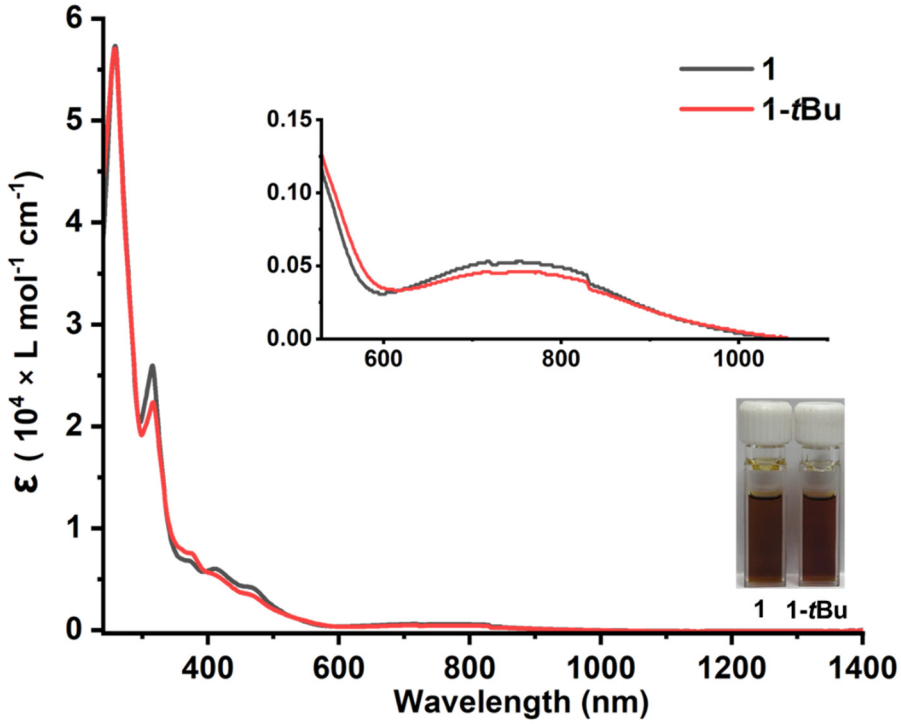

Fig. S7. UV-vis-NIR absorption spectrum of **1** (2.8×10^{-5} M, sample label: 3-P61-U-7, spin concentration 100%) and **1-*t*Bu** (3.2×10^{-5} M, label: 6-P101-O-7, spin concentration 99%) in CH_2Cl_2. Insert spectra: Zoom of the UV-vis-NIR absorption spectra at λ = 570–1200 nm. Insert pictures: The corresponding samples in the UV cells under the regular condition. **1**: Bands at λ_{max} = 259, 316 and 760 nm have the following extinction coefficients (L mol^{-1} cm^{-1}): $\varepsilon_{259} = 5.7 \times 10^4$, $\varepsilon_{316} = 2.3 \times 10^4$ and $\varepsilon_{760} = 5.7 \times 10^2$. **1-*t*Bu**: Bands at λ_{max} = 256, 315 and 753 nm have the following extinction coefficients (L mol^{-1} cm^{-1}): $\varepsilon_{256} = 5.7 \times 10^4$, $\varepsilon_{315} = 2.2 \times 10^4$ and $\varepsilon_{753} = 4.4 \times 10^2$.

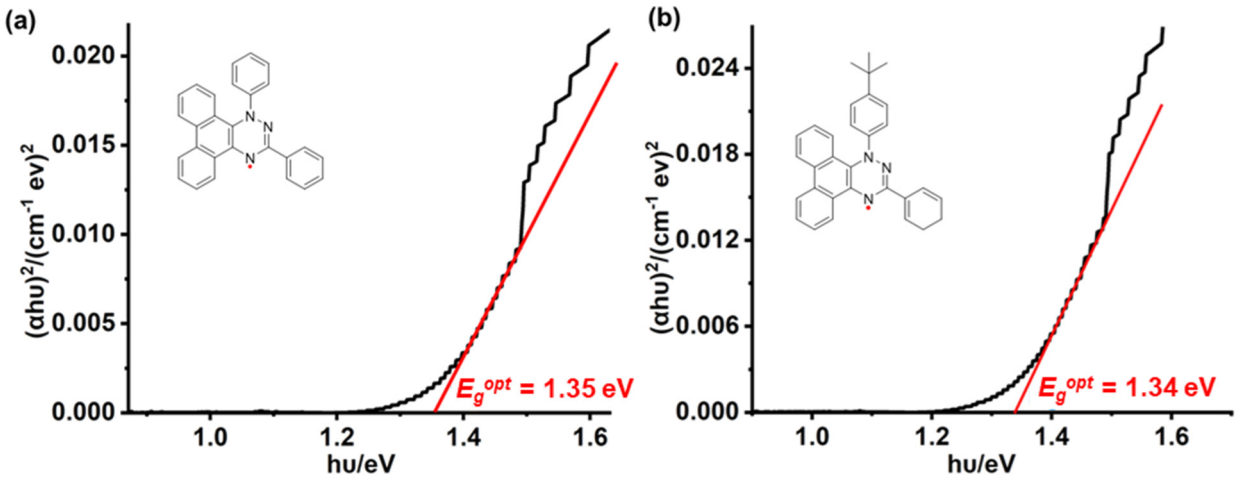

Fig. S8. The determinations of E_g^{opt} for **1** (0.075 mM, label: 3-P61-U-7, spin concentration 100%) and **1-*t*Bu** (0.1 mM, label: 6-P101-O-7, spin concentration 99%).

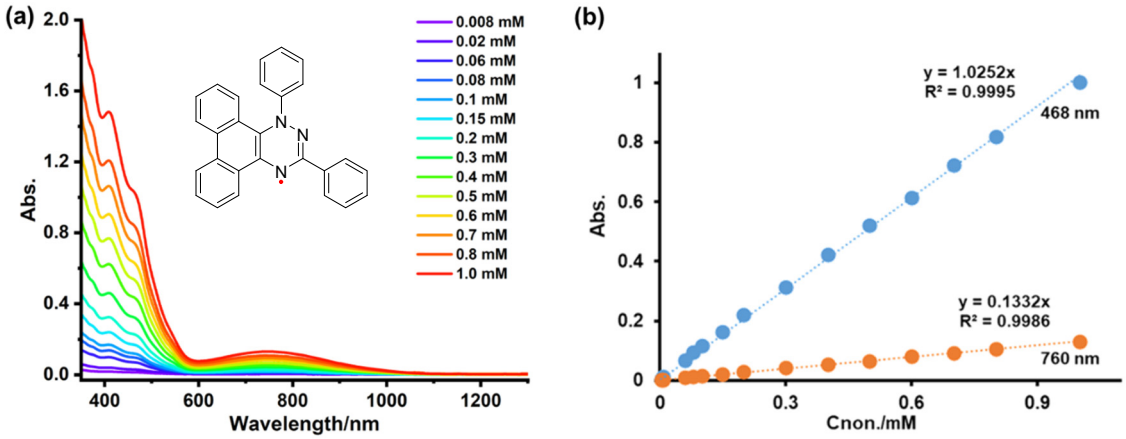

Fig. S9. (a) UV-vis-NIR absorption spectrum of **1** (label: 3-P61-U-7, spin concentration 100%) at different concentrations in CH_2Cl_2; Light path-length was 5 mm. (b) The corresponding absorption intensity at 468 and 760 nm, respectively, as a function of the concentration.

8. Electron Paramagnetic Resonance Spectroscopy

DPPH powder (g = 2.0037) was used as a *g*-value reference. Each of the solutions was drawn into an EPR-quality quartz capillary tube (0.6-mm I.D.). The capillary was stoppered with parafilm and placed in a 5-mm O.D. EPR sample tube, then positioned immediately in the EPR cavity. Series of spectra was obtained at 295 K.

Spin concentrations. Compound **1** and **1-*t*Bu** was dissolved with toluene in a 25 mL volumetric flask, respectively, to give a roughly 1 mM sample solution. Similarly, TEMPO (3.91 mg) was dissolved with toluene in 25 mL volumetric bottle to give a 1.0 mM standard radical sample. The

EPR spectra were obtained at 295 K. The spin concentrations of the radicals were determined by comparing the double-integrated EPR signal intensity of its solution with that of the TEMPO standard of known concentration.

Spectra for simulation. To perform spectral simulation, diluted solutions of the free radicals were prepared. Compound **1** (1.44 mg) was dissolved with dichloromethane (DCM) or toluene in a 25 mL volumetric flask to give a 0.15 mM sample solution; and compound **1-*t*Bu** (2.20 mg) was dissolved with toluene in a 25 mL volumetric flask to give a 0.20 mM sample solution. The corresponding EPR spectra of **1** in DCM and **1-*t*Bu** in toluene acquired at 295 K are shown in Fig. S10 and S11. The EPR spectrum of **1** in toluene exhibited insufficient resolution for reliable simulation under the fast-motion approximation.

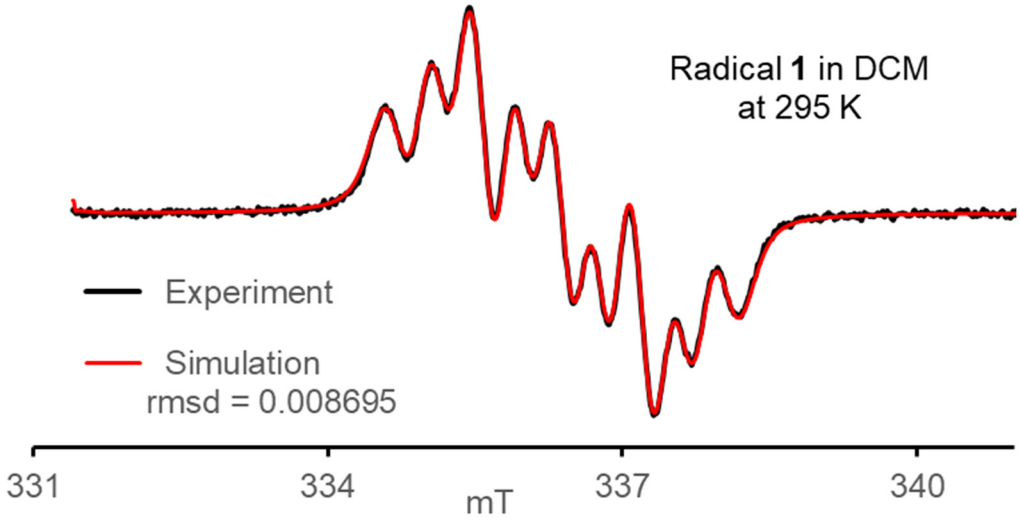

No.	Item	Value	Standard Deviation	95% Confidence Interval	
1	arg1.g	2.00293	4.61725×10^{5} (0.002%)	2.002842	–2.003022
2	arg1.A(1,1)	21.89440	0.08093118 (0.370%)	21.73578	–22.05302
3	arg1.A(1,2)	12.58950	0.4870437 (3.869%)	11.63491	–13.54409
4	arg1.A(1,3)	11.76190	0.8227526 (6.995%)	10.14933	–13.37447
5	arg1.lwpp(1,1)	0.283922	0.03232706 (11.386%)	0.2205621	–0.3472819
6	arg1.lwpp(1,2)	0.146061	0.04211096 (28.831%)	0.06352503	–0.228597

Fig. S10. EPR spectra (9.4294 GHz, modulation amplitude = 0.05 mT) of radical **1** (0.15 mM, label: 3-P61-U-7, spin concentration 100%) in DCM. Simulation: g = 2.0029, $\alpha_{N(1)}$ = 21.89 MHz (n =1), $\alpha_{N(2)}$ = 12.59 MHz (n =1), $\alpha_{N(3)}$ = 11.76 MHz (n =1); correlation coefficient near 1.0 between Lorentzian and Gaussian components of the Voigt line shape.

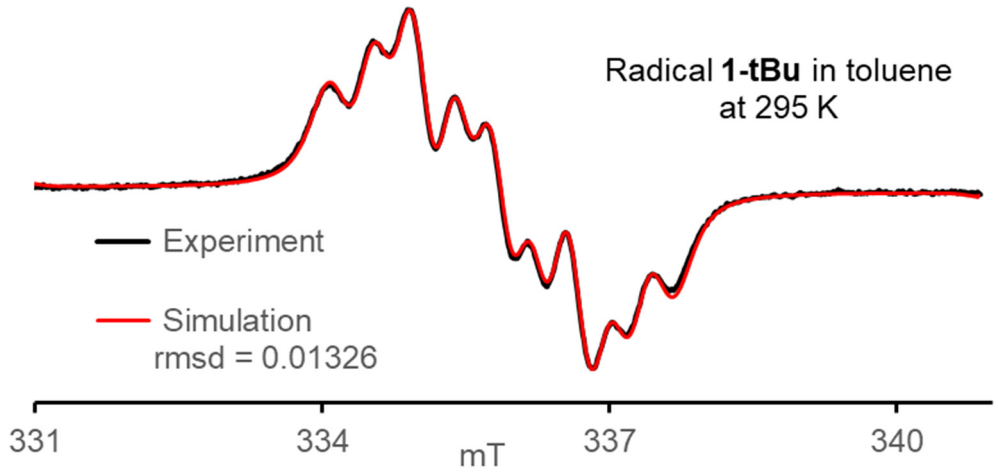

No.	Item	Value	Standard Deviation	95% Confidence Interval	
1	arg1.g	2.003191	1.83365×10^{5} (0.001 %)	2.003155	–2.003227
2	arg1.A(1,1)	21.82530	2.320289 (10.631 %)	17.27762	–26.37298
3	arg1.A(1,2)	12.96110	3.253666 (25.103 %)	6.584032	–19.33817
4	arg1.A(1,3)	11.24130	3.432502 (30.535 %)	4.513719	–17.96888
5	arg1.lwpp(1,1)	0.281702	0.01172936 (4.164 %)	0.2587129	–0.3046911
6	arg1.lwpp(1,2)	0.199497	0.01389118 (6.963 %)	0.1722708	–0.2267232

Fig. S11. EPR spectrum (9.4168 GHz, modulation amplitude = 0.05 mT) of radical **1-*t*Bu** (0.20 mM, label: 6-P101-O-7, spin concentration 99%) in toluene. Simulation: $g = 2.0032$, $\alpha_{N(1)} = 21.83$ MHz (n =1), $\alpha_{N(2)} = 12.96$ MHz (n =1), $\alpha_{N(3)} = 11.24$ MHz (n =1); correlation coefficient near 1.0 between Lorentzian and Gaussian components of the Voigt line shape.

Table S14. DFT-calculated isotropic ^{14}N hyperfine coupling constants (in MHz) for **1**, **2** and **Blatter** in different media. Insert figures: (a) Illustration of the general structure and labelling of the three nitrogen atoms in the Blatter-type radicals; (b) Plot of experimental *vs.* DFT-calculated ^{14}N hyperfine coupling constants for neutral radical **1** in DCM. The solid line represents the linear regression fit through the predicted values, with the regression equation and $R^2 = 0.97$ shown in the figure demonstrating excellent agreement with the fitted model. The strong correlation supports the assignment of the observed species to neutral radical **1**.

Species	Basis Set	Medium	Solvent Model	Hyperfine Coupling Constants (MHz)		
				N1	**N2**	**N4**
1	M062X/def2TZVP	gas phase	/	20.0785	14.2083	16.1387
	M062X/def2TZVP	DCM	SMD	21.6004	13.9795	15.9426
	UB3LYP/6-31G(d,p)	toluene	PCM	19.1213	13.1013	14.1864
2	M062X/def2TZVP	gas phase	/	18.7857	15.5993	16.9163
	M062X/def2TZVP	DCM	SMD	20.1715	14.8650	16.6362
	UB3LYP/6-31G(d,p)	toluene	PCM	17.0315	13.6422	14.5744
Blatter	M062X/def2TZVP	gas phase	/	19.6935	17.1791	17.7218
	M062X/def2TZVP	DCM	SMD	21.4430	15.8929	17.5773
	UB3LYP/6-31G(d,p)	toluene	PCM	18.4066	15.2504	15.4786

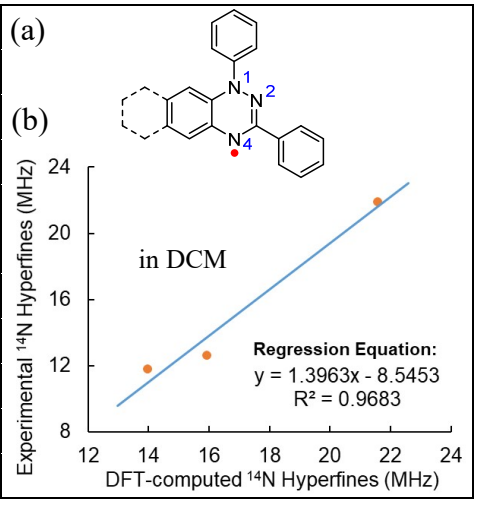

9. Electrochemistry Measurements

The cyclic and differential pulse voltammetry measurements were carried out at 25 °C in a glovebox under argon atmosphere.

In the measurements, radical **Blatter** (1.42 mg, prepared according to the procedure reported in the literature[S10], **1** (1.92 mg, label: 9-P62-U-7, spin concentration 98%) and **1-*t*Bu** (2.20 mg, label: 9-P59-O-7, spin concentration 100%) were first evacuated under high vacuum for 3 hours. Freshly prepared dichloromethane was obtained from solvent purification system, then distilled from calcium hydride under nitrogen. Supporting electrolyte tetrabutylammonium hexafluorophosphate (*n*-Bu_4NPF_6) was recrystallized 3× from methanol, then dried under high vacuum for 48 hours at 70 °C. In an argon glovebox, the radicals and *n*-Bu_4NPF_6 were dissolved in 5 mL dichloromethane to give a solution with the concentration of 1 mM for **1** and **1-*t*Bu** containing *n*-Bu_4NPF_6 (0.1 M), respectively.

Three electrodes were employed, including a glass carbon electrode (4 mm in diameter) as the working electrode, a platinum wire as counter electrode and an Ag electrode as the reference one. Cyclic and differential pulse voltammograms with the scanning rates in the 100 mV s^{-1} were obtained (Fig. 12). In the end of each measurement, ferrocene (0.93 mg, ferrocene: radical = 1:1, mol/mol) was added to the cell and the peak potentials were referenced to the Fc/Fc^+ couple (0.46 V *vs* SCE).[S25] A background measurement was performed under the identical condition using the same solvent and supporting electrolyte (0.1 M *n*-Bu_4NPF_6 in dichloromethane) in the absence of the radicals. The background current was subtracted from each voltammogram to obtain the net Faradaic responses.

A detailed investigation into the electrochemical reaction mechanisms and fundamental kinetics of compounds **1** and **1-*t*Bu** was next conducted using variable scan-rate and concentration-dependent cyclic voltammetries. For the variable scan-rate measurements, in the glovebox, compound **1** (20.03 mg, label: 9-P62-U-7, spin concentration: 98%) and **1-*t*Bu** (22.91 mg, label: 9-P59-O-7, spin concentration: 100%) was dissolved into dichloromethane in a 2 mL volumetric flask, respectively, to give a stock solution, each with a concentration of 26 mM. These stock solutions were subsequently diluted to a final concentration of 1.0 mM in 25 mL of dichloromethane in volumetric flask containing *n*-Bu_4NPF_6 (0.1 M) as the supporting electrolyte. For each measurement, 2 mL of the resulting solution was used to perform CV scans over a potential range of –1.2 to 0.9 V (vs. Fc/Fc^+) at different scan rates. The background current obtained at the corresponding scan rate was subtracted from each CV to yield the net cyclic voltammogram. The results are presented in Fig. S13–S16. Subsequently, CV experiments were carried out at different radical concentrations. Specifically, the 26 mM stock solutions of the radicals were serially diluted to prepare 2 mL samples with concentrations ranging from 0.20 to 1.4 mM, each containing $[n\text{-}Bu_4N]^+[PF_6]^-$ (0.1 M). Cyclic voltammetry was performed over the potential window of –1.2 to 0.9 V with a fixed scanning rate of 100 mV s^{-1}. The Background

CV was acquired under the same conditions (0.1 M *n*-Bu$_4$NPF$_6$ in dichloromethane, scan rate = 100 mV s^{-1}) and subtracted from each concentration-dependent voltammogram. The corresponding results are shown in Fig. S17–S20.

Through the study of the electrochemical behavior of **1** and **1-*t*Bu**, we found that the compounds have the same reversible electrochemical behavior as the Blatter free radical (Fig. 6b and Fig. S12, Table 1). The compounds have one reversible oxidation potential peaks ($E_{1/2}^{0/+1}$ = 0.09 V for **1** and $E_{1/2}^{0/+1}$ = 0.06 V for **1-*t*Bu**) and one reversible reduction potential peak ($E_{1/2}^{-1/0}$ = –0.66 V for **1** and $E_{1/2}^{-1/0}$ = –0.72 V for **1-*t*Bu**). Compared with the original Blatter radical ($E_{1/2}^{0/+1}$ = 0.28 V, $E_{1/2}^{-1/0}$ = –0.92 V), the oxidation potential is decreased and the reduction potential is increased. The electrochemical energy gap of **1** and **1-*t*Bu** are therefore determined to be 0.75 eV and 0.78 eV, respectively.

Variable scan-rate and concentration-dependent cyclic voltammetries reveal key characteristics of a reversible, diffusion-controlled, single-electron transfer process. This is supported by a linear relationship of both the anodic and cathodic peak currents (i_p) with the square root of the scan rate ($v^{1/2}$, see Fig. S14–S15) and the radical concentration (Fig. S18–S19), coupled with the invariance of the respective peak potentials (Fig. S16 and S20).

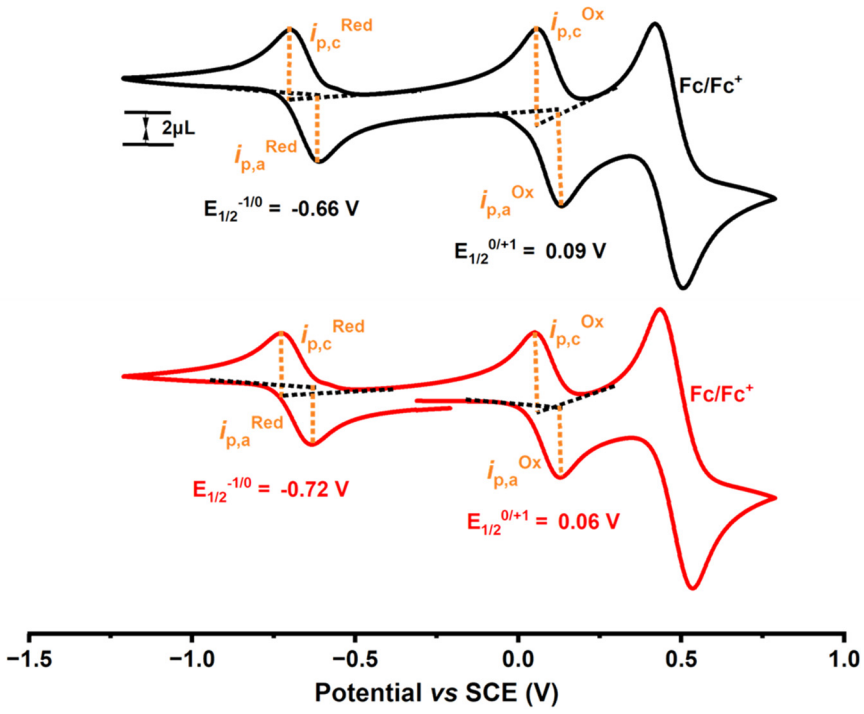

Fig. S12. Cyclic voltammetry of radicals **1** (1 mM) and **1-*t*Bu** (1 mM) in dichloromethane containing *n*-Bu$_4$NPF$_6$ (0.1 M) as an electrolyte. Reference electrode = Ag/AgCl; scan rate = 100 mV s^{-1}; temperature = 25 °C. Fc/Fc$^+$ (0.46 V) was used as an internal reference.

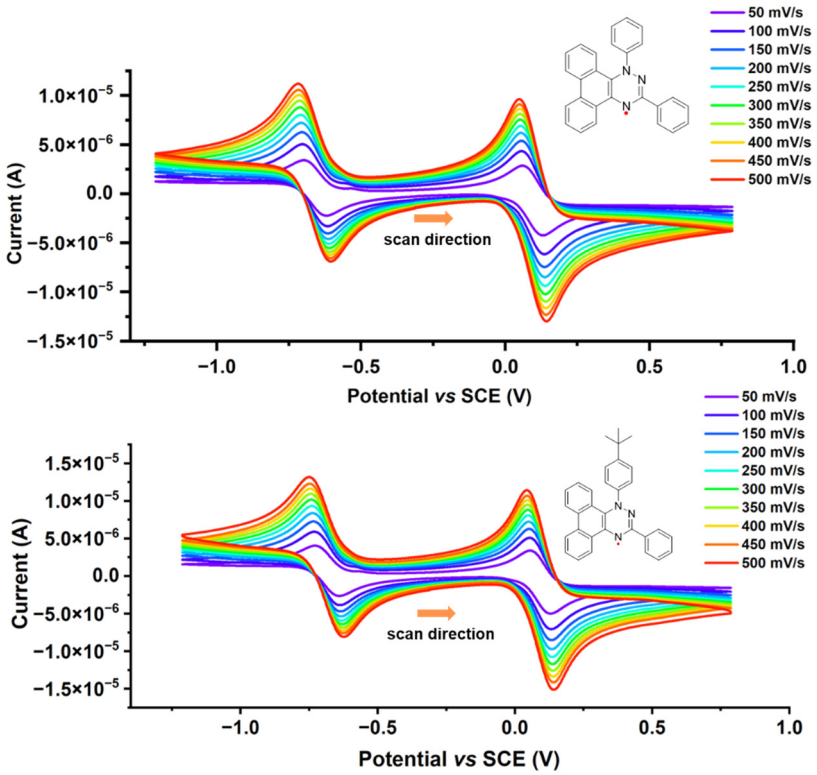

Fig. S13. Variable scan-rate cyclic voltammetry of radicals **1** (1.0 mM) and **1-*t*Bu** (1.0 mM) in DCM containing *n*-Bu_4NPF_6 (0.1 M) as an electrolyte. Reference electrode = Ag/AgCl; temperature = 25 °C. Fc/Fc^+ (0.462 V) was used as an internal reference.

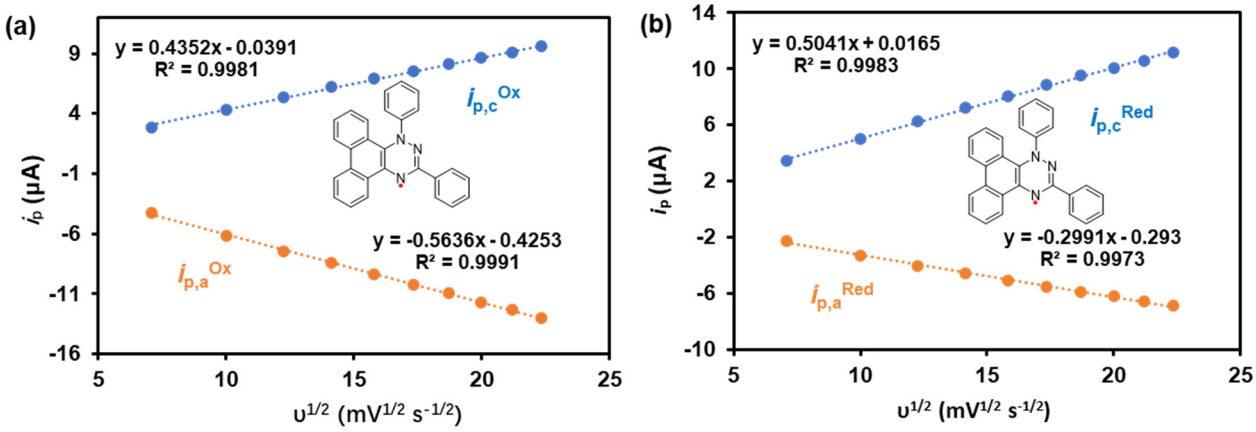

Fig. S14. Plots of peak currents (i_p) *versus* the square root ($v^{1/2}$) of scan rate for radical **1**. Data are derived from the spectra shown in Fig. S13. $i_{p,a}^{Ox}$, the anodic peak current for the first redox couple, corresponding to the oxidation of the neutral radical to its cation; $i_{p,c}^{Ox}$, the cathodic peak current for the first redox couple, corresponding to the reduction of the generated cation back to the neutral radical; $i_{p,c}^{Red}$, the cathodic peak current for the second redox couple, corresponding to the reduction of the neutral radical to its anion; $i_{p,a}^{Red}$, the anodic peak current for the second redox couple, corresponding to the oxidation of the generated anion back to the neutral radical. For illustrations of these different peak currents, see Fig. S13.

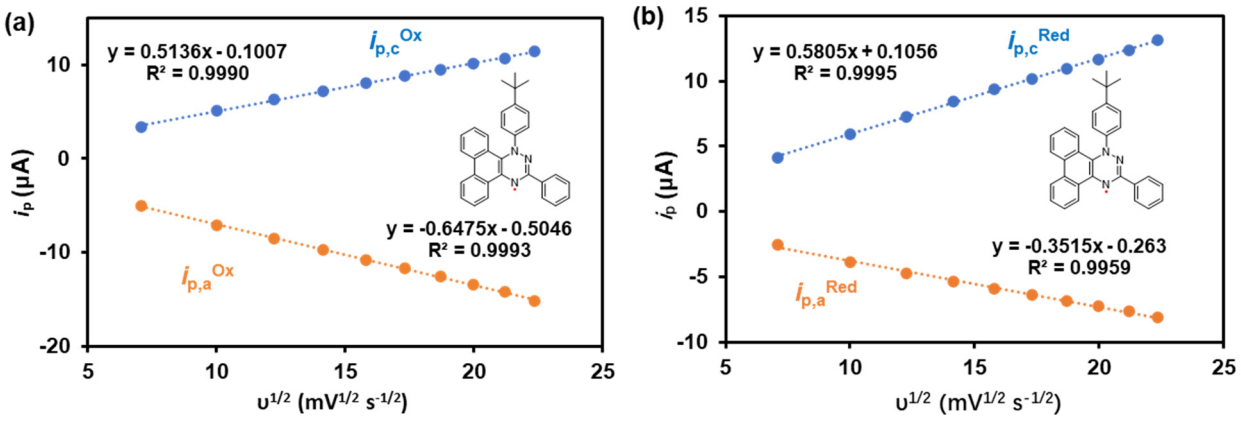

Fig. S15. Plots of peak currents (i_p) *versus* the square root ($\nu^{1/2}$) of scan rate for radical **1-*t*Bu**. Data are derived from the spectra shown in Fig. S13. $i_{p,a}^{Ox}$, the anodic peak current for the first redox couple, corresponding to the oxidation of the neutral radical to its cation; $i_{p,c}^{Ox}$, the cathodic peak current for the first redox couple, corresponding to the reduction of the generated cation back to the neutral radical; $i_{p,c}^{Red}$, the cathodic peak current for the second redox couple, corresponding to the reduction of the neutral radical to its anion; $i_{p,a}^{Red}$, the anodic peak current for the second redox couple, corresponding to the oxidation of the generated anion back to the neutral radical. For illustrations of these different peak currents, see Fig. S12.

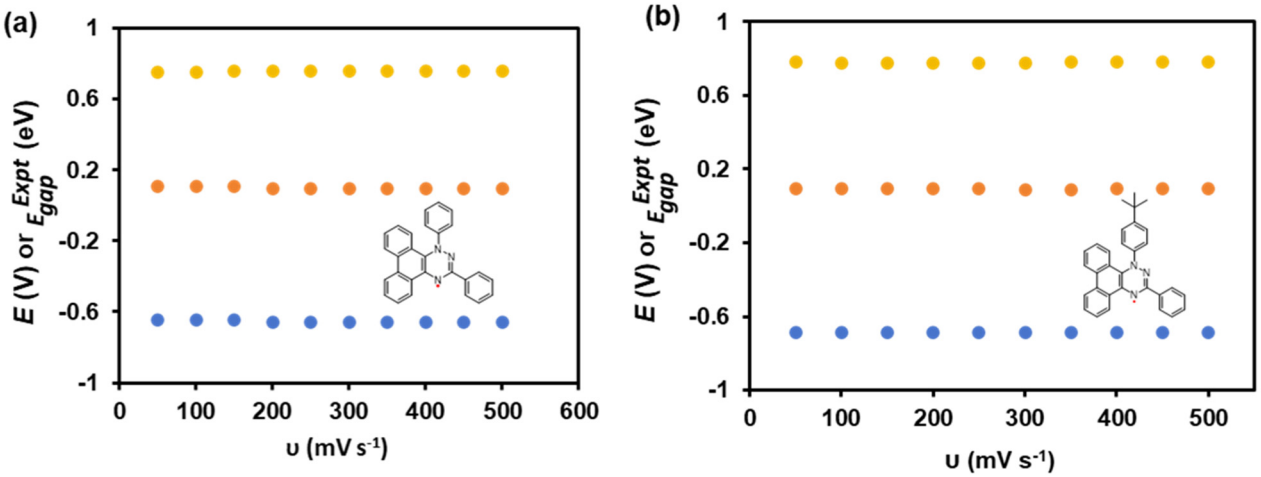

Fig. S16. The experimental oxidation ($E_{1/2}^{-1/0}$) and reduction ($E_{1/2}^{0/+1}$) potentials as well as the redox gaps (E_{gap}^{Expt}) at different scan rates for **1** and **1-*t*Bu**. Data are derived from the spectra shown in Fig. S13.

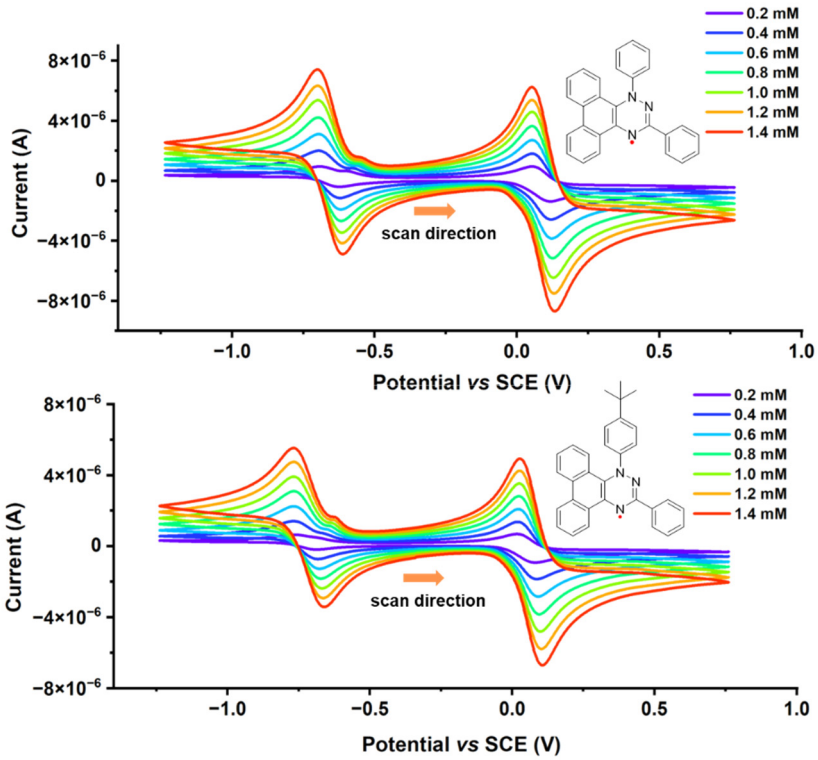

Fig. S17. Concentration-dependent cyclic voltammetry of radicals **1** and **1-*t*Bu** in DCM containing *n*-Bu$_4$NPF$_6$ (0.1 M) as an electrolyte. Reference electrode = Ag/AgCl; scan rate = 100 mV s^{-1}; temperature = 25 °C. Fc/Fc$^+$ (0.462 V) was used as an internal reference.

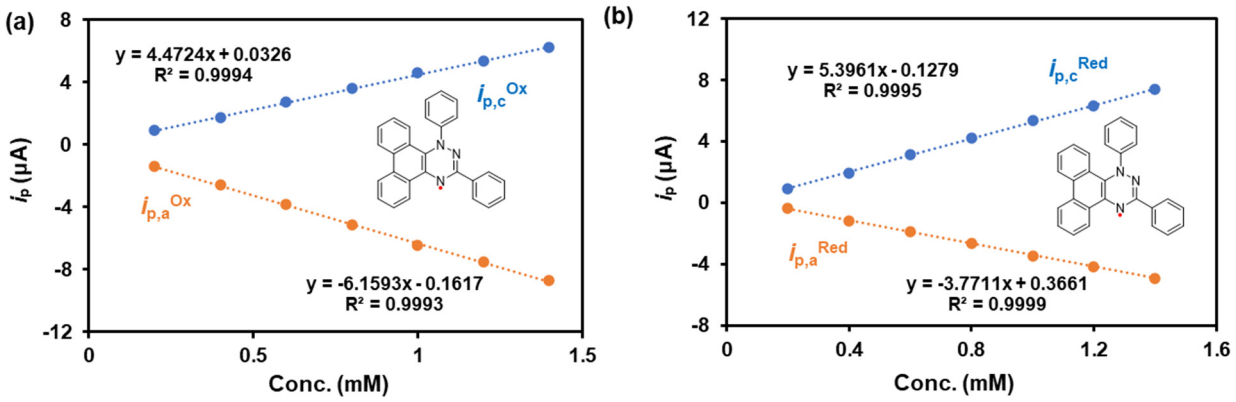

Fig. S18. Plots of peak currents (i_p) *versus* the concentration (Conc.) of **1** under a fixed scan rate of 100 mV s^{-1}. Data are derived from the spectra shown in Fig. S17. $i_{p,a}^{Ox}$, the anodic peak current for the first redox couple, corresponding to the oxidation of the neutral radical to its cation; $i_{p,c}^{Ox}$, the cathodic peak current for the first redox couple, corresponding to the reduction of the generated cation back to the neutral radical; $i_{p,c}^{Red}$, the cathodic peak current for the second redox couple, corresponding to the reduction of the neutral radical to its anion; $i_{p,a}^{Red}$, the anodic peak current for the second redox couple, corresponding to the oxidation of the generated anion back to the neutral radical. For illustrations of these different peak currents, see Fig. S12.

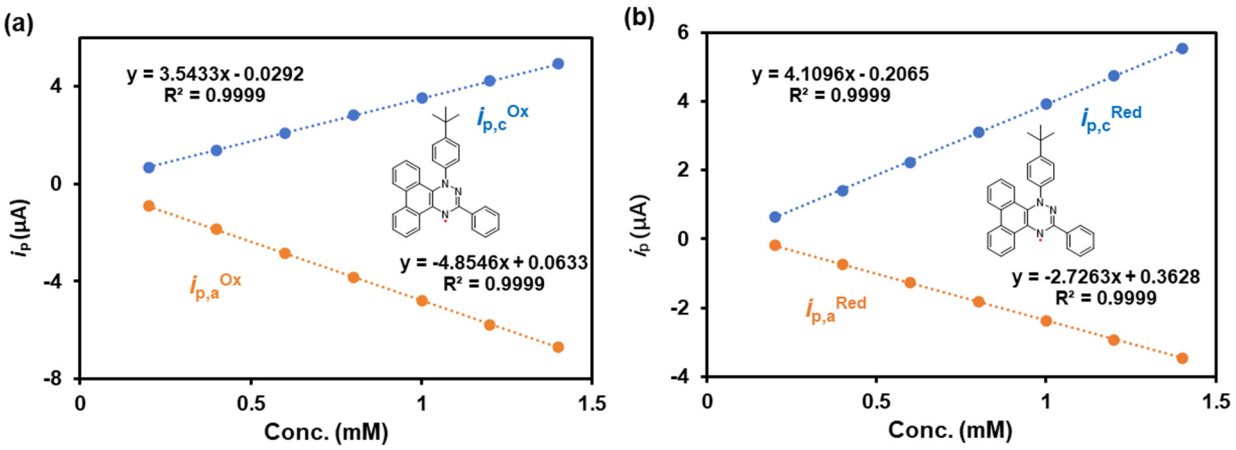

Fig. S19. Plots of peak currents (i_p) *versus* the concentration (Conc.) of **1-*t*Bu** under a fixed scan rate of 100 mV s^{-1}. Data are derived from the spectra shown in Fig. S17. $i_{p,a}^{Ox}$, the anodic peak current for the first redox couple, corresponding to the oxidation of the neutral radical to its cation; $i_{p,c}^{Ox}$, the cathodic peak current for the first redox couple, corresponding to the reduction of the generated cation back to the neutral radical; $i_{p,c}^{Red}$, the cathodic peak current for the second redox couple, corresponding to the reduction of the neutral radical to its anion; $i_{p,a}^{Red}$, the anodic peak current for the second redox couple, corresponding to the oxidation of the generated anion back to the neutral radical. For illustrations of these different peak currents, see Fig. S12.

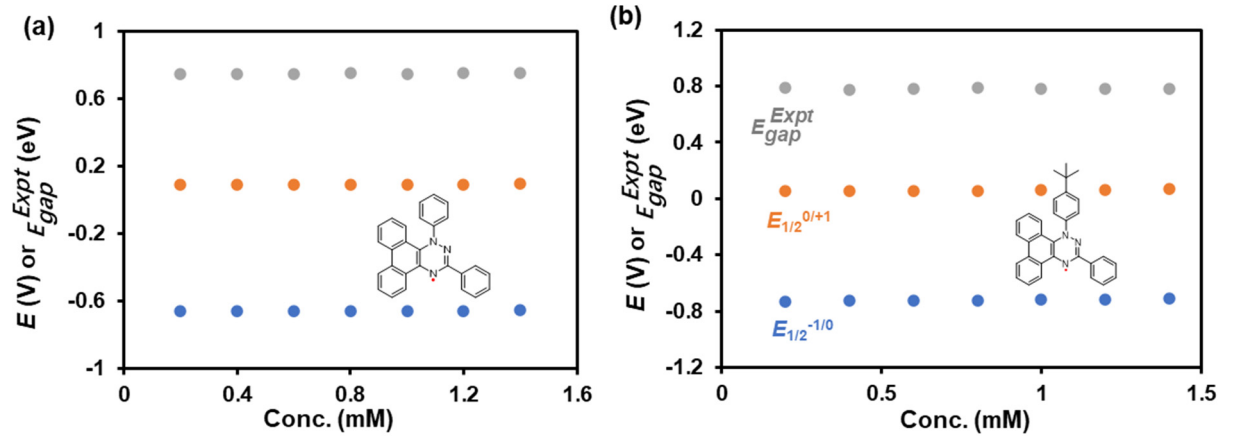

Fig. S20. The experimental oxidation ($E_{1/2}^{-1/0}$) and reduction ($E_{1/2}^{0/+1}$) potentials as well as the redox gaps (E_{gap}^{Expt}) at different concentrations of **1** and **1-*t*Bu**. Data are derived from the spectra shown in Fig. S17.

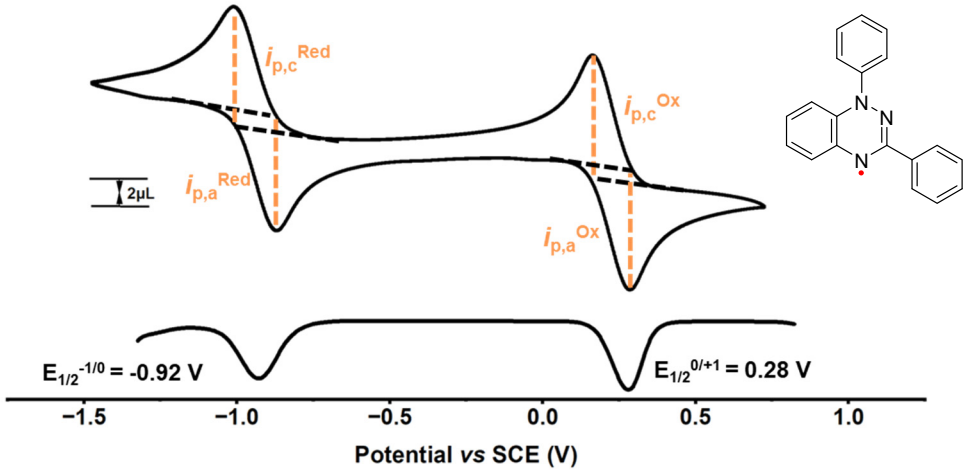

Fig. S21. Cyclic voltammetry of **Blatter** (1 mM) in dichloromethane containing *n*-Bu_4NPF_6 (0.1 M) as an electrolyte. Reference electrode = Ag/AgCl; scan rate = 100 mV s^{-1}; temperature = 25 °C. Fc/Fc^+ (0.46 V) was used as an internal reference ($i_{p,c}^{Red}$ = 8.57 μA, $i_{p,a}^{Red}$ = -8.53 μA, $i_{p,c}^{Ox}$ = 9.03 μA, $i_{p,a}^{Ox}$ = -8.91 μA).

10. Computational Details

General Methods. DFT calculations were performed using the Gaussian 09 program package[S26] in Linux operating system. At first, the geometries for the studies radicals were obtained by full system optimization at the M06-2X/def2-TZVP level of theory,[S27] using SMD[S28] solvation model for dichloromethane. Dispersion was taken into account using Grimme's empirical dispersion correction (D3 version) (empiricaldispersion=GD3).[S29] Frequencies were also calculated at the same level of theory to ensure the stationary points represented the minima on the potential energy surfaces. Orbital plots were obtained using cube files with "coarse" setting and the surfaces plotted with isodensity 0.02.

Based on the optimized geometries in dichloromethane, NICS(1)zz and 2D-NICS for all the studies radicals were calculated using the GIAO-B3LYP/6-31g(d,p) method and SMD model. For $NICS(1)_{zz}$ computations, the ghost atoms (Bq) are located at the distance of 1 Å above or below the center of entire mass of the ring systems. The excitation energies, oscillators, and rotational strengths of 30 lowest-lying singlet excited states of **1** and **1-*t*Bu** were calculated using TD-DFT(ub3lyp/6-31+g(d,p)/SMD). The Boltzmann-averaged UV-vis-NIR spectra were obtained by using the Gaussian functions with half-width of 0.42 eV through the aid of Multiwfn3.4.[S30]

Radicals **1** and **1-*t*Bu** were also fully optimized in the gas phase at the M06-2X-GD3/def2-TZVP level of theory. The spin density plots for the radicals in the gas phase were visualized by GaussView 6.0, using "medium" setting and an isodensity of 0.003 electron $Bohr^{-3}$ for surface plotting.

The redox potentials were calculated at the M06-2X-GD3/def2-TZVP level of theory using the method based on Born-Haber cycle (Scheme S3),[S31] where the standard Gibbs free energies of redox half reactions consist of the free energy change in the gas phase and the solvation free energies of the oxidized and reduced species:

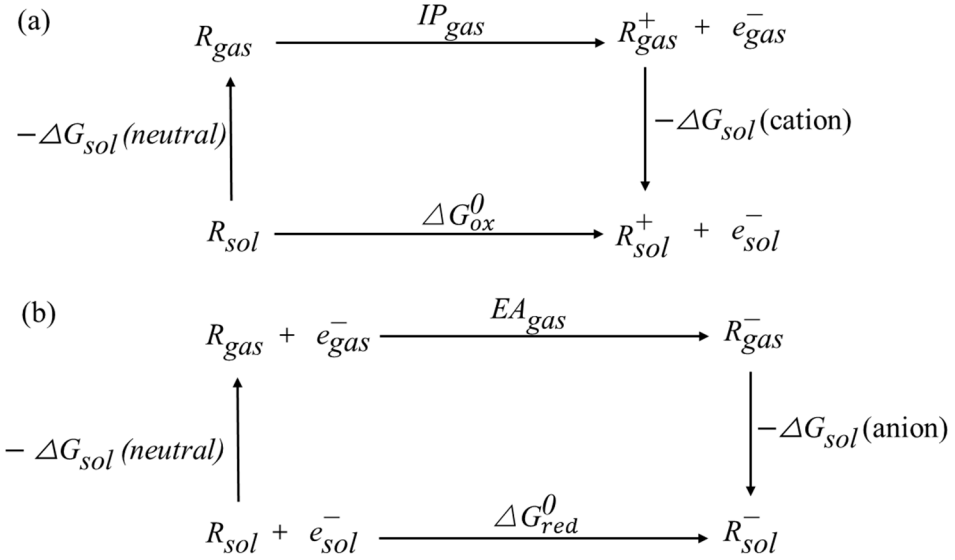

Scheme S3. The Born-Haber cycle.

In the computations, the gas-phase ionization potentials (IP_{gas}) are determined by the enthalpy changes between the cationic and neutral molecules, whereas the gas-phase electron affinities (EA_{gas}) are the differences between neutral and anionic molecules:

$$IP_{gas} = (E^0 + ZPVE + E_{therm})_{cation} - (E^0 + ZPVE + E_{therm})_{neutral} \quad \text{(S1)}$$

$$EA_{gas} = (E^0 + ZPVE + E_{therm})_{neutral} - (E^0 + ZPVE + E_{therm})_{anion} \quad \text{(S2)}$$

where E^0 is the total electronic energy, ZPVE the zero-point vibrational energy and E_{therm} the thermal correction to the energy. The free energies of the oxidation (ΔG^0_{ox}) and reduction reactions (ΔG^0_{red}) were determined based on the obtained IP_{gas} and EA_{gas}, corrected by solvation effects through Eqs. S3 and S4:

$$\Delta G_{ox}^{0} = IP_{gas} + \Delta G_{sol}(cation) - \Delta G_{sol}(neutral) \quad \text{(S3)}$$

$$\Delta G_{red}^{0} = -EA_{gas} + \Delta G_{sol}(anion) - \Delta G_{sol}(neutral) \quad \text{(S4)}$$

where ΔG_{sol}, including $\Delta G_{sol}(neutral)$, $\Delta G_{sol}(cation)$ and $\Delta G_{sol}(anion)$, denote the solvation free energy for each species. The corresponding thermodynamic redox potentials, E_{ox} and E_{red}, were calculated by Faraday's law:

$$E_{ox} = \frac{\Delta G_{ox}^{0}}{nF} \quad \text{(S5)}$$

$$E_{red} = \frac{-\Delta G_{red}^{0}}{nF} \quad \text{(S6)}$$

where n is the number of electrons transferred (n =1 in the studies cases) and F is the Faraday constant. The differential solvation stabilization energy ($\Delta\Delta G_{sol}$) was determined by,

$$\Delta\Delta G_{sol} = -\Delta G_{sol}(anion) - \Delta G_{sol}(cation) + 2\,\Delta G_{sol}(neutral) \quad \text{(S7)}$$

The results are shown in Fig. 2 and Table 1 in the main text as well as Fig. S22–S30 and Table S15–S22.

Table S15. The DFT (SMD M06-2X-GD3/def2-TZVP) calculations for the radicals Blatter and **1**–**8** in dichloromethane: charge (e), spin multiplicity, energies (E°, hartree), zero-point vibrational energies (ZPVE, hartree), ZPVE-corrected energy (E°+ZPVE, hartree), sum of electronic and thermal free energies (G, hartree, 298 K), Sum of electronic and thermal Enthalpies (H, hartree, 298 K), total entropy (electronic, translational, rotational and vibrational, S, cal·mol^{-1}·K^{-1}, 298 K), dipole moment (total, μ, Debye), and imaginary and lowest vibrational frequencies (cm^{-1}). [a]

Species	Chrg.[b]	Spin Multip-licity	Point grp.[c]	E°	ZPVE	E°+ZPVE	G (298 K)	H (298 K)	S (298 K)	<S^2>	μ	RMS Gradt.[d] (×10^{-6})	Lowest Vibrational Frequencies
Blatter	0	2	C_1	–896.658916358	0.28542	–896.373497	–896.419484	–896.356498	132.566	0.7680	4.40	2	18.1, 52.7
1	0	2	C_1	-1203.93863275	0.380381	-1203.558252	-1203.610284	-1203.535914	156.524	0.7669	3.76	3	28.2, 29.5
1-*t*Bu	0	2	C_1	-1361.17552287	0.492750	-1360.682773	-1360.742489	-1360.654851	184.450	0.7669	4.30	2	7.75, 22.9
2	0	2	C_1	-1280.17920394	0.393449	-1279.785755	-1279.837762	-1279.762873	157.617	0.7722	4.05	9	37.4, 40.6
3	0	2	C_1	-1618.17578148	0.368856	-1617.806926	-1617.86328	-1617.78291	169.154	0.7696	5.89	2	12.6, 29.4
4	0	2	C_1	-970.693729912	0.268676	-970.425054	-970.469342	-970.408429	128.201	0.7670	3.36	2	39.4, 53.0
5	0	2	C_1	-1293.65839634	0.265401	-1293.392996	-1293.439136	-1293.375624	133.673	0.7675	2.94	5	20.1, 40.0
6	0	2	C_1	-1233.75170597	0.291198	-1233.460508	-1233.511042	-1233.440006	149.508	0.7679	3.17	1	32.7, 37.9
7	0	2	C_1	-1277.96638644	0.362705	-1277.603681	-1277.654826	-1277.581633	154.047	0.7686	3.67	2	30.6, 36.5
8	0	2	C_1	-1667.2030796	0.563166	-1666.639914	-1666.707973	-1666.606583	213.393	0.7690	3.57	2	13.5, 18.5

[a] For different energy units, 1 Hartree = 627.5095 kcal mol^{-1} = 27.2114 eV. [b] Charge. [c] Symmetry point group of the geometry. [d] In Cartesian coordinates.

10.1 Simulated UV-vis spectra

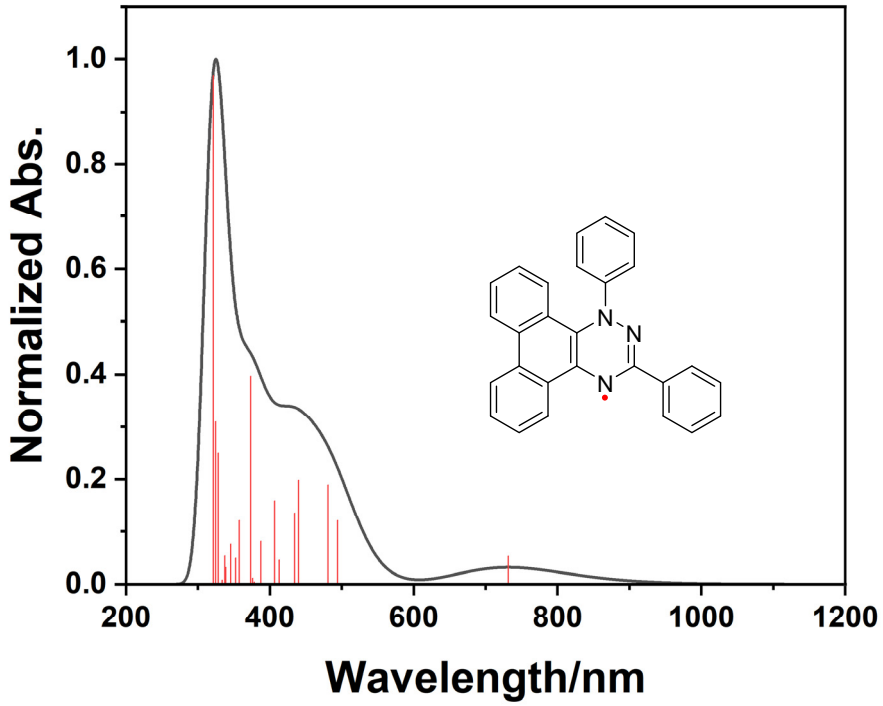

Fig. S22. TD-DFT(ub3lyp/6-31+g(d,p)/SMD)-computed UV-vis-NIR absorption spectrum of **1** in dichloromethane.

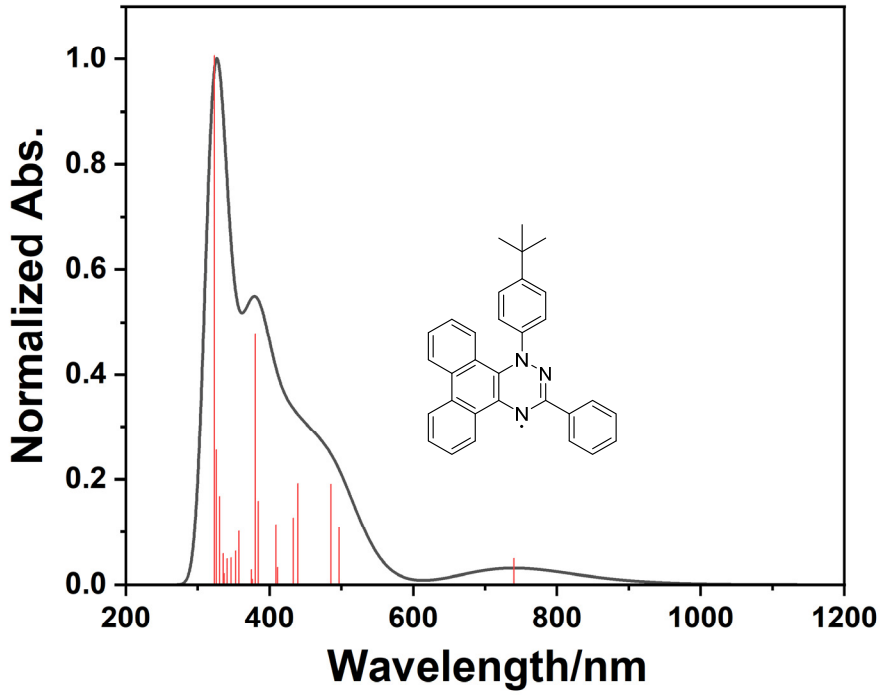

Fig. S23. TD-DFT(ub3lyp/6-31+g(d,p)/SMD)-computed UV-vis-NIR absorption spectrum of **1-*t*Bu** in dichloromethane.

Table S16. Electronic transitions of **1** calculated at the TD-DFT(ub3lyp/6-31+g(d,p) level: main contribution, $<S^2>$, energies (eV), wavelength (nm), and oscillator strength (*f*).

Excited State	Main contribution	$<S^2>$	Energy[eV]	Wavelength[nm]	Osc. strength(*f*)
1	α-HOMO→α-LUMO	0.813	1.6951	731.41	0.0133
2	β-HOMO→ β-LUMO α-HOMO→α-LUMO+1	0.868	2.5103	493.90	0.0301
3	α-HOMO→α-LUMO+1 β-HOMO→ β-LUMO	0.854	2.5787	480.80	0.0473
4	β-HOMO-1→ β-LUMO α-HOMO→ α-LUMO+2	1.317	2.8197	439.70	0.0495
5	α-HOMO→ α-LUMO+2 β-HOMO-1→ β-LUMO	1.073	2.8560	434.12	0.0339
6	β-HOMO-5→ β-LUMO β-HOMO-6→ β-LUMO β-HOMO-3→ β-LUMO	0.920	3.0013	413.10	0.0114
7	β-HOMO-2→ β-LUMO α-HOMO→ α-LUMO+2 α-HOMO→ α-LUMO+3 α-HOMO→ α-LUMO+4	1.199	3.0485	406.71	0.0397
8	α-HOMO→ α-LUMO+3 β-HOMO-2→ β-LUMO α-HOMO→ α-LUMO+4	1.063	3.2019	387.22	0.0203
9	α-HOMO→ α-LUMO+3 α-HOMO→ α-LUMO+4	1.334	3.2767	378.38	0.0010
10	α-HOMO→ α-LUMO+4 α-HOMO-1→ α-LUMO+2	2.068	3.2973	376.02	0.0029
11	α-HOMO→ α-LUMO+2 β-HOMO-2→ β-LUMO	1.594	3.3223	373.18	0.0992
12	β-HOMO-3→ β-LUMO α-HOMO→ α-LUMO+4	0.999	3.4702	357.28	0.0302
13	α-HOMO-1→ α-LUMO α-HOMO→ α-LUMO+6	1.937	3.5206	352.17	0.0124
14	α-HOMO→ α-LUMO+5 α-HOMO→ α-LUMO+6 β-HOMO-1→ β-LUMO+2 α-HOMO-1→ α-LUMO	1.839	3.5910	345.26	0.0189
15	β-HOMO-4→ β-LUMO β-HOMO-5→ β-LUMO	1.038	3.6596	338.80	0.0080
16	β-HOMO-6→ β-LUMO β-HOMO-4→ β-LUMO β-HOMO-5→ β-LUMO	0.987	3.6778	337.12	0.0135
17	α-HOMO→ α-LUMO+5 α-HOMO→ α-LUMO+6	0.914	3.7180	333.47	0.0020
18	β-HOMO→ β-LUMO+1 β-HOMO-3→β-LUMO+1 α-HOMO-4→ α-LUMO β-HOMO-4→ β-LUMO	2.235	3.7760	328.34	0.0624
19	β-HOMO-1→β-LUMO+2 β-HOMO-2→β-LUMO+1 β-HOMO→ β-LUMO+1	1.956	3.8209	324.49	0.0774
20	α-HOMO-1→ α-LUMO β-HOMO→ β-LUMO+1	1.349	3.8603	321.18	0.2423

Table S17. Electronic transitions of **1-*t*Bu** calculated at the TD-DFT(ub3lyp/6-31+g(d,p) level: main contribution, $<S^2>$, energies (eV), wavelength (nm), and oscillator strength (*f*).

Excited State	Main contribution	$<S^2>$	Energy[eV]	Wavelength[nm]	Osc. strength(*f*)
1	α-HOMO→α-LUMO	0.812	1.6755	739.97	0.0136
2	β-HOMO→ β-LUMO α-HOMO→α-LUMO+1	0.874	2.4954	496.84	0.0294
3	α-HOMO→α-LUMO+1 β-HOMO→ β-LUMO	0.854	2.5537	485.50	0.0521
4	α-HOMO→ α-LUMO+2 β-HOMO-1→ β-LUMO	1.510	2.8207	439.56	0.0523
5	β-HOMO-1→ β-LUMO α-HOMO→ α-LUMO+2	0.888	2.8633	433.01	0.0345
6	β-HOMO-6→ β-LUMO β-HOMO-5→ β-LUMO β-HOMO-4→ β-LUMO	0.926	3.0162	411.06	0.0090
7	β-HOMO-2→ β-LUMO α-HOMO→ α-LUMO+3	1.082	3.0323	408.88	0.0311
8	α-HOMO→ α-LUMO+3 β-HOMO-3→ β-LUMO	1.246	3.2284	384.04	0.0432
9	α-HOMO→ α- 376.10 LUMO+2 β-HOMO-2→ β-LUMO	1.627	3.2604	380.27	0.1306
10	β-HOMO→ β-LUMO+1 β-HOMO-1→β-LUMO+2	2.345	3.2965	376.10	0.0028
11	α-HOMO→ α-LUMO+3	0.898	3.3081	374.79	0.0078
12	β-HOMO-3→ β-LUMO α-HOMO→ α-LUMO+4	1.060	3.4699	357.32	0.0276
13	α-HOMO→ α-LUMO+6 α-HOMO-1→ α-LUMO α-HOMO→ α-LUMO+5	1.771	3.5151	352.71	0.0175
14	α-HOMO→ α-LUMO+5 β-HOMO-1→ β-LUMO+1 α-HOMO-1→ α-LUMO	1.966	3.5808	346.25	0.0139
15	β-HOMO-5→ β-LUMO β-HOMO-6→ β-LUMO	0.906	3.6373	340.87	0.0134
16	α-HOMO→α-LUMO+5 β-HOMO-5→ β-LUMO α-HOMO→ β-LUMO+6	1.118	3.6820	336.73	0.0057
17	α-HOMO→ α-LUMO+5 β-HOMO-4→β-LUMO	1.177	3.6957	335.48	0.0160
18	β-HOMO-4→β-LUMO β-HOMO→β-LUMO+1	2.000	3.7520	330.45	0.0457
19	β-HOMO-1→β-LUMO+2 β-HOMO-1→ β-LUMO+1 β-HOMO-2→ β-LUMO+1	1.960	3.8069	325.69	0.0696
20	α-HOMO-1→ α-LUMO β-HOMO→ β-LUMO+1	1.324	3.8349	323.30	0.2742

10.2 Molecular Orbitals

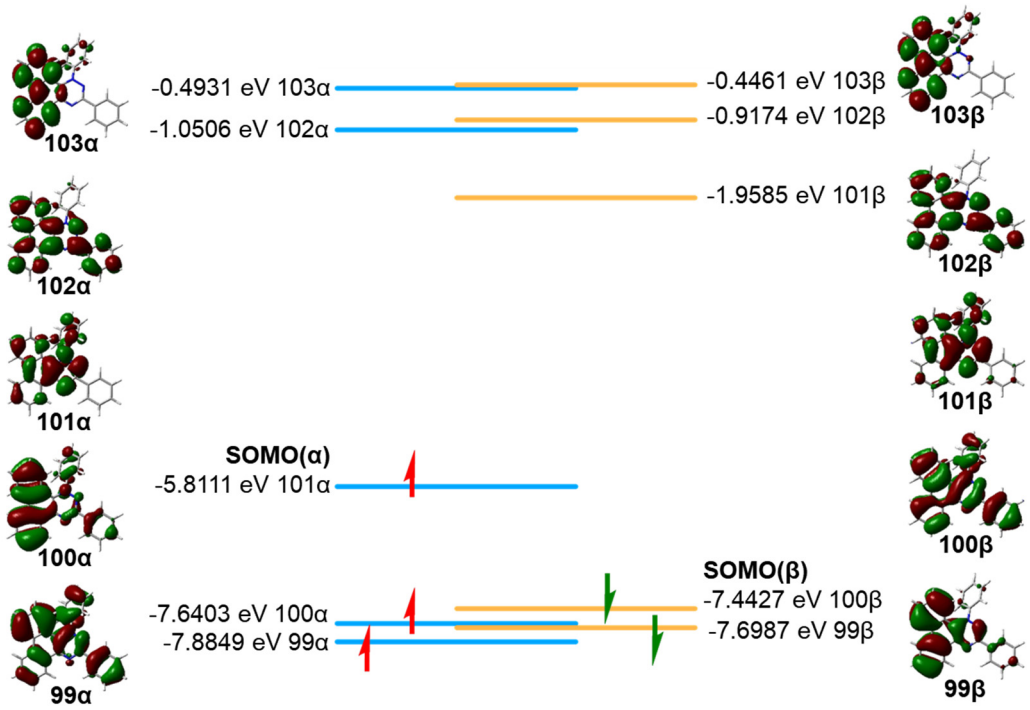

Fig. S24. Plots of the frontier molecular orbitals of **1** (Isovalue = 0.02 electron Bohr^{-3}).

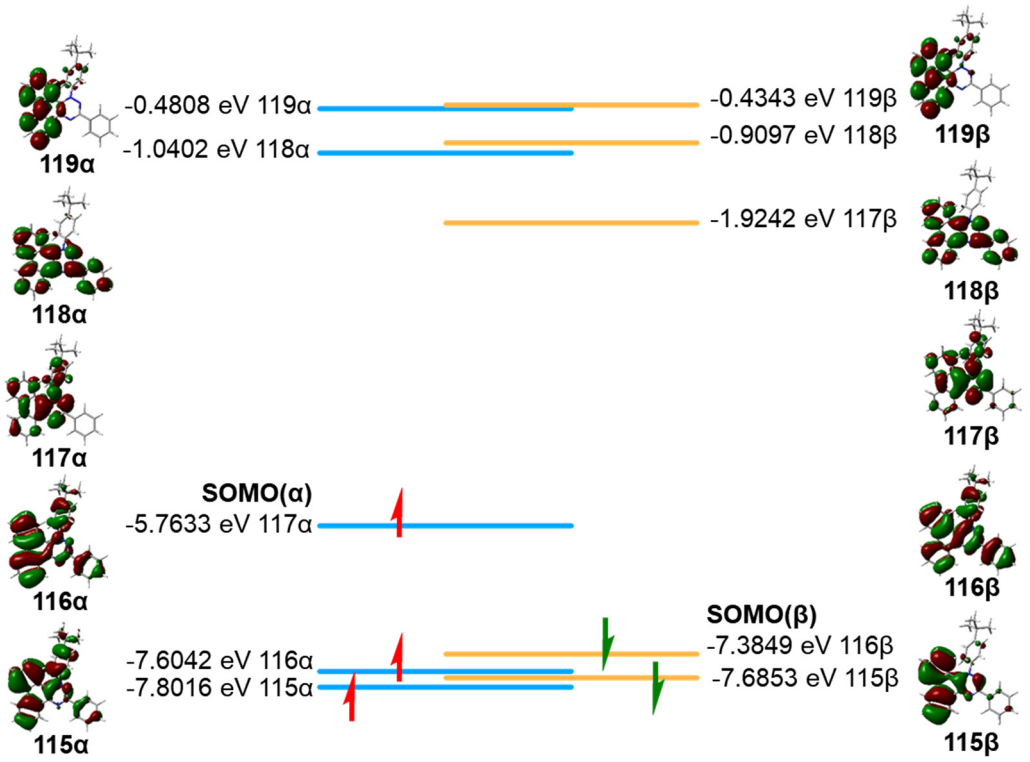

Fig. S25. Plots of the frontier molecular orbitals of **1-*t*Bu** (Isovalue = 0.02 electron Bohr^{-3}).

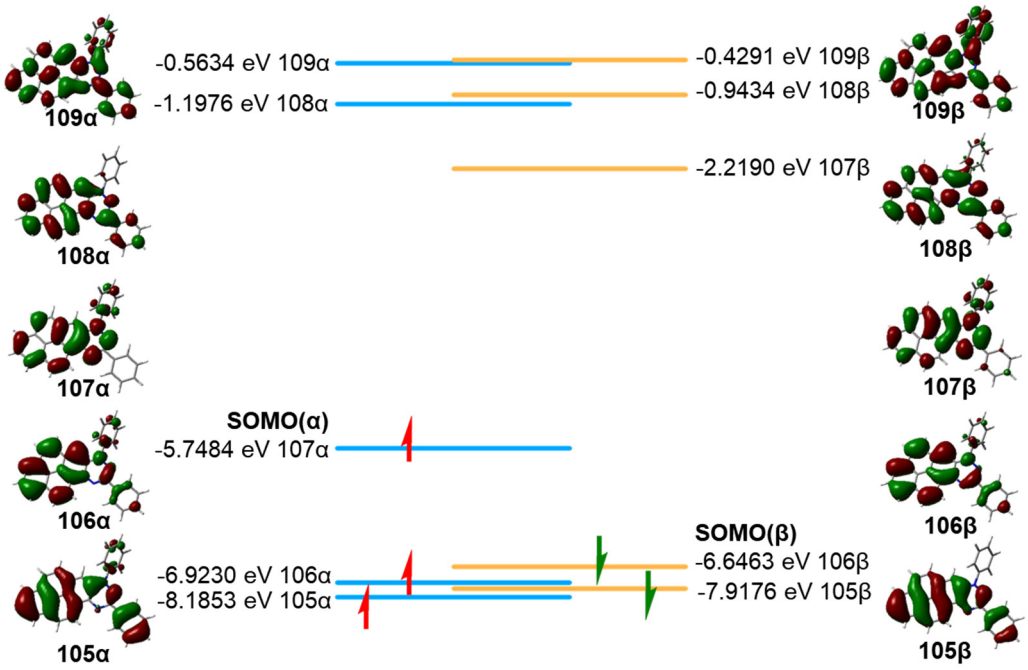

Fig. S26. Plots of the frontier molecular orbitals of **2** (Isovalue = 0.02 electron Bohr^{-3}).

Table S18. The DFT (M06-2X-GD3/def2-TZVP//SMD) calculated frontier molecular orbitals of **Blatter** and **1**–**8** in dichloromethane.

Species	**Blatter**	**1**	**1-*t*Bu**	**2**	**3**	**4**	**5**	**6**	**7**	**8**
SOMO (α) (eV)	-5.9613	-5.8110	-5.7632	-5.7484	-5.9438	-5.9278	-5.9875	-6.1567	-5.8958	-5.8483
LUMO (α) (eV)	-0.6371	-1.0505	-1.0402	-1.1976	-1.0878	-0.7816	-0.7871	-0.8966	-0.7988	-0.9529
HOMO (β) (eV)	-7.6115	-7.4427	-7.3849	-6.6463	-7.3684	-7.1267	-6.8973	-7.8105	-6.9804	-6.8928
SUMO (β) (eV)	-1.9246	-1.9585	-1.9242	-2.2190	-2.1849	-2.0767	-2.1896	-2.1304	-2.1229	-2.0127

10.3 Charge and Spin densities

Table S19. Mulliken atomic charge distributions and spin densities for **Blatter**, **1**, **1-*t*Bu** and **2**–**8** at the M06-2X-GD3/def2-TZVP (gas phase) level.

Blatter				**1**			
		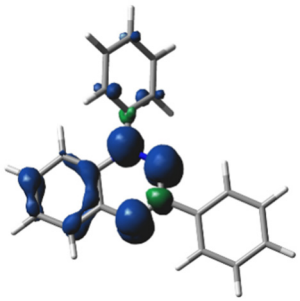		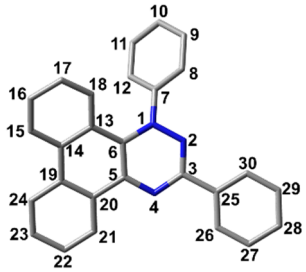		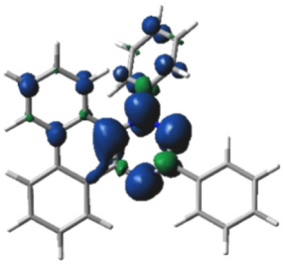	
Charges		**Spin densities**		**Charges**		**Spin densities**	
1N	0.04263	1N	0.261726	1 N	0.044023	1 N	0.284072
2N	-0.288958	2N	0.34128	2 N	-0.287861	2 N	0.267318
3C	0.228259	3C	-0.120701	3 C	0.243922	3 C	-0.102406
4N	-0.319082	4N	0.32385	4 N	-0.376812	4 N	0.307203
5C	0.182865	5C	-0.003107	5 C	0.249645	5 C	-0.034504
6C	0.067459	6C	0.053621	6 C	-0.050925	6 C	0.162156
7C	0.209305	7C	-0.039506	7 C	0.083821	7 C	-0.045711
8C	-0.088063	8C	0.041096	8 C	-0.013763	8 C	0.04809
9C	0.033835	9C	-0.021009	9 C	0.03188	9 C	-0.029882
10C	-0.007298	10C	0.037074	10 C	-0.009831	10 C	0.054106
11C	0.022956	11C	-0.020696	11 C	0.026867	11 C	-0.031204
12C	-0.026447	12C	0.037109	12 C	-0.005516	12 C	0.058128
13C	-0.039055	13C	-0.002036	13 C	0.014737	13 C	-0.043003
14C	0.004375	14C	0.071689	14 C	0.089821	14 C	0.049334
15C	0.005351	15C	0.025337	15 C	-0.063497	15 C	-0.026429
16C	-0.062737	16C	0.028189	16 C	-0.020314	16 C	0.054026
17C	0.071674	17C	0.012619	17 C	0.014623	17 C	-0.031147
18C	-0.03257	18C	-0.01707	18 C	-0.006658	18 C	0.054343
19C	0.008012	19C	0.010772	19 C	0.109287	19 C	0.000277
20C	0.002436	20C	-0.013346	20 C	0.000715	20 C	-0.00608
21C	0.001249	21C	0.00907	21 C	-0.037439	21 C	0.010295
22C	-0.016195	22C	-0.015961	22 C	0.012493	22 C	-0.000966
				23 C	-0.005456	23 C	0.007624
				24 C	-0.07132	24 C	0.000815
				25 C	0.057407	25 C	0.01657
				26 C	-0.023963	26 C	-0.01434
				27 C	0.004267	27 C	0.008998
				28 C	0.00245	28 C	-0.011558
				29 C	0.003275	29 C	0.007882
				30 C	-0.015877	30 C	-0.014005

2				3			
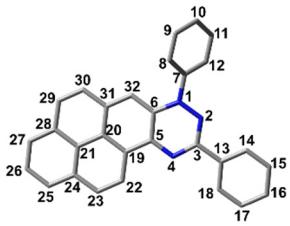		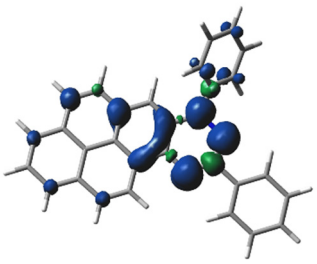		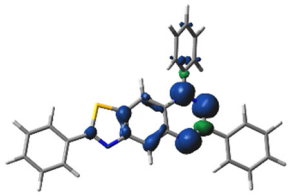			
Charges		**Spin densities**		**Charges**		**Spin densities**	
1 N	0.056668	1 N	0.247717	1 N	0.054833	1 N	0.246288
2 N	-0.292194	2 N	0.311704	2 N	-0.296732	2 N	0.350233
3 C	0.221385	3 C	-0.116449	3 C	0.223195	3 C	-0.120557
4 N	-0.361723	4 N	0.315270	4 N	-0.31581	4 N	0.314244
5 C	0.242439	5 C	-0.033388	5 C	0.226571	5 C	-0.005467
6 C	0.020067	6 C	0.077620	6 C	0.029771	6 C	0.02738
7 C	0.212048	7 C	-0.036073	7 C	0.20198	7 C	-0.034046
8 C	-0.088788	8 C	0.037575	8 C	-0.086709	8 C	0.03374
9 C	0.033206	9 C	-0.019080	9 C	0.036407	9 C	-0.017049
10 C	-0.006101	10 C	0.033701	10 C	-0.003478	10 C	0.030145
11 C	0.022960	11 C	-0.018732	11 C	0.023656	11 C	-0.016998
12 C	-0.025021	12 C	0.033505	12 C	-0.020463	12 C	0.030651
13 C	0.070220	13 C	0.015433	13 C	-0.057242	13 C	0.030611
14 C	-0.021560	14 C	-0.015001	14 C	0.001459	14 C	0.047907
15 C	0.003757	15 C	0.008904	15 C	0.189102	15 C	0.02243
16 C	0.000183	16 C	-0.013421	16 C	-0.180584	16 C	0.043495
17 C	0.006996	17 C	0.010573	17 C	0.07662	17 C	0.012054
18 C	-0.027678	18 C	-0.016997	18 C	-0.033047	18 C	-0.017181
19 C	0.025495	19 C	0.038105	19 C	0.008564	19 C	0.010804
20 C	0.022130	20 C	0.002057	20 C	0.002411	20 C	-0.013354
21 C	0.032033	21 C	0.021942	21 C	0.002197	21 C	0.008969
22 C	-0.079356	22 C	-0.006735	22 C	-0.020142	22 C	-0.015501
23 C	-0.023503	23 C	0.032667	23 N	-0.24468	23 N	-0.010327
24 C	0.080250	24 C	-0.009956	24 S	0.018996	24 S	-0.008242
25 C	-0.049372	25 C	0.024831	25 C	0.136788	25 C	0.037629
26 C	0.004996	26 C	-0.009792	26 C	0.062018	26 C	-0.012548
27 C	-0.042728	27 C	0.035447	27 C	-0.034673	27 C	0.012774
28 C	0.079855	28 C	-0.016396	28 C	-0.014085	28 C	-0.007418
29 C	-0.053778	29 C	0.054534	29 C	0.012807	29 C	0.013715
30 C	-0.088331	30 C	-0.039175	30 C	0.018184	30 C	-0.007149
31 C	0.106727	31 C	0.057696	31 C	-0.017917	31 C	0.01277
32 C	-0.081280	32 C	-0.008085				

4				5			
		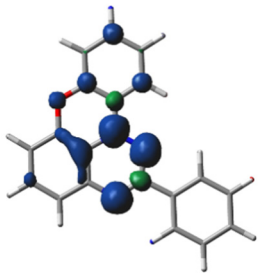				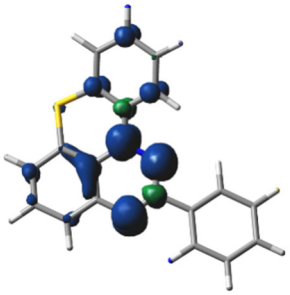	
Charges		**Spin densities**		**Charges**		**Spin densities**	
1 N	0.094327	1 N	0.262491	1 N	0.069952	1 N	0.257867
2 N	-0.32254	2 N	0.312183	2 N	-0.322431	2 N	0.319739
3 C	0.243403	3 C	-0.10853	3 C	0.245960	3 C	-0.113781
4 N	-0.31923	4 N	0.292314	4 N	-0.319217	4 N	0.303975
5 C	0.203216	5 C	-0.00642	5 C	0.196901	5 C	-0.010938
6 C	-0.0023	6 C	0.081037	6 C	0.040613	6 C	0.077030
7 C	0.057422	7 C	-0.06361	7 C	0.116649	7 C	-0.069865
8 C	0.217153	8 C	0.078324	8 C	-0.018564	8 C	0.075684
9 C	-0.07168	9 C	-0.04097	9 C	-0.004006	9 C	-0.038638
10 C	0.020459	10 C	0.083229	10 C	-0.004742	10 C	0.073065
11 C	-0.00137	11 C	-0.03759	11 C	0.004582	11 C	-0.038769
12 C	0.026922	12 C	0.070364	12 C	0.020748	12 C	0.069773
13 C	0.199103	13 C	0.010056	13 C	-0.021760	13 C	-0.002062
14 C	-0.07629	14 C	0.024773	14 C	-0.013088	14 C	0.050247
15 C	0.04847	15 C	0.031774	15 C	0.021719	15 C	0.017022
16 C	-0.09603	16 C	-0.00492	16 C	-0.083802	16 C	0.013304
17 C	0.059479	17 C	0.010619	17 C	0.075538	17 C	0.011566
18 C	-0.02823	18 C	-0.01442	18 C	-0.029455	18 C	-0.015332
19 C	0.009251	19 C	0.009224	19 C	0.009127	19 C	0.009409
20 C	0.003125	20 C	-0.01069	20 C	0.004659	20 C	-0.011753
21 C	0.000444	21 C	0.007321	21 C	-0.001980	21 C	0.007644
22 C	-0.00816	22 C	-0.01326	22 C	-0.015482	22 C	-0.013600
23 O	-0.25695	23 O	0.026701	23 S	0.028081	23 S	0.028414

6				7			
		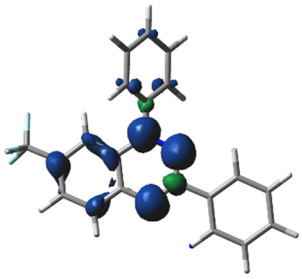				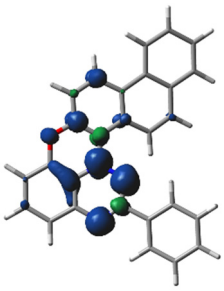	
Charges		**Spin densities**		**Charges**		**Spin densities**	
1N	0.049637	1N	0.269128	1N	0.076793	1N	0.270877
2N	-0.287504	2N	0.336553	2N	-0.345494	2N	0.293772
3C	0.234281	3C	-0.114073	3C	0.257343	3C	-0.102517
4N	-0.320497	4N	0.318331	4N	-0.322465	4N	0.290321
5C	0.195003	5C	-0.017021	5C	0.197855	5C	-0.01147
6C	0.059988	6C	0.049664	6C	0.003706	6C	0.083834
7C	0.208716	7C	-0.038546	7C	0.018916	7C	-0.07592
8C	-0.021367	8C	0.035765	8C	0.266678	8C	0.101065
9C	0.025617	9C	-0.019851	9C	-0.109944	9C	-0.043558
10C	-0.001577	10C	0.035676	10C	-0.039655	10C	0.070359
11C	0.039153	11C	-0.020393	11C	0.080684	11C	-0.028488
12C	-0.088112	12C	0.039616	12C	0.091735	12C	0.058891
13C	-0.025133	13C	0.025914	13C	0.202177	13C	0.006051
14C	-0.029333	14C	0.071751	14C	-0.084557	14C	0.025818
15C	-0.007299	15C	0.002963	15C	0.053417	15C	0.023657
16C	-0.051267	16C	0.037092	16C	-0.099976	16C	0.00032
17C	0.073655	17C	0.010732	17C	0.078045	17C	0.009059
18C	-0.029553	18C	-0.015515	18C	-0.033435	18C	-0.013074
19C	0.010178	19C	0.009899	19C	0.012117	19C	0.008443
20C	0.006264	20C	-0.011699	20C	0.002576	20C	-0.009681
21C	0.004305	21C	0.007879	21C	-0.007478	21C	0.006347
22C	-0.015499	22C	-0.013747	22C	-0.008552	22C	-0.011339
23C	0.508275	23C	-0.002278	23C	-0.048735	23C	-0.014574
24F	-0.180329	24F	-0.000075	24C	-0.058427	24C	0.028215
25F	-0.178441	25F	0.001366	25C	0.103737	25C	-0.01349
26F	-0.179161	26F	0.000869	26C	-0.049973	26C	0.00607
				27C	0.000029	27C	-0.007229
				28C	-0.007557	28C	0.007977
				29C	-0.079124	29C	-0.006342
				30C	0.109524	30C	0.015612
				31O	-0.259959	31O	0.03099

8

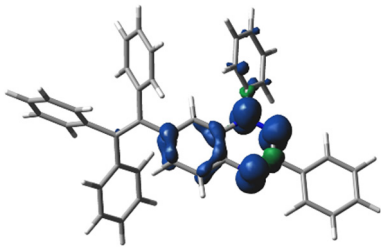

Charges		Spin densities	
1N	0.052084	1N	0.255934
2N	-0.296369	2N	0.327022
3C	0.234176	3C	-0.117275
4N	-0.31934	4N	0.317491
5C	0.21641	5C	-0.013236
6C	0.05121	6C	0.05278
7C	0.215184	7C	-0.04118
8C	-0.083649	8C	0.045217
9C	0.026592	9C	-0.023382
10C	-0.004553	10C	0.040698
11C	0.020072	11C	-0.022584
12C	-0.029703	12C	0.04024
13C	-0.056892	13C	0.00618
14C	-0.050757	14C	0.093131
15C	0.049453	15C	-0.005437
16C	-0.081398	16C	0.037723
17C	0.06973	17C	0.012394
18C	-0.032927	18C	-0.016621
19C	0.006495	19C	0.010486
20C	0.00173	20C	-0.013123
21C	0.000472	21C	0.008837
22C	-0.018219	22C	-0.01539
23C	0.081841	23C	-0.006018
24C	-0.046632	24C	-0.002133
25C	-0.005649	25C	-0.000392
26C	0.003485	26C	-0.001205
27C	0.000912	27C	0.000569
28C	0.029659	28C	-0.001202
29C	0.10406	29C	0.01445
30C	-0.072414	30C	-0.002182
31C	0.032854	31C	0.003208
32C	-0.005739	32C	-0.001576
33C	0.004153	33C	0.003385
34C	-0.004245	34C	-0.001954
35C	0.00256	35C	0.002778
36C	-0.08751	36C	0.005379
37C	0.000802	37C	0.004025
38C	-0.00196	38C	-0.001444
39C	0.007707	39C	0.00532
40C	-0.004231	40C	-0.001831

41C	0.037238	41C	0.001443
42C	-0.046692	42C	-0.000525

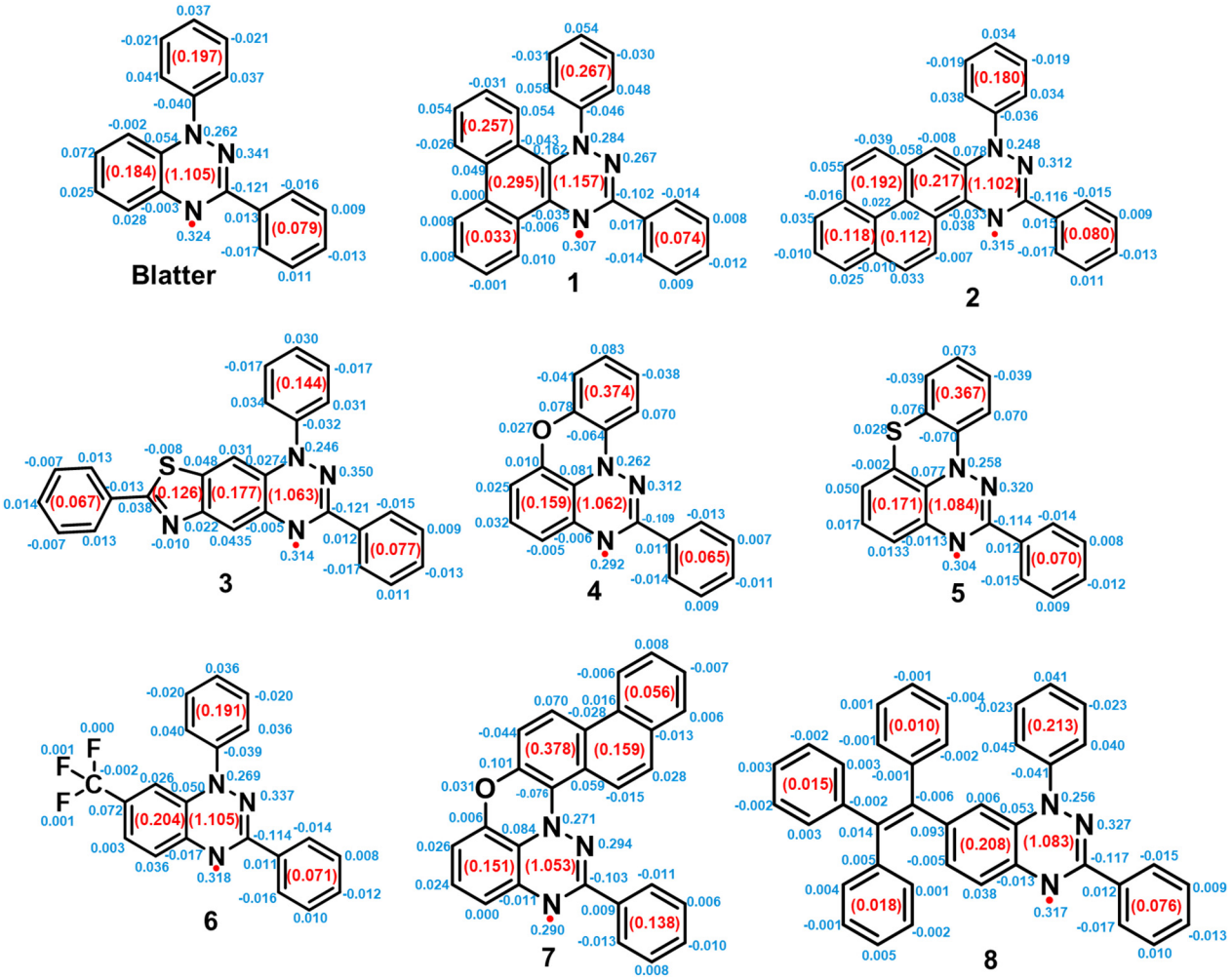

Fig. S27. DFT(M06-2X-GD3/def2-TZVP) calculated spin populations on atoms (blue numbers) and summed values of six atoms on the rings (red numbers in parentheses) for the studied radicals.

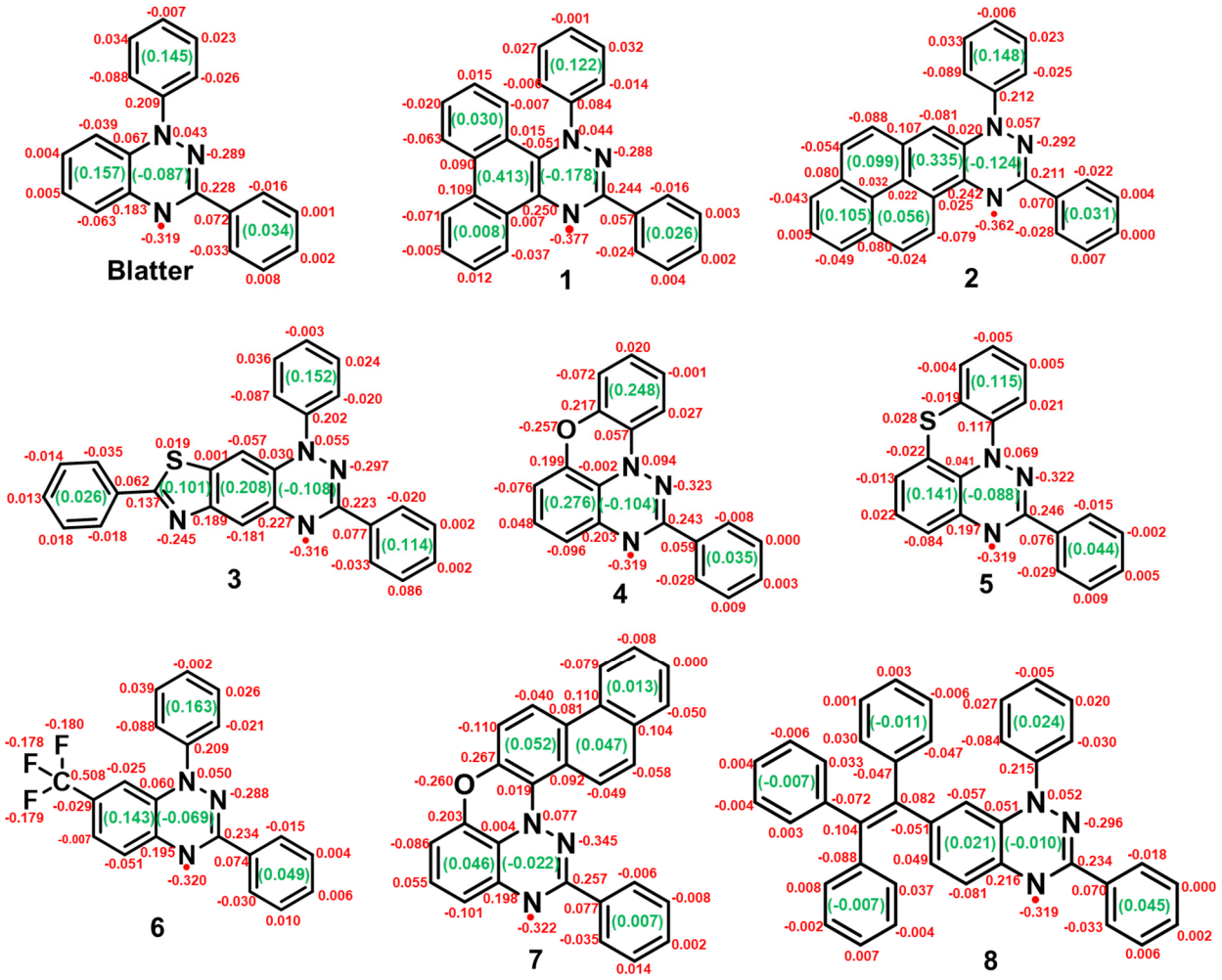

Fig. S28. DFT(M06-2X-GD3/def2-TZVP) calculated Mulliken charges on atoms (red numbers) and the summed values of six atoms on the ring (green numbers in parentheses) for the studied radicals.

10.4 Electrochemical Gaps Calculations

Table S20. The DFT (M06-2X-GD3/def2-TZVP//SMD M06-2X-GD3/def2-TZVP) calculations for the redox potentials of **Blatter** and **1**–**8**: energies ($E°$, hartree), zero-point vibrational energies (ZPVE, hartree), thermal correction to energies (TC-E, hartree), total electronic and thermal energies (U, hartree, 298 K), dipole moment (total, μ, Debye), imaginary and lowest vibrational frequencies (cm^{-1}), relative electronic and thermal energies (Rel. U, hartree), the gas-phase ionization potentials (IP_{gas}, eV), the gas-phase electron affinities (EA_{gas}, eV), the solvation free energies of the neutral species ($\Delta G_{sol}(neut)$, eV), the solvation free energies of the cations ($\Delta G_{sol}(cat.)$, eV), the solvation free energies of the anions ($\Delta G_{sol}(anion)$, eV), The differential solvation stabilization energy ($\Delta\Delta G_{sol}$, eV), the free energies of the oxidation (ΔG^0_{ox}, hartree) and reduction reactions (ΔG^0_{red}, hartree), thermodynamic oxidation (E_{ox}, eV) and reduction (E_{red}, eV) potentials, and the electrochemical gaps (E^{Calc}_{gap}, eV).[a]

Species	Task [b]	State	Medium	Chrg.[c]	Spin Multip-licity	Point grp.[d]	$E°$	ZPVE	TC-E	H (298 K)	<S^2>	μ	RMS Gradt.[e] ($\times10^{-6}$)	Lowest Vibrational Frequencies	IP_{gas}	EA_{gas}	ΔG_{sol} (Neut.)	ΔG_{sol} (Cat.)	ΔG_{sol} (Anion)	$\Delta\Delta G_{sol}$	ΔG^0_{ox}	ΔG^0_{ox}	E_{ox}	E_{red}	E^{Calc}_{gap}
Blatter	Basic Opt.	Neutral	Gas Phase	0	2	C_1	–896.629570596	0.285481	0.302555	–896.327960	0.7691	3.10	1	30.0, 37.6	6.222	1.834	–0.7917	–2.2877	–2.2998	3.004	0.1737	–0.1228	4.726	3.343	1.383
	SPE [f]	Neutral	DCM	0	2	C_1	–896.658666471	/	/	/	/	/	/	/											
	SPE [f]	Cation	Gas Phase	+1	0	C_1	–896.394157354	/	/	/	/	/	/	/											
	SPE [f]	Anion	Gas Phase	–1	0	C_1	–896.680943289	/	/	/	/	/	/	/											
	Basic Opt.	Cation	Gas Phase	+1	0	C_1	–896.402563017	0.287238	0.303251	-896.099312	/	4.86	3	27.6, 34.5											
	SPE [g]	Cation	DCM	+1	0	C_1	–896.486637382	/	/	/	/	/	/	/											
	Basic Opt.	Anion	Gas Phase	–1	0	C_1	–896.695079588	0.283506	0.299699	-896.39538	/	1.45	2	26.6, 44.2											
	SPE [h]	Anion	DCM	–1	0	C_1	–896.779596196	/	/	/	/	/	/	/											
1	Basic Opt.	Neutral	Gas Phase	0	2	C_1	-1203.90210572	0.380086	0.401556	-1203.500550	0.7680	2.49	5	20.9, 26.7	5.855	2.065	-0.9878	-2.3283	-2.4070	2.760	0.1659	-0.1280	4.514	3.484	1.030
	SPE [f]	Neutral	DCM	0	2	C_1	-1203.93840764	/	/	/	/	/	/	/											
	SPE [f]	Cation	Gas Phase	+1	0	C_1	-1203.67758707	/	/	/	/	/	/	/											
	SPE [f]	Anion	Gas Phase	–1	0	C_1	-1203.96031803	/	/	/	/	/	/	/											
	Basic Opt.	Cation	Gas Phase	+1	0	C_1	-1203.68938388	0.382740	0.403990	-1203.285394	/	3.05	4	25.7, 36.8											
	SPE [g]	Cation	DCM	+1	0	C_1	-1203.77494999	/	/	/	/	/	/	/											
	Basic Opt.	Anion	Gas Phase	–1	0	C_1	-1203.97628232	0.378339	0.399861	-1203.576421	/	2.11	7	28.6, 33,3											
	SPE [h]	Anion	DCM	–1	0	C_1	-1204.06473535	/	/	/	/	/	/	/											
2	Basic Opt.	Neutral	Gas Phase	0	2	C_1	-1280.13975331	0.393169	0.415218	-1279.724536	0.7741	2.72	2	28.3, 39.0	5.931	2.150	-1.0691	-2.3573	-2.3646	2.584	0.1706	-0.1266	4.643	3.446	1.197
	SPE [f]	Neutral	DCM	0	2	C_1	-1280.17904091	/	/	/	/	/	/	/											
	SPE [f]	Cation	Gas Phase	+1	0	C_1	-1279.9167763	/	/	/	/	/	/	/											
	SPE [f]	Anion	Gas Phase	–1	0	C_1	-1280.20646305	/	/	/	/	/	/	/											
	Basic Opt.	Cation	Gas Phase	+1	0	C_1	-1279.92354827	0.395049	0.416989	-1279.506560	/	3.23	2	25.0, 36.8											
	SPE [g]	Cation	DCM	+1	0	C_1	-1280.01017938	/	/	/	/	/	/	/											
	Basic Opt.	Anion	Gas Phase	–1	0	C_1	-1280.21630481	0.390458	0.412742	-1279.803563	/	0.61	1	19.4, 30.4											
	SPE [h]	Anion	DCM	–1	0	C_1	-1280.30320354	/	/	/	/	/	/	/											
3	Basic Opt.	Neutral	Gas Phase	0	2	C_1	-1618.13701304	0.369144	0.392225	-1617.744788	0.7705	4.03	1	25.1, 29.9	6.072	2.070	-1.0495	-2.3401	-2.4147	2.656	0.1757	-0.1263	4.781	3.435	1.346
	SPE [f]	Neutral	DCM	0	2	C_1	-1618.17558221	/	/	/	/	/	/	/											

Continued from previous page ...

Species	Task [b]	State	Medium	Chrg.[c]	Spin Multip-licity	Point grp.[d]	$E°$	ZPVE	TC-E	H (298 K)	<S^2>	μ	RMS Gradt.[e] (×10^{-6})	Lowest Vibrational Frequencies	IP_{gas}	EA_{gas}	ΔG_{sol} (Neut.)	ΔG_{sol} (Cat.)	ΔG_{sol} (Anion)	$\Delta\Delta G_{sol}$	ΔG^0_{ox}	ΔG^0_{ox}	E_{ox}	E_{red}	E^{Calc}_{gap}
	SPE[f]	Cation	Gas Phase	+1	0	C_1	-1617.90759625	/	/	/	/	/	/	/											
	SPE[f]	Anion	Gas Phase	–1	0	C_1	-1618.20105354	/	/	/	/	/	/	/											
	Basic Opt.	Cation	Gas Phase	+1	0	C_1	-1617.91528238	0.370697	0.393622	-1617.521661	/	3.95	5	26.4, 31.4											
	SPE[g]	Cation	DCM	+1	0	C_1	-1618.00127906	/	/	/	/	/	/	/											
	Basic Opt.	Anion	Gas Phase	–1	0	C_1	-1618.21121528	0.367066	0.390349	-1617.820866	/	5.74	3	18.9, 22.2											
	SPE[h]	Anion	DCM	–1	0	C_1	-1618.2999562	/	/	/	/	/	/	/											
4	Basic Opt.	Neutral	Gas Phase	0	2	C_1	-970.666466347	0.268584	0.284366	-970.382100	0.7678	2.25	2	19.7, 48.0											
	SPE[f]	Neutral	DCM	0	2	C_1	-970.693593759	/	/	/	/	/	/	/											
	SPE[f]	Cation	Gas Phase	+1	0	C_1	-970.430521381	/	/	/	/	/	/	/											
	SPE[f]	Anion	Gas Phase	–1	0	C_1	-970.724087958	/	/	/	/	/	/	/											
	Basic Opt.	Cation	Gas Phase	+1	0	C_1	-970.437284441	0.270635	0.286205	-970.151079	/	3.78	4	21.9, 48.0	6.286	1.829	-0.7382	-2.2495	-2.2406	3.014	0.1755	-0.1224	4.775	3.331	1.444
	SPE[g]	Cation	DCM	+1	0	C_1	-970.519953238	/	/	/	/	/	/	/											
	Basic Opt.	Anion	Gas Phase	–1	0	C_1	-970.730994084	0.265446	0.281685	-970.449309	/	1.54	3	25.0, 41.9											
	SPE[h]	Anion	DCM	–1	0	C_1	-970.813335003	/	/	/	/	/	/	/											
5	Basic Opt.	Neutral	Gas Phase	0	2	C_1	-1293.63014846	0.265330	0.281777	-1293.348372	0.7684	1.94	1	21.0, 27.4											
	SPE[f]	Neutral	DCM	0	2	C_1	-1293.65825686	/	/	/	/	/	/	/											
	SPE[f]	Cation	Gas Phase	+1	0	C_1	-1293.39191727	/	/	/	/	/	/	/											
	SPE[f]	Anion	Gas Phase	–1	0	C_1	-1293.69266061	/	/	/	/	/	/	/											
	Basic Opt.	Cation	Gas Phase	+1	0	C_1	-1293.39989618	0.267408	0.283724	-1293.116172	/	3.28	1	8.65, 25.1	6.318	1.996	-0.7649	-2.2514	-2.2590	2.981	0.1776	-0.1283	4.832	3.490	1.342
	SPE[g]	Cation	DCM	+1	0	C_1	-1293.48263569	/	/	/	/	/	/	/											
	Basic Opt.	Anion	Gas Phase	–1	0	C_1	-1293.7016207	0.263341	0.279898	-1293.421722	/	1.80	6	38.6, 42.5											
	SPE[h]	Anion	DCM	–1	0	C_1	-1293.78464041	/	/	/	/	/	/	/											
6	Basic Opt.	Neutral	Gas Phase	0	2	C_1	-1233.72321033	0.291316	0.310985	-1233.412226	0.7689	2.60	1	27.8, 28.6											
	SPE[f]	Neutral	DCM	0	2	C_1	-1233.75147919	/	/	/	/	/	/	/											
	SPE[f]	Cation	Gas Phase	+1	0	C_1	-1233.47677819	/	/	/	/	/	/	/											
	SPE[f]	Anion	Gas Phase	–1	0	C_1	-1233.78746881	/	/	/	/	/	/	/											
	Basic Opt.	Cation	Gas Phase	+1	0	C_1	-1233.48548343	0.293099	0.312599	-1233.172884	/	3.33	5	31.0, 33.9	6.513	2.209	-0.7692	-2.3457	-2.1006	2.908	0.1814	-0.1301	4.936	3.540	1.396
	SPE[g]	Cation	DCM	+1	0	C_1	-1233.57168778	/	/	/	/	/	/	/											
	Basic Opt.	Anion	Gas Phase	–1	0	C_1	-1233.80192659	0.288644	0.308519	-1233.493408	/	0.79	3	18.8, 23.0											
	SPE[h]	Anion	DCM	–1	0	C_1	-1233.87912244	/	/	/	/	/	/	/											
7	Basic Opt.	Neutral	Gas Phase	0	2	C_1	-1277.93009541	0.362661	0.383867	-1277.546228	0.7694	2.39	3	24.9, 31.1	6.130	1.995	-0.9842	-2.3698	-2.3970	2.798	0.1744	-0.1252	4.744	3.408	1.336
	SPE[f]	Neutral	DCM	0	2	C_1	-1277.96626316	/	/	/	/	/	/	/											

Continued from previous page ...

Species	Task [b]	State	Medium	Chrg.[c]	Spin Multip-licity	Point grp.[d]	*E*°	ZPVE	*TC*-*E*	*H* (298 K)	<S²>	μ	RMS Gradt.[e] (×10⁻⁶)	Lowest Vibrational Frequencies	IP_{gas}	EA_{gas}	ΔG_{sol} (Neut.)	ΔG_{sol} (Cat.)	ΔG_{sol} (Anion)	$\Delta\Delta G_{sol}$	ΔG_{ox}^{0}	ΔG_{ox}^{0}	E_{ox}	E_{red}	E_{gap}^{Calc}
	SPE[f]	Cation	Gas Phase	+1	0	C_1	-1277.69986415	/	/	/	/	/	/	/											
	SPE[f]	Anion	Gas Phase	–1	0	C_1	-1277.99309849	/	/	/	/	/	/	/											
	Basic Opt.	Cation	Gas Phase	+1	0	C_1	-1277.70664740	0.364708	0.385700	-1277.320948	/	3.57	2	27.7, 28.4											
	SPE[g]	Cation	DCM	+1	0	C_1	-1277.79373731	/	/	/	/	/	/	/											
	Basic Opt.	Anion	Gas Phase	–1	0	C_1	-1278.00085445	0.359713	0.381301	-1277.619553	/	1.27	3	23.0, 30.0											
	SPE[h]	Anion	DCM	–1	0	C_1	-1278.08894217	/	/	/	/	/	/	/											
8	Basic Opt.	Neutral	Gas Phase	0	2	C_1	-1667.15377623	0.563761	0.596057	-1666.557719	0.7702	3.40	2	14.2, 18.9	5.874	2.000	-1.3324	-2.5378	-2.6842	2.557	0.1716	-0.1232	4.669	3.352	1.316
	SPE[f]	Neutral	DCM	0	2	C_1	-1667.20274247	/	/	/	/	/	/	/											
	SPE[f]	Cation	Gas Phase	+1	0	C_1	-1666.93111028	/	/	/	/	/	/	/											
	SPE[f]	Anion	Gas Phase	–1	0	C_1	-1667.21333028	/	/	/	/	/	/	/											
	Basic Opt.	Cation	Gas Phase	+1	0	C_1	-1666.93932665	0.565374	0.597476	-1666.341851	/	4.04	2	14.3, 21.2											
	SPE[g]	Cation	DCM	+1	0	C_1	-1667.03259044	/	/	/	/	/	/	/											
	Basic Opt.	Anion	Gas Phase	–1	0	C_1	-1667.2247309	0.561064	0.593497	-1666.631234	/	9.32	1	12.4, 16.7											
	SPE[h]	Anion	DCM	–1	0	C_1	-1667.32337328	/	/	/	/	/	/	/											

[a] For different energy units, 1 Hartree = 627.5095 kcal mol^{-1} = 27.2114 eV. [b] The computational tasks, including basic geometry optimizations/frequency analysis (Basic Opt.) and single-point energy calculations (SPE) herein. [c] Charge. [d] Symmetry point group of the geometry. [e] In Cartesian coordinates. [f] Based on the optimized geometry of the neutral species in gas phase. [g] Based on the optimized geometry of the cations in gas phase. [h] Based on the optimized geometry of the anions in gas phase.

Table S21. Summary of the DFT-computed solvation free energies for radicals **Blatter** and **1** – **8**: solvation energies at the neutral (ΔG_{sol}(Neut.), eV), cationic (ΔG_{sol}(Cat.), eV), and anionic (ΔG_{sol}(Anion), eV) states, differential solvation stabilization energies ($\Delta\Delta G_{sol}$, eV)[a], and the corresponding (or twice) differential energies in three different states of charge ($2\Delta\Delta G_{sol}$(Neut.), $\Delta\Delta G_{sol}$(Cat.) and $\Delta\Delta\Delta G_{sol}$(Anion), eV)) relative to that of **Blatter**. Data are derived from Table S20.

Species	ΔG_{sol}(Neut.)	$2\Delta\Delta G_{sol}$(Neut.)[b]	ΔG_{sol}(Cat.)	$\Delta\Delta G_{sol}$(Cat.)[c]	ΔG_{sol}(Anion)	$\Delta\Delta G_{sol}$(Anion)[d]	$\Delta\Delta G_{sol}$	$\Delta\Delta\Delta G_{sol}$
Blatter	-0.7917	**0.0000**	-2.2877	**0.0000**	-2.2998	**0.0000**	3.004	**0.000**
1	-0.9878	-0.3922	-2.3283	-0.0406	-2.4070	-0.1072	2.760	-0.244
2	-1.0691	-0.5548	-2.3573	-0.0696	-2.3646	-0.0648	2.584	-0.420
3	-1.0495	-0.5156	-2.3401	-0.0524	-2.4147	-0.1149	2.656	-0.348
4	-0.7382	0.1070	-2.2495	0.0382	-2.2406	0.0592	3.014	0.010
5	-0.7649	0.0536	-2.2514	0.0363	-2.2590	0.0408	2.981	-0.023
6	-0.7692	0.0450	-2.3457	-0.0580	-2.1006	0.1992	2.908	-0.096
7	-0.9842	-0.3850	-2.3698	-0.0821	-2.3970	-0.0972	2.798	-0.206
8	-1.3324	-1.0814	-2.5378	-0.2501	-2.6842	-0.3844	2.557	-0.447

[a] Differential solvation stabilization energies, $\Delta\Delta G_{sol} = 2\Delta G_{sol}$(Neut.) – ΔG_{sol}(Cat.) – ΔG_{sol}(Anion). [b] Twice the differential solvation energies of the neutrals relative to **Blatter**, $2\Delta\Delta G_{sol}$(Neut.) = 2 × (ΔG_{sol}(Neut.) – ΔG_{sol}(Neut., **Blatter**)). [c] Differential cationic-state solvation energies relative to **Blatter**, $\Delta\Delta G_{sol}$(Cat.) = ΔG_{sol}(Cat.) – ΔG_{sol}(Cat., **Blatter**). [d] Differential anionic-state solvation energies relative to **Blatter**, $\Delta\Delta G_{sol}$(Anion) = ΔG_{sol}(Anion) – ΔG_{sol}(Anion, **Blatter**).

Table S22. DFT-computed static polarizabilities (α, a.u.) and neutral-state solvation free energies (ΔG_{sol}(neut), eV) for radicals **Blatter** and **1** – **8**.[a] Data of ΔG_{sol}(Neut) are derived from Table S17. The corresponding plot of α_{iso} *vs* ΔG_{sol}(Neut) is shown in Fig. S29.

Species	α_{xx}	α_{xy}	α_{yy}	α_{xz}	α_{yz}	α_{zz}	α_{avg} [b]	ΔG_{sol}(Neut)
Blatter	327.095	7.486	298.963	4.993	7.323	132.594	252.88	-0.7917
1	447.53	3.695	434.605	-2.082	-23.057	188.976	357.04	-0.9878
2	629.354	21.216	437.114	-9.489	-4.117	178.844	415.10	-1.0691
3	625.665	1.238	396.451	-11.357	-5.145	181.469	401.20	-1.0495
4	354.897	3.275	311.593	0.001	0.003	112.875	259.79	-0.7382
5	368.492	1.936	329.564	-7.774	-4.987	127.857	275.30	-0.7649
6	354.931	3.89	303.552	-13.801	6.971	143.706	267.40	-0.7692
7	512.942	33.404	438.046	-20.822	9.005	161.473	370.82	-0.9842
8	671.654	8.305	524.78	-13.506	10.261	326.831	507.76	-1.3324

[a] Polarizabilities were computed at the M06-2X/def2-TZVP level of theory in the gas phase. Solvation free energies were obtained using the SMD solvation model (dichloromethane) at the same level. [b] Average polarizability, $\alpha_{avg} = (\alpha_{xx} + \alpha_{yy} + \alpha_{zz})/3$.

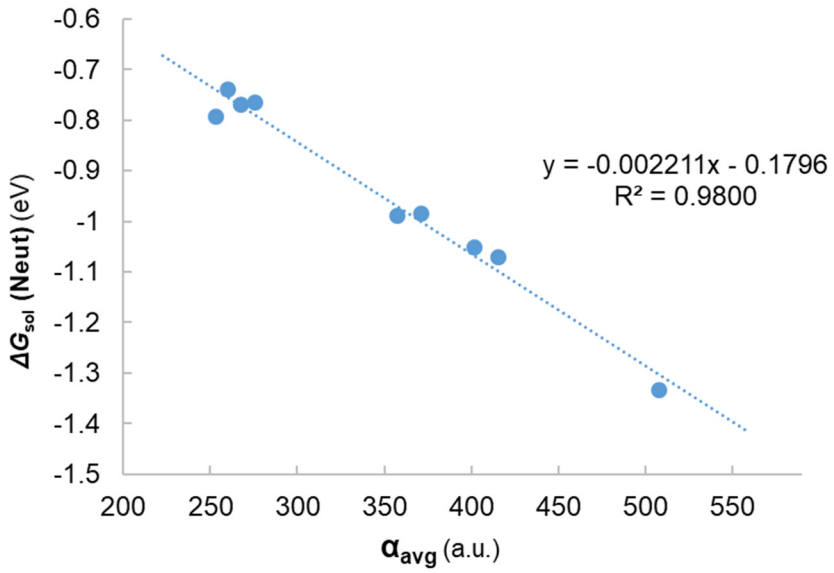

Fig. S29. Plot of DFT(M06-2X-GD3/def2-TZVP)-calculated solvation free energy for the neutral species (ΔG_{sol}(neut), eV) in DCM *versus* their average static polarizabilities (α_{avg}, a.u.). The linear fit ($R^2 = 0.98$) demonstrates a strong correlation between increased polarizability and enhanced neutral-state solvation.

10.5 NICS Calculations

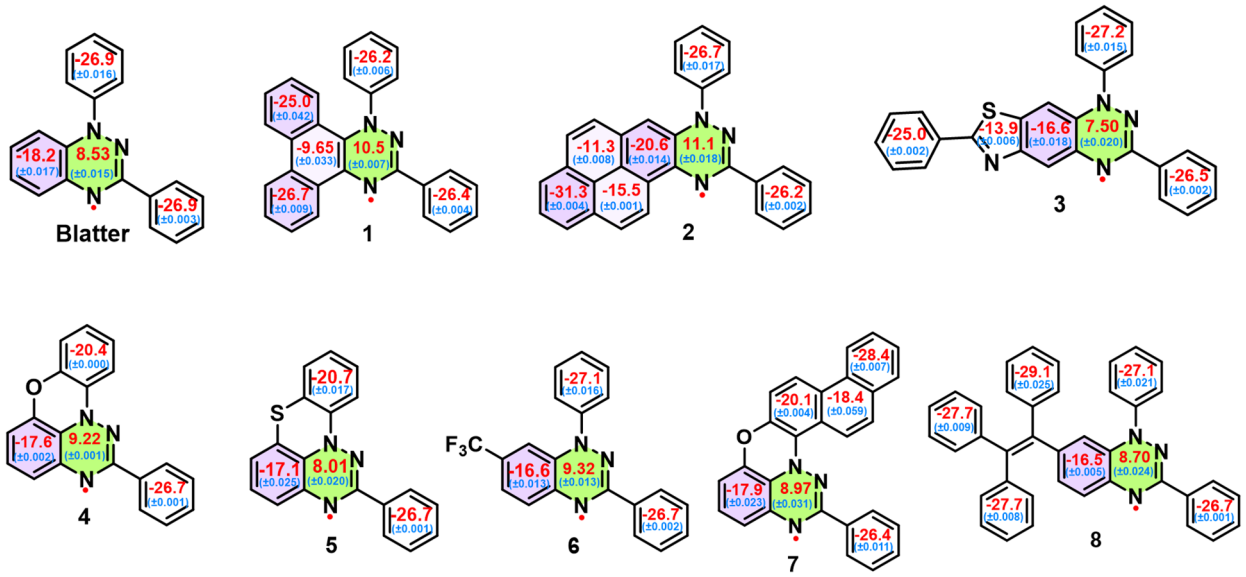

Fig. S30. DFT(SMD M06-2X-GD3/def2-TZVP) calculated NICS(1)zz values for the radicals in DCM. The values are indicated in red numbers. Hydrogen atoms are omitted for clarity in the structures.

10.6 Statistical Analyses of Correlation between ρ_{FR} and E_{gap}

As noted in the main text, the cyclic voltammetry of radical **8** reported in the literature[S7] shows a reduction wave suggestive of a multi-electron process, likely resulting in an underestimated reduction potential and hence an overestimated electrochemical gap. Linear regression analyses were carried out on the correlation between the experimentally determined electrochemical gap (E_{gap}^{Expt}) and DFT-calculated total spin density on the triazinyl-fused six-membered ring (ρ_{FR}) as well as that between the DFT-calculated electrochemical gaps (E_{gap}^{Calc}) and ρ_{FR} for the set of radicals including all the studied ones (**Blatter**, **1**, **1-*t*Bu**, and **2** – **8**), which confirms the overestimation of the actual electrochemical gap, as demonstrated by the abnormally larger standard residual for radical **8** in the correlation between E_{gap}^{Expt} and ρ_{FR} (Fig. S31), compared to that in E_{gap}^{Calc} vs ρ_{FR} (Fig. S32). Radical **8** is thus omitted from the correlation analysis.

In addition to Fig. 7 in the main text, Figs. S33 and S34 show the correlations between ρ_{FR} and the experimentally determined electrochemical gap (E_{gap}^{Expt}) for other two sets of radicals: (1) **Blatter**, **1**, **1-*t*Bu**, and **2** – **7** (Fig. S33) and (2) **1**, **1-*t*Bu**, **2** – **5** and **7** (i.e., includes only the π-extended (**1**, **1-*t*Bu**, **2**, **3**) and the π-planarized (**4**, **5** and **7**) Blatter derivatives) (Fig. S34).

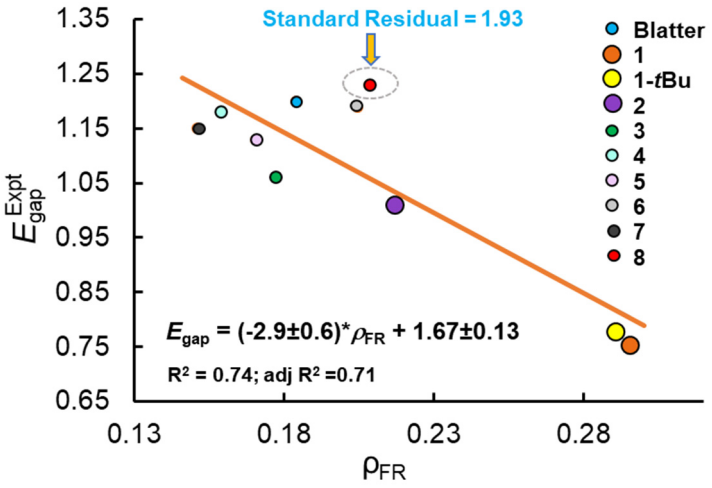

Fig. S31. Plot of experimentally determined electrochemical gap (E_{gap}^{Expt}) *vs* DFT-calculated total spin density on the triazinyl-fused six-membered ring (ρ_{FR}) for the set of radicals including **Blatter**, **1**, **1-*t*Bu**, and **2** – **8**. The solid line represents the linear regression fit through the predicted values, with the regression equation and adjusted R^2 = 0.71 shown in the figure. Error bars for slope and intercept correspond to 95 % confidence interval; P-value is 1.369×10^{-3} and 1.238×10^{-6} for the slope and the intercept, respectively; standard residual for **8** = 1.93.

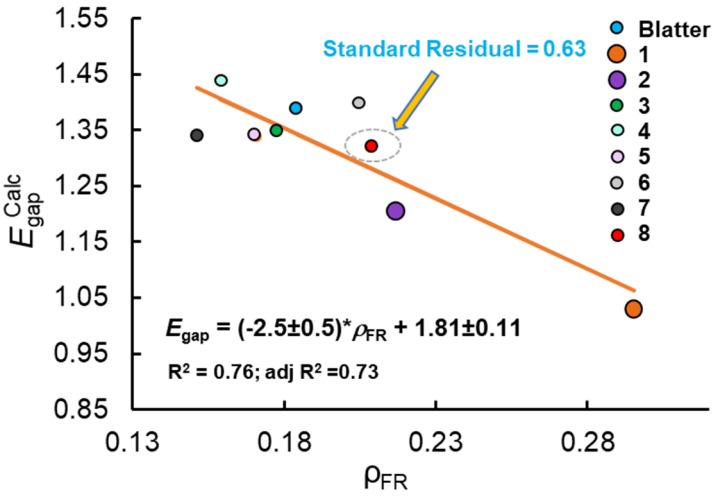

Fig. S32. Plot of DFT-calculated electrochemical gap (E_{gap}^{Calc}) *vs* total spin density on the triazinyl-fused six-membered ring (ρ_{FR}) for a set of radicals including **Blatter** and **1** – **8**. The solid line represents the linear regression fit through the predicted values, with the regression equation and adjusted R^2 = 0.73 shown in the figure. Error bars for slope and intercept correspond to 95 % confidence interval; P-value is 0.00218 and 6.316×10^{-7} for the slope and the intercept, respectively; standard residual for **8** = 0.63.

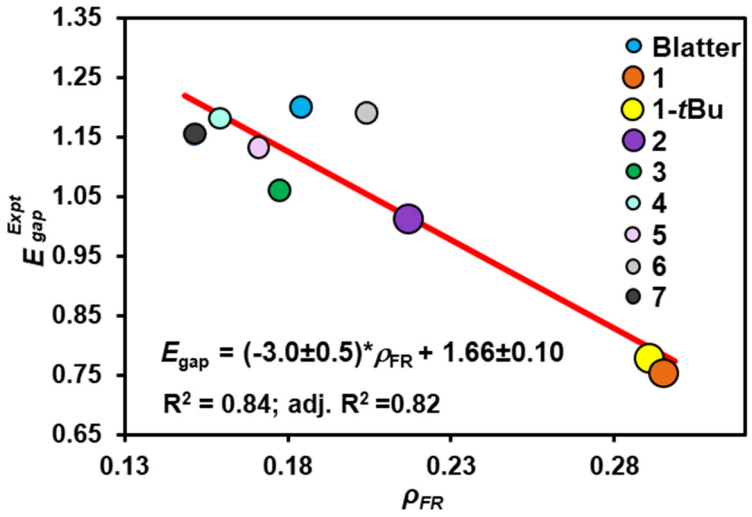

Fig. S33. Plot of experimentally determined electrochemical gap (E_{gap}^{Expt}) *vs* total spin density on the triazinyl-fused six-membered ring (ρ_{FR}) for the set of radicals including **Blatter**, **1**, **1-*t*Bu**, and **2** – **7**. The solid line represents the linear regression fit through the predicted values, with the regression equation and adjusted R^2 = 0.822 shown in the figure. Error bars for slope and intercept correspond to 95 % confidence interval; P-value is 0.000460 and 8.042×10^{-7} for the slope and the intercept, respectively; standard residual for **6** = 2.00.

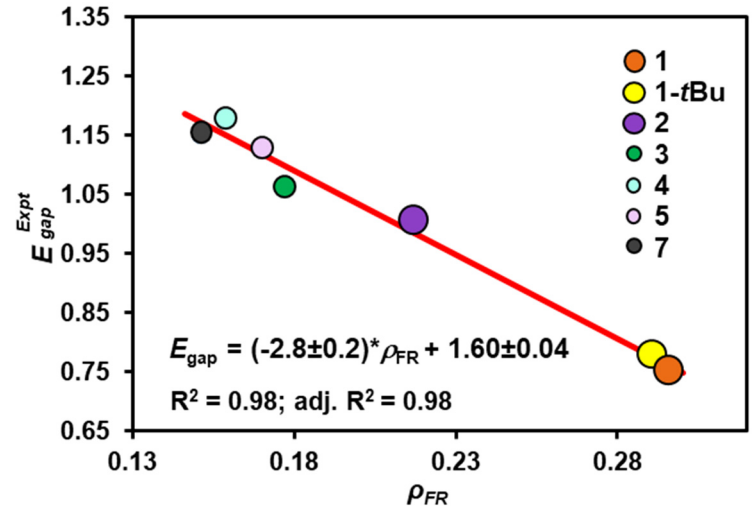

Fig. S34. Plot of DFT-calculated electrochemical gap (E_{gap}^{Expt}) *vs* total spin density on the triazinyl-fused six-membered ring (ρ_{FR}) for the set of radicals including only the π-extended (**1**, **1-*t*Bu**, **2**, **3**) and the π-planarized (**4**, **5** and **7**) Blatter derivatives. The solid line represents the linear regression fit through the predicted values, with the regression equation and adjusted R^2 = 0.976 shown in the figure. Error bars for slope and intercept correspond to 95 % confidence interval; P-value is 2.024×10^{-4} and 1.756×10^{-7} for the slope and the intercept, respectively.

10.7 DFT Calculations on a Molecular Pair Extracted from the Crystal Structure

To assess whether intermolecular interactions exist in the deposited monolayer, a pair of molecules of radical **1** extracted from its crystal structure was employed as a dimer model. The two molecules are arranged parallelly with an intermolecular distance of 14.6 Å, which is 7.2 Å smaller than the average intermolecular distance observed in the vapor-deposited monolayer (21.8 Å).

Single-point calculations were performed on these two molecules using several functionals and basis sets. Initial attempts with UM062X-D3/def2TZVP yielded unphysical results, in which the wavefunction of the broken-symmetry singlet state did not converge properly, and the inclusion of the D3 dispersion correction introduced excessively long-range interactions that are unlikely to be relevant at this separation. In contrast, calculations using UM062X/def2TZVP and UB3LYP/def2TZVP (both without D3 correction) produced reasonable and mutually consistent results. As a reference, single-molecule calculations on a monomer were also performed at the UM062X/def2TZVP level.

The computational results are summarized in Table S23. For the molecular pair, the open-shell singlet and triplet states are essentially degenerate, with a small coupling constant $J = 0.25$ K, which indicates negligible spin–spin coupling between the two radicals at this distance. The binding energy, evaluated as $\Delta E = 2E_{\text{monomer}} - E_{\text{dimer(OS)}}$, was found to be −0.02098 kcal mol^{-1}, effectively zero within computational accuracy. These results suggest that the intermolecular interactions are negligible at the 14.6 Å separation, and are expected to be even weaker at the larger distance observed in the monolayer.

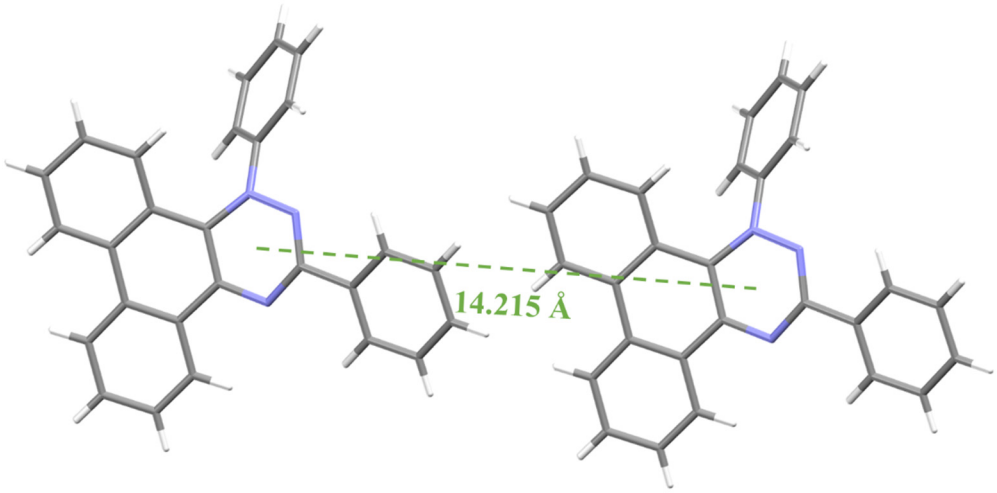

Fig. S35. Intermolecular distance (ca. 14.215 Å) in the structure of **Dimer_parallel**.

Table S23. The DFT single-point calculations on a molecular pair of **1** (**1**$_2$) extracted from its crystal structure and a monomer (**1**) in the gas phase: charge (e), spin multiplicity, energies (E°, hartree), expectation value of total spin squared (<S^2>), singlet-triplet energy gaps (ΔE_U(S–T), kcal·mol^{-1}), projected singlet-triplet energy gaps (ΔE_{S-T}, kcal·mol^{-1}) and intermolecular coupling constant (J, K). [a]

Species	Basis Set	State	Chrg.[b]	Spin Multip -licity	Point grp.[c]	E°	Converg.[d] (×10^{-8})	<S^2>	ΔE_U(S–T)	ΔE_{S-T}	J
1$_2$	UM062X/def2TZVP	Triplet	0	3	C_1	-2407.25944803	0.22	2.0387	0.000489458	0.0009979	0.251
		BS-singlet	0	1	C_1	-2407.25944725	0.22	1.0387			
	UB3LYP/Def2TZVP	Triplet	0	3	C_1	-2408.23995907	0.51	2.0332	0.000489458	0.0009952	0.251
		BS-singlet	0	1	C_1	-2408.23995829	0.27	1.0332			
1	UM062X/def2TZVP	Doublet	0	2	C_1	–1203.89843429	0.68	0.768	/	/	/

[a] For different energy units, 1 Hartree = 627.5095 kcal mol^{-1} = 27.2114 eV = 315774.65 K. [b] Charge. [c] Symmetry point group of the geometry. [d] The density matrix RMS convergence.

11. Thin Films

The experiments were performed with an ultra-high-vacuum BOSON-STM system operated at a low temperature of 6 K. The Au(111) single crystal was cleaned by repeated cycles of Ar^+ sputtering at 1.0 keV followed by annealing at 620 K for 7 min. Radical **1** was thermally sublimed (sublimation temperature: 108 ℃ – 127 ℃) from a K-cell evaporator onto the clean Au(111) surface kept at RT. All STM images were obtained in the constant-current modes. dI/dV spectra were acquired using lock-in detection of the tunneling current by adding a 3 mV_{peak} modulation at 613 Hz to the sample bias at the set point of 100 mV, 20 pA.

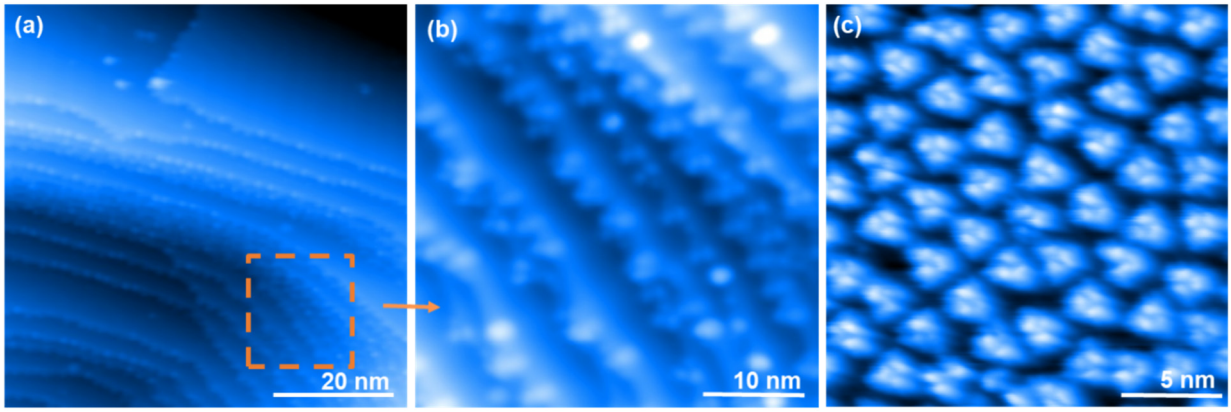

Fig. S36. Adsorption of radical **1** onto the Au(111) surface. (a–b) Deposition at 108–115 °C for 2 min: The (a) overview and (b) magnified STM images of the film (set point: (a) 200 mV, 20 pA; (b) 200 mV, 20 pA) (The orange dashed rectangle in (a) indicates the same regions in (b)); (c) Deposition at 123–127 °C for 50 s: STM image of the film (set point: 700 mV, 20 pA).

12. Routine ^{1}H NMR, ^{13}C NMR and HRMS Spectra of Compounds

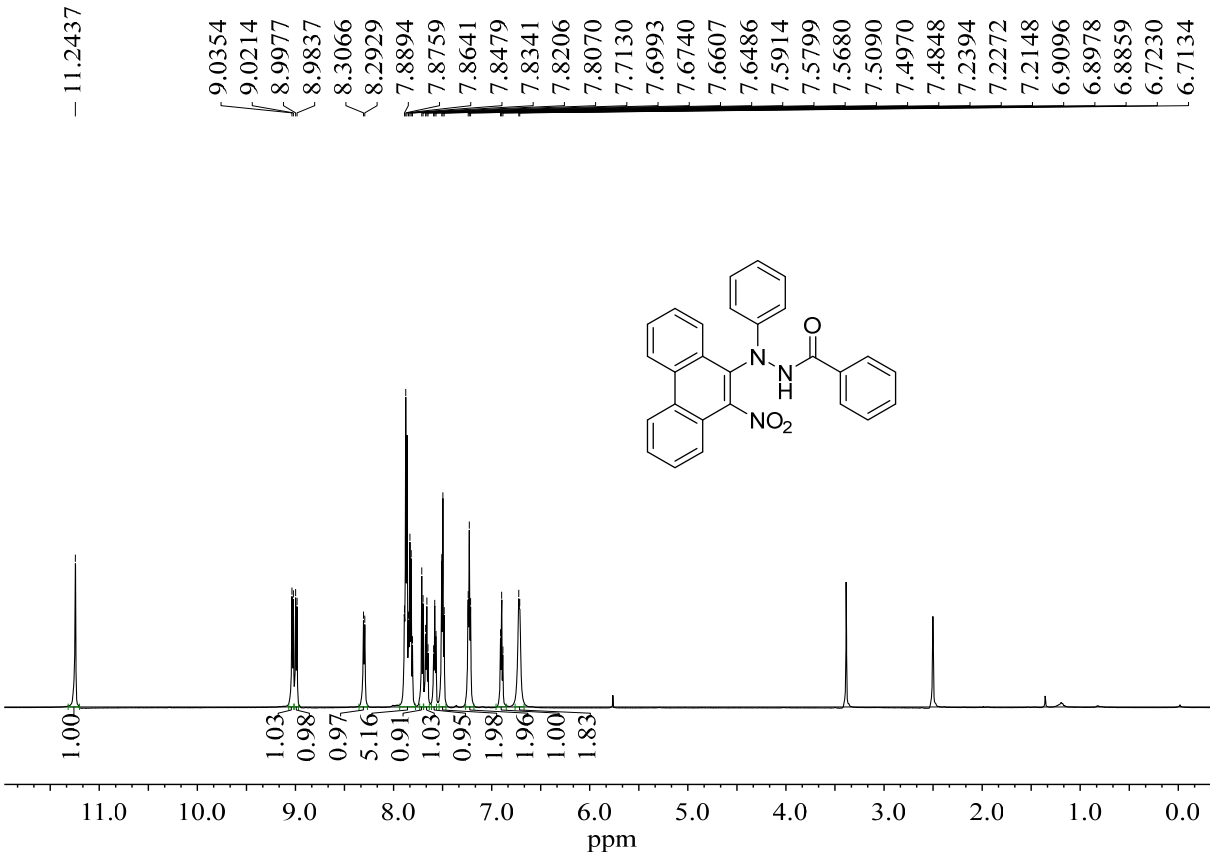

Fig. S37. ^{1}H NMR spectrum (600 MHz, 298 K, $(CD_3)_2SO$) of **12** (sample label: 5–P45–U–5).

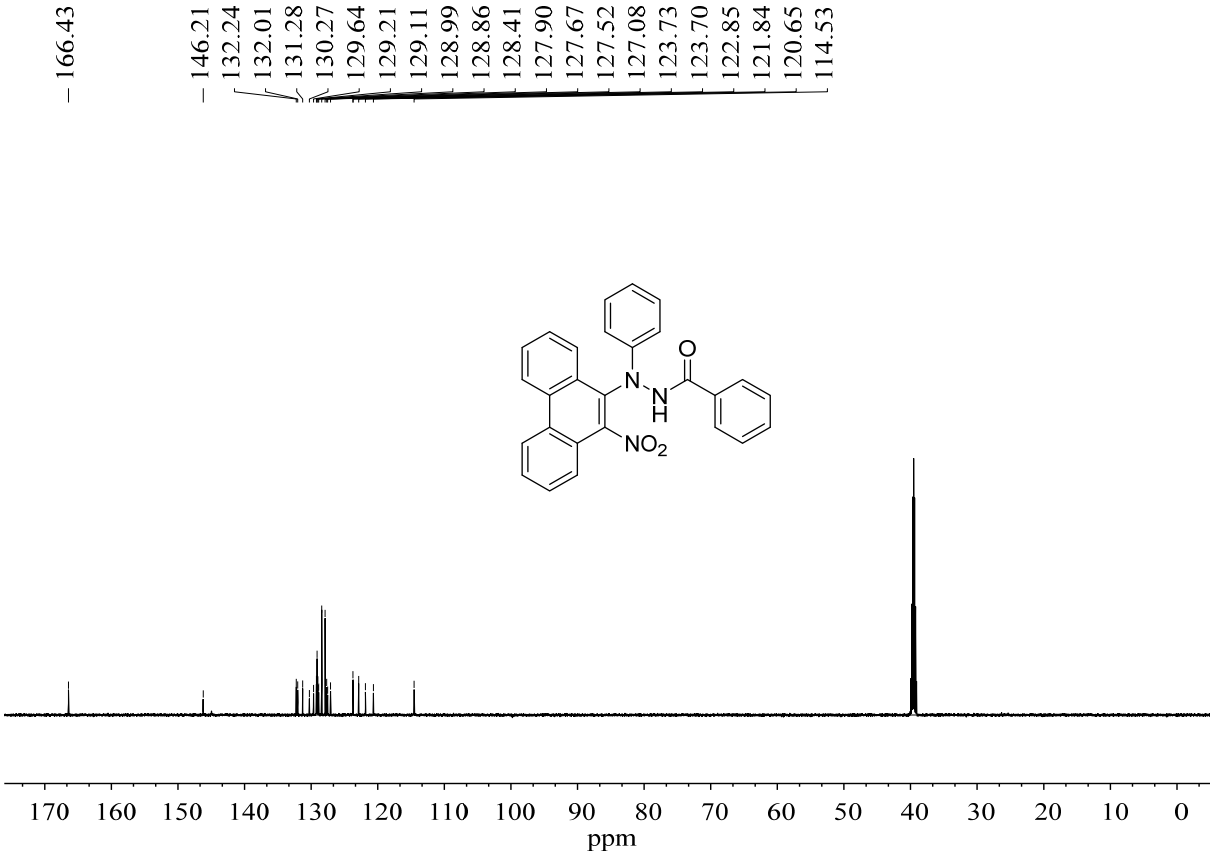

Fig. S38. ^{13}CNMR spectra (150 MHz, 298K, $(CD_3)_2SO$) of **12** (sample label: 5–P45–U–5).

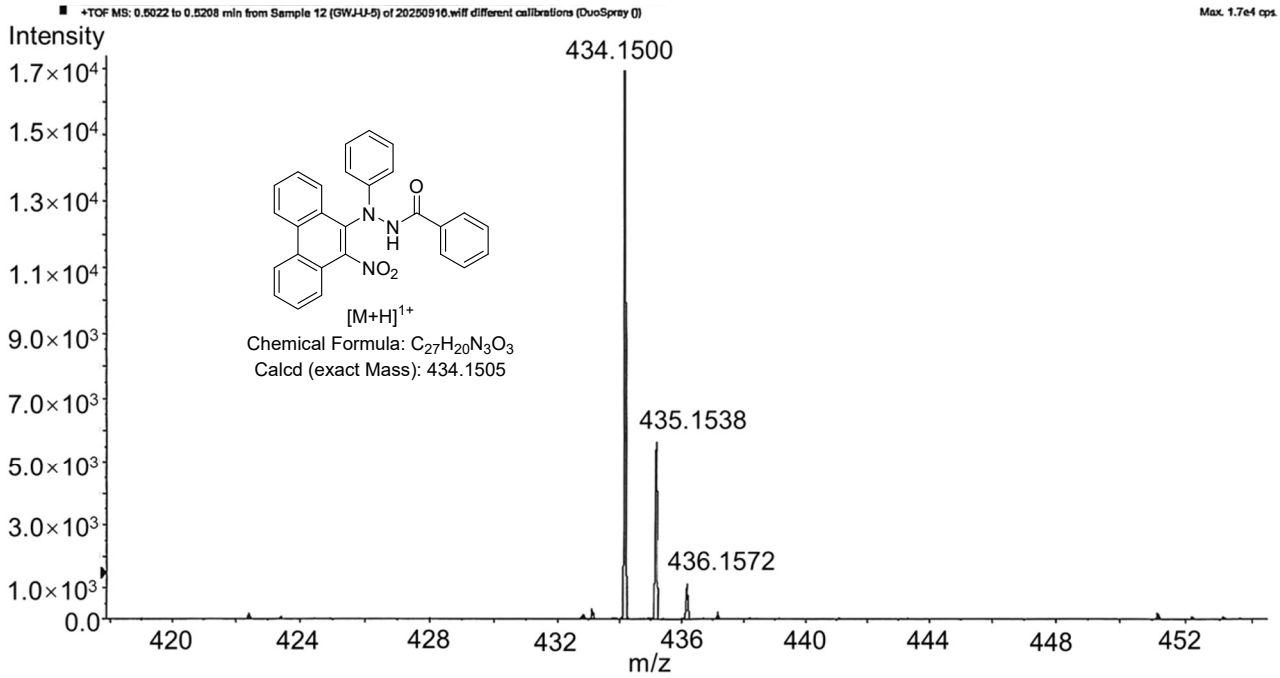

Fig. S39. HRMS (ESI−TOF) spectrum of molecular **12** (sample label: 5–P45–U–5), obtained in the positive ion mode using acetone as the mobile flow phase. $[M+H]^+$: Calcd $C_{27}H_{20}N_3O_3$ 434.1505, found 434.1500 (-1.15 ppm).

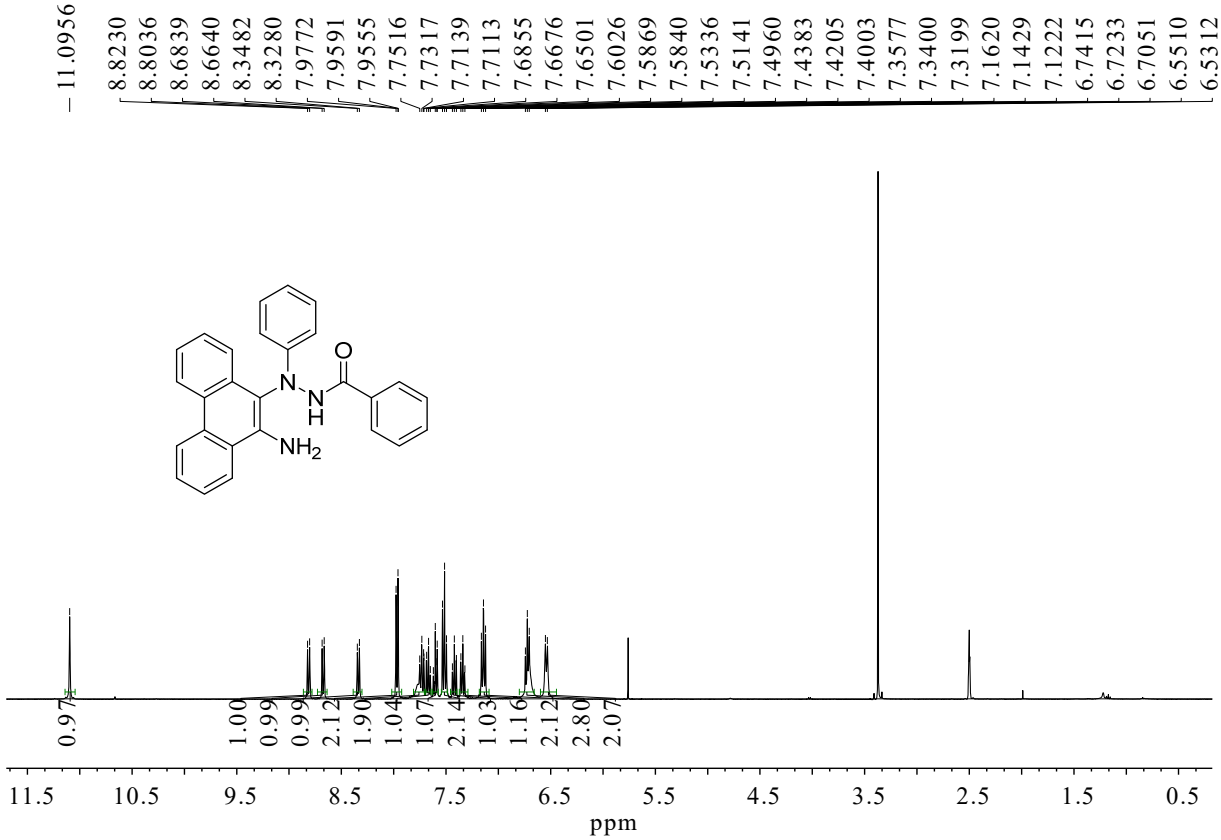

Fig. S40. ^{1}H NMR spectrum (400 MHz, 298 K, $(CD_3)_2SO$) of **13** (sample label: 4–P147–U-6).

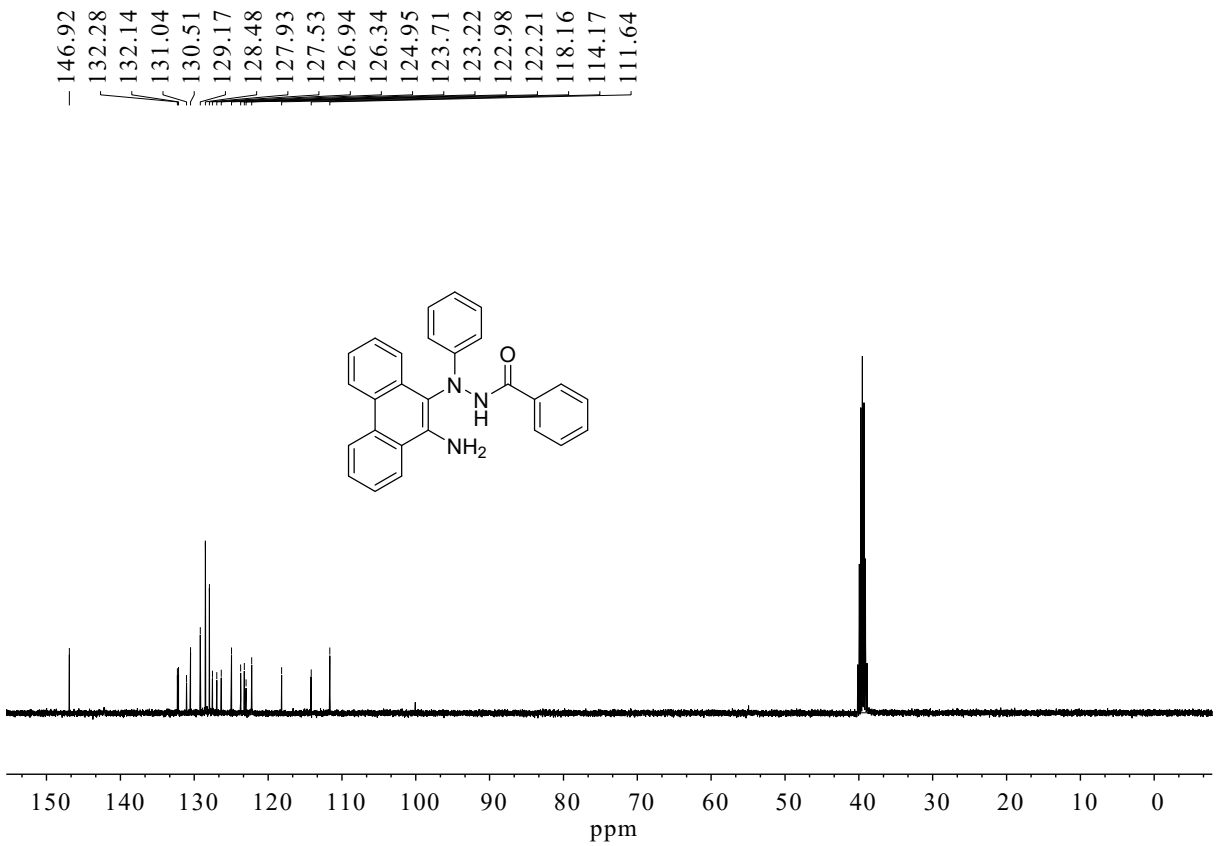

Fig. S41. ^{13}C NMR spectra (100 MHz, 298 K, $(CD_3)_2SO$) of **13** (sample label: 4–P147–U-6).

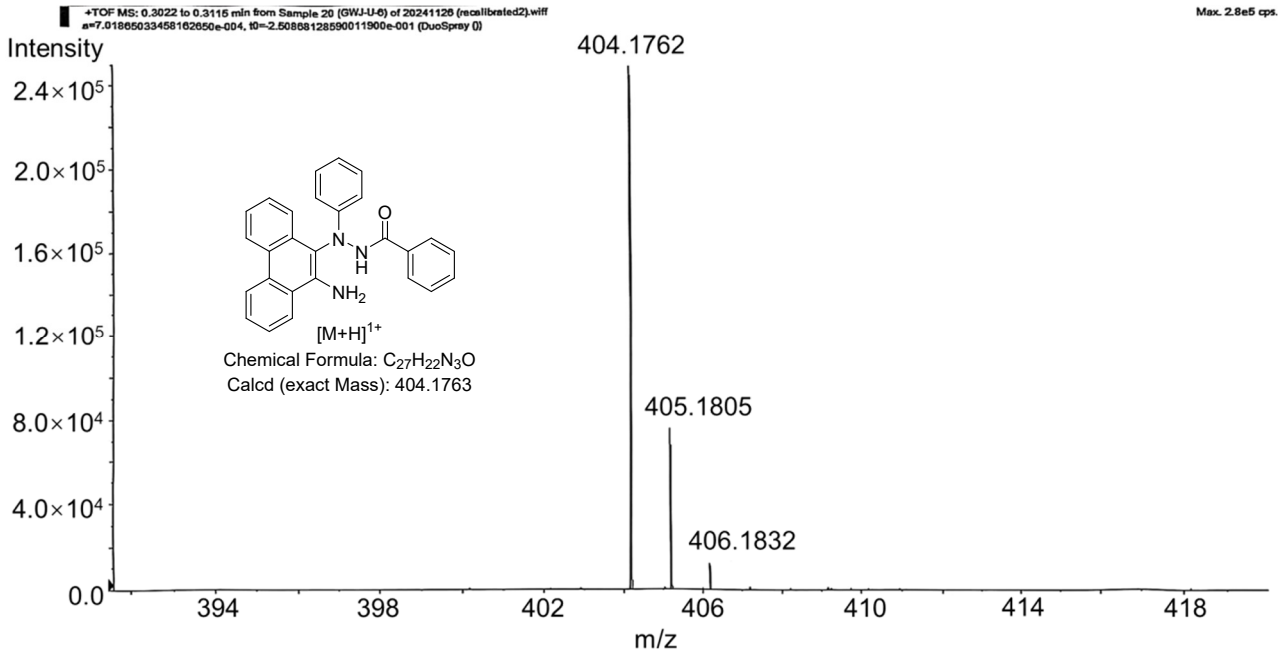

Fig. S42. HRMS (ESI−TOF) spectrum of molecular **13** (sample label: 4–P147–U-6), obtained in the positive ion mode using methanol as the mobile flow phase. $[M + H]^{1+}$: Calcd $C_{27}H_{22}N_3O$ 404.1763, found 404.1762 (-0.25 ppm).

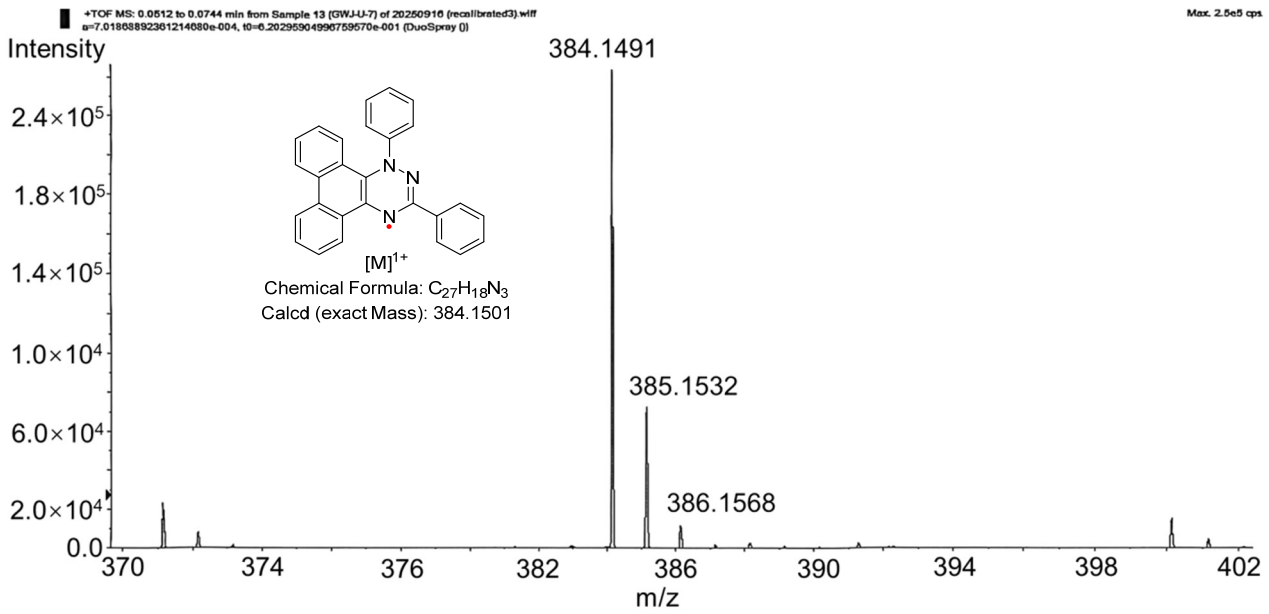

Fig. S43. HRMS (ESI−TOF) spectrum of molecular **1** (sample label: 5–P61–U-7), obtained in the positive ion mode using methanol as the mobile flow phase. $[M]^+$: Calcd: $C_{27}H_{18}N_3$ 384.1501, found 384.1491 (-2.60 ppm).

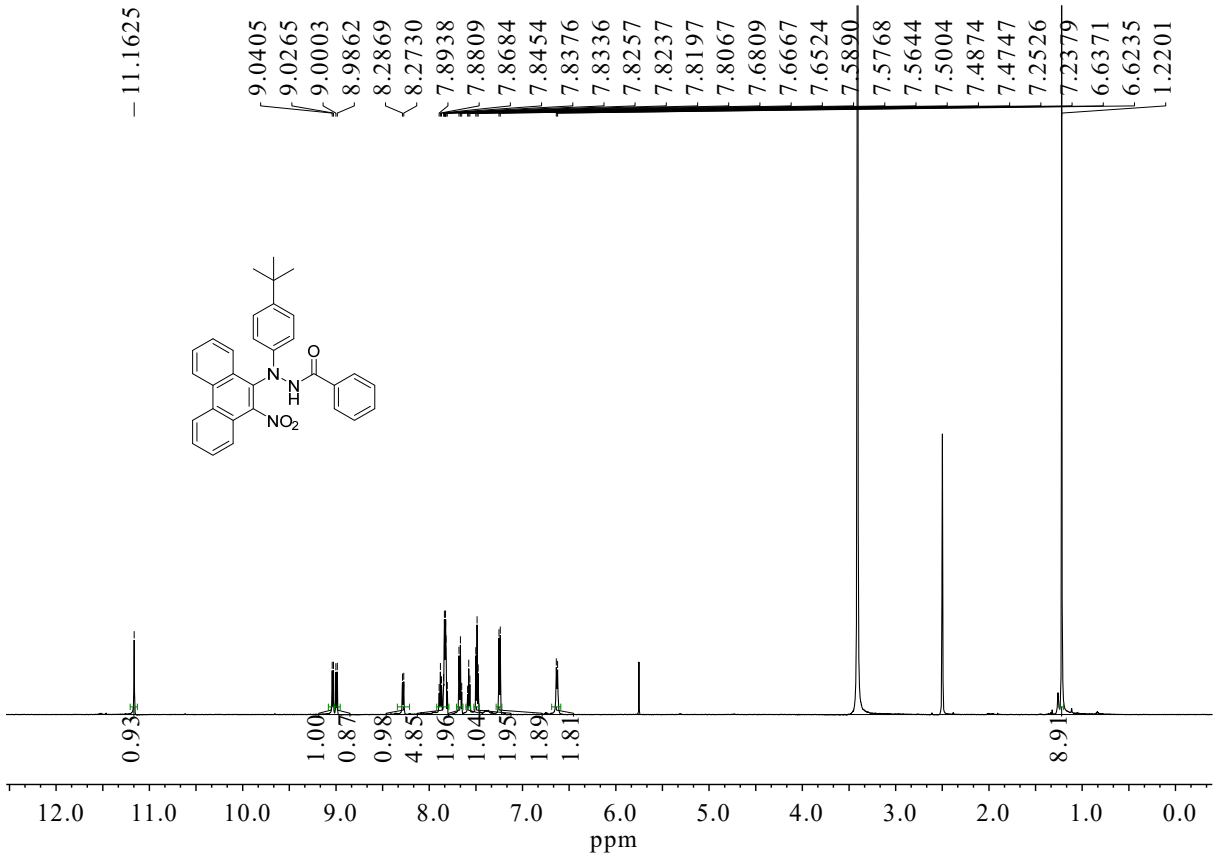

Fig. S44. ^{1}H NMR spectrum (600 MHz, 298 K, $(CD_3)_2SO$) of **15** (sample label: 5–P116–O–5).

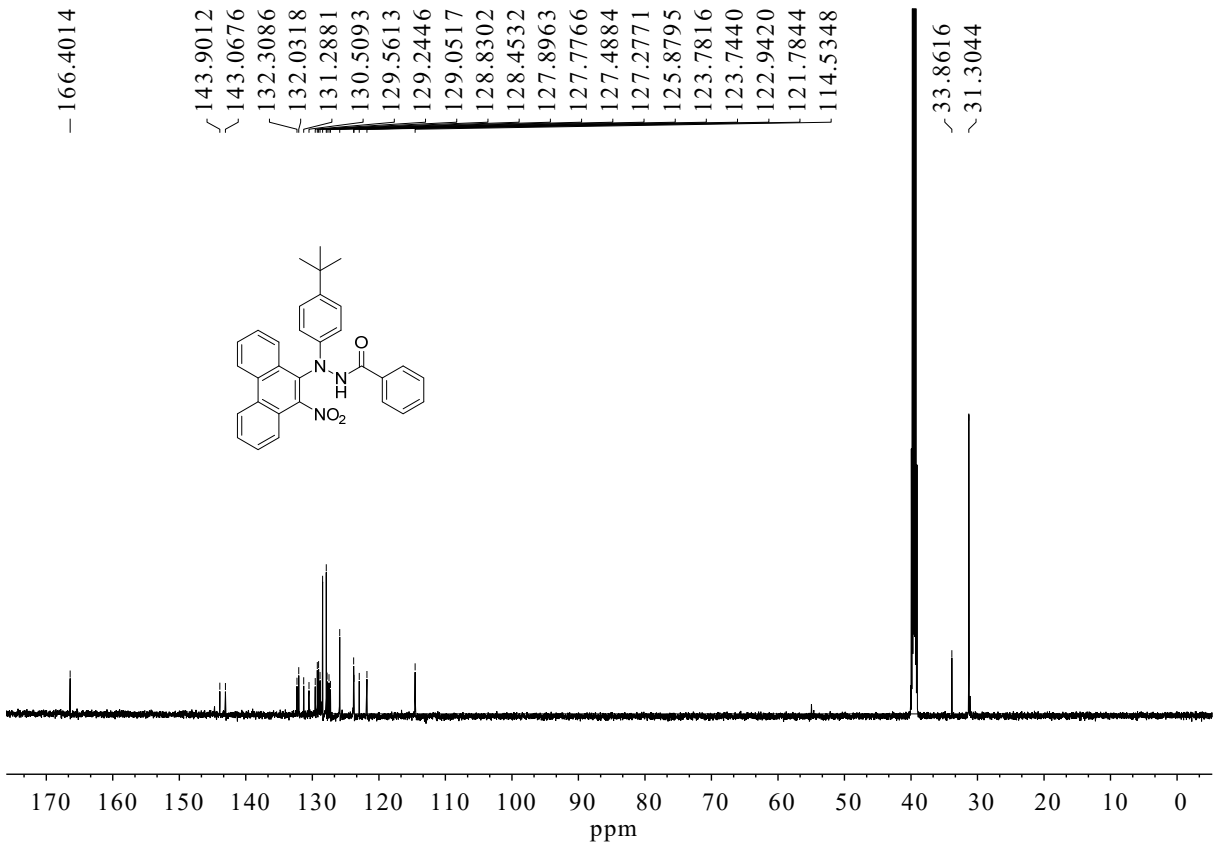

Fig. S45. ^{13}C NMR spectra (150 MHz, 298 K, $(CD_3)_2SO$) of **15** (sample label: 5–P116–O–5).

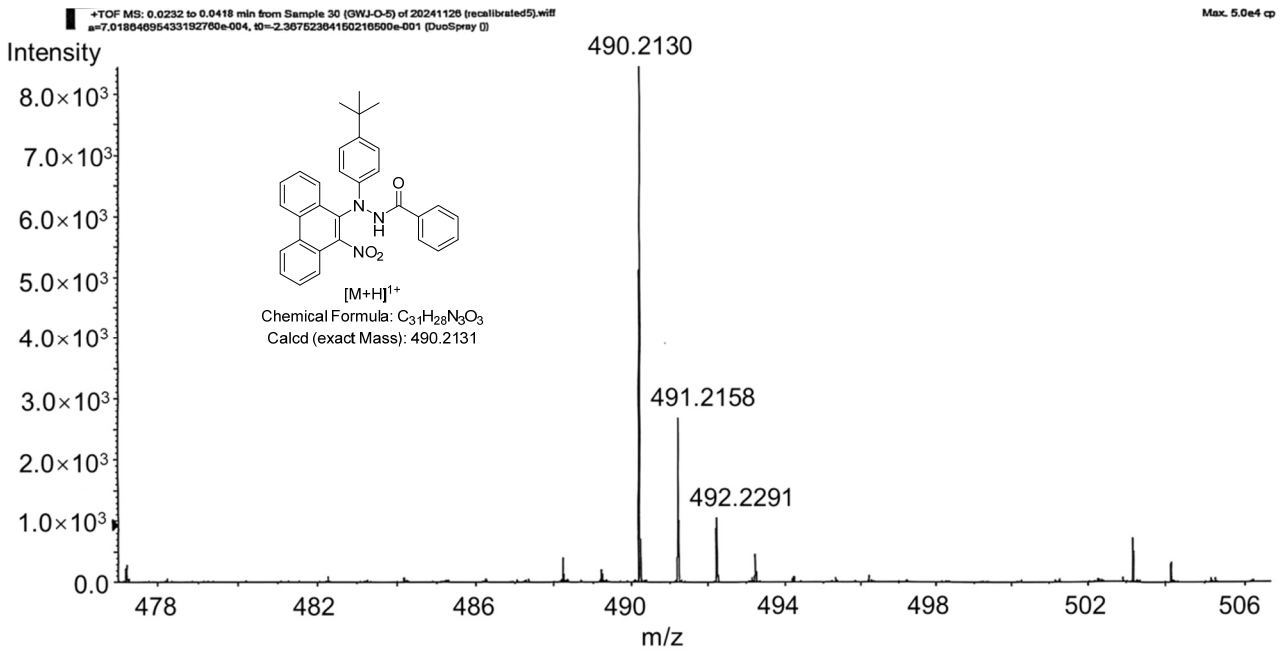

Fig. S46. HRMS (ESI−TOF) spectrum of molecular **15** (sample label: 5–P116–O–5), obtained in the positive ion mode using acetone as the mobile flow phase. $[M + H]^{1+}$: Calcd $C_{31}H_{28}N_3O_3$ 490.2131, found 490.2130 (-0.20 ppm).

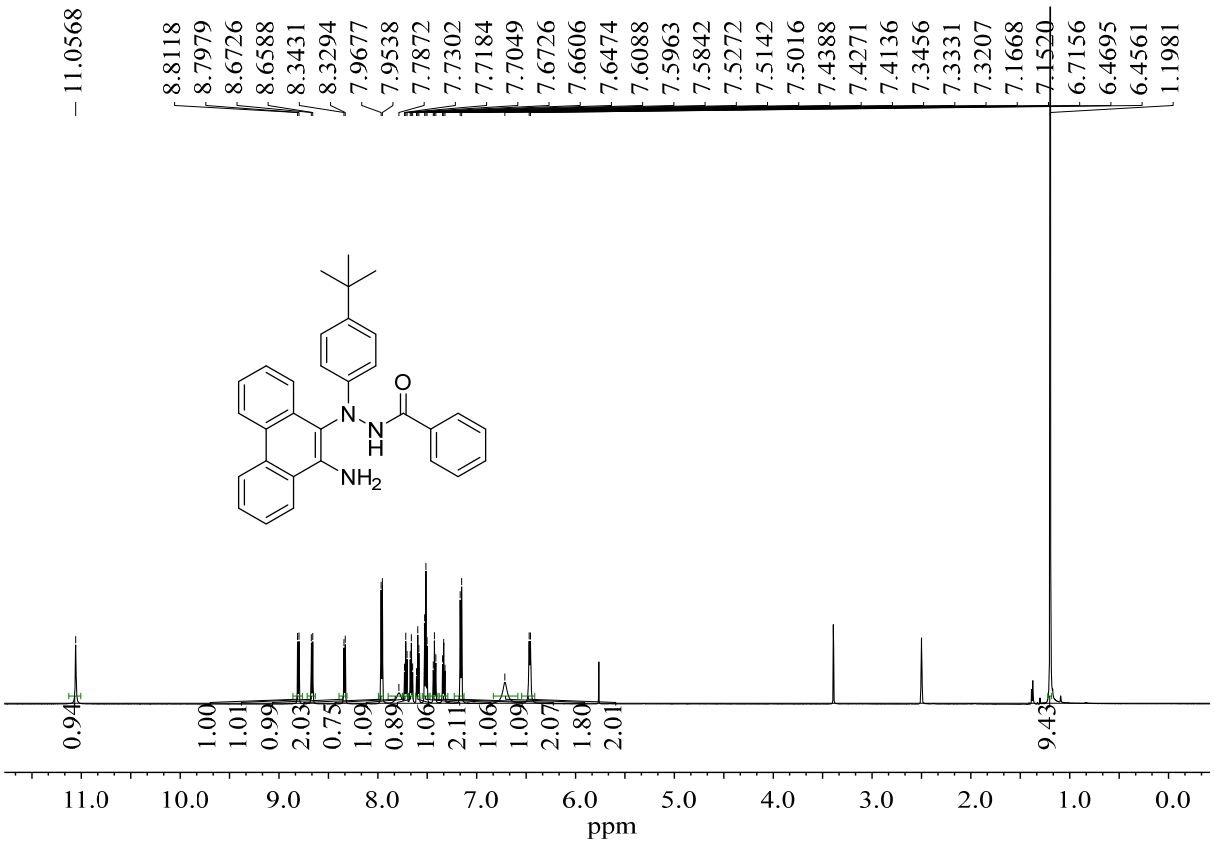

Fig. S47. ^{1}H NMR spectrum (600 MHz, 298 K, $(CD_3)_2SO$) of **16** (sample label: 6–P93–O-6).

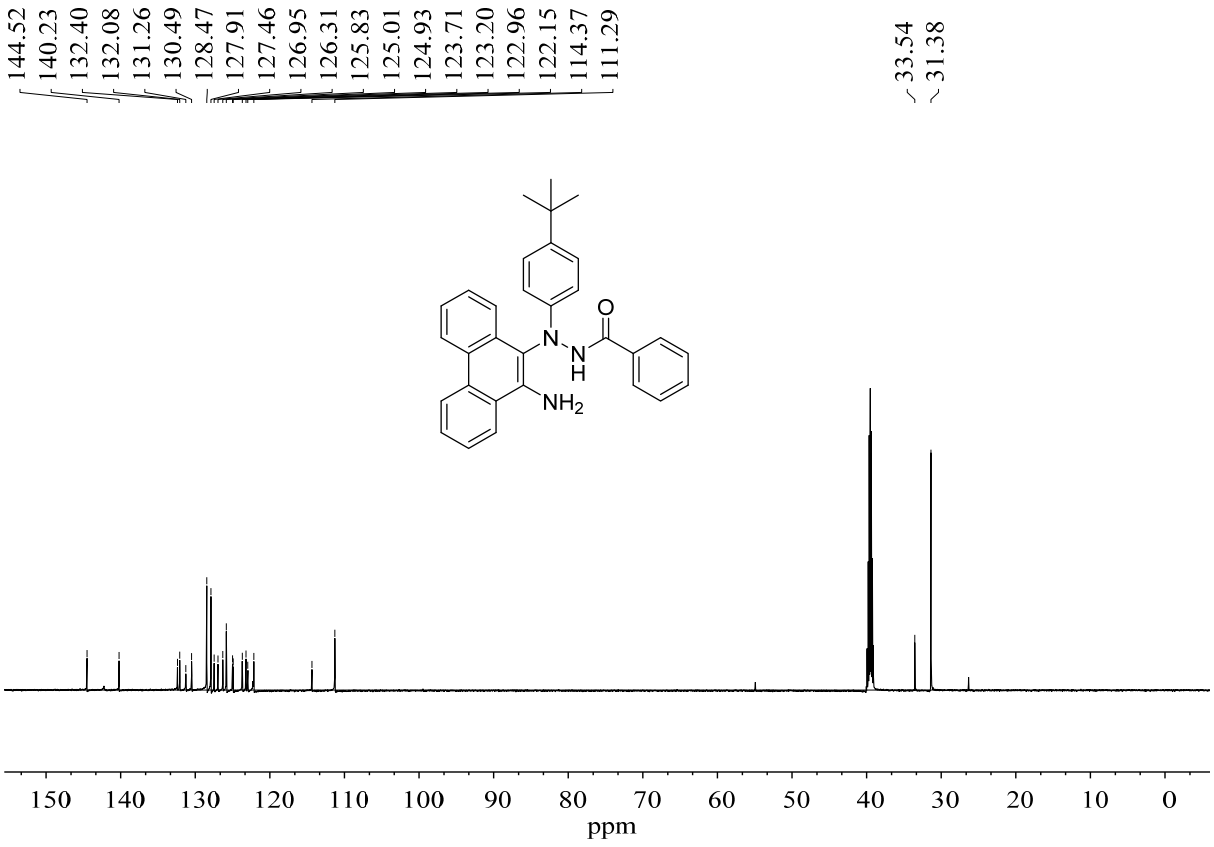

Fig. S48. ^{13}C NMR spectra (150 MHz, 298 K, $(CD_3)_2SO$) of **16** (sample label: 6–P93–O-6).

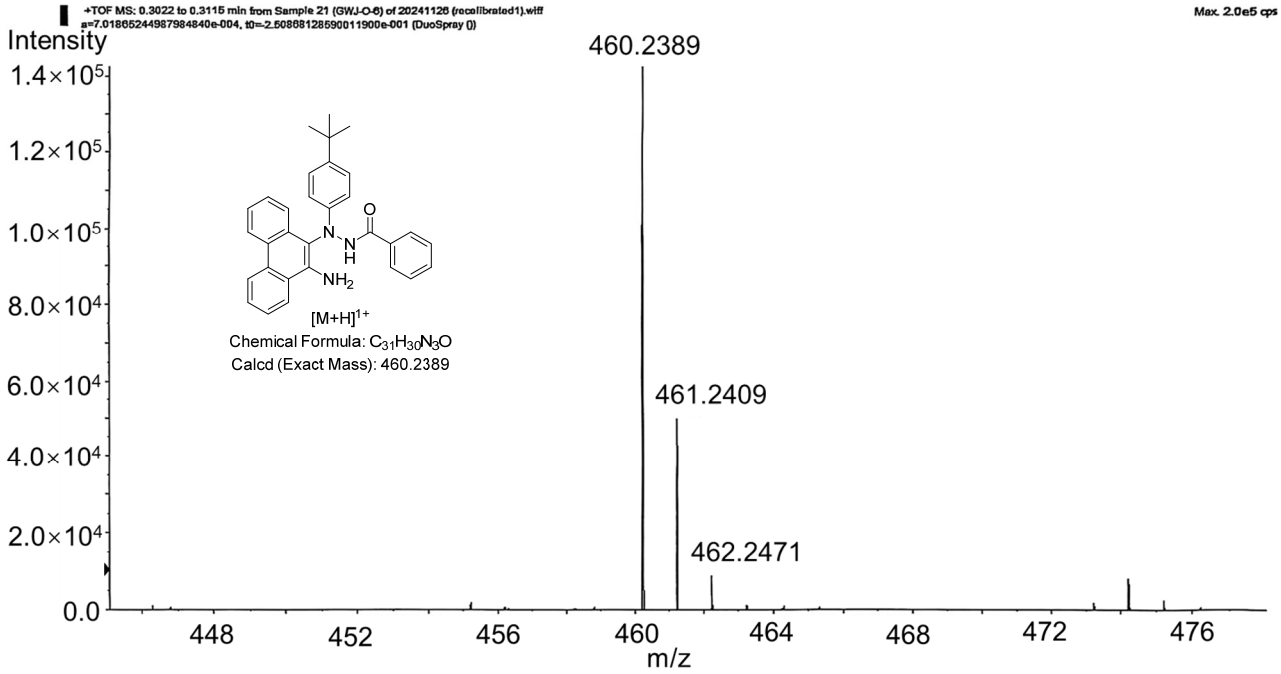

Fig. S49. HRMS (ESI−TOF) spectrum of molecular **16** (sample label: 6–P93–O-6), obtained in the positive ion mode using methanol as the mobile flow phase. $[M + H]^{1+}$: Calcd $C_{31}H_{30}N_3O$ 460.2389, found 460.2389 (0.00 ppm).

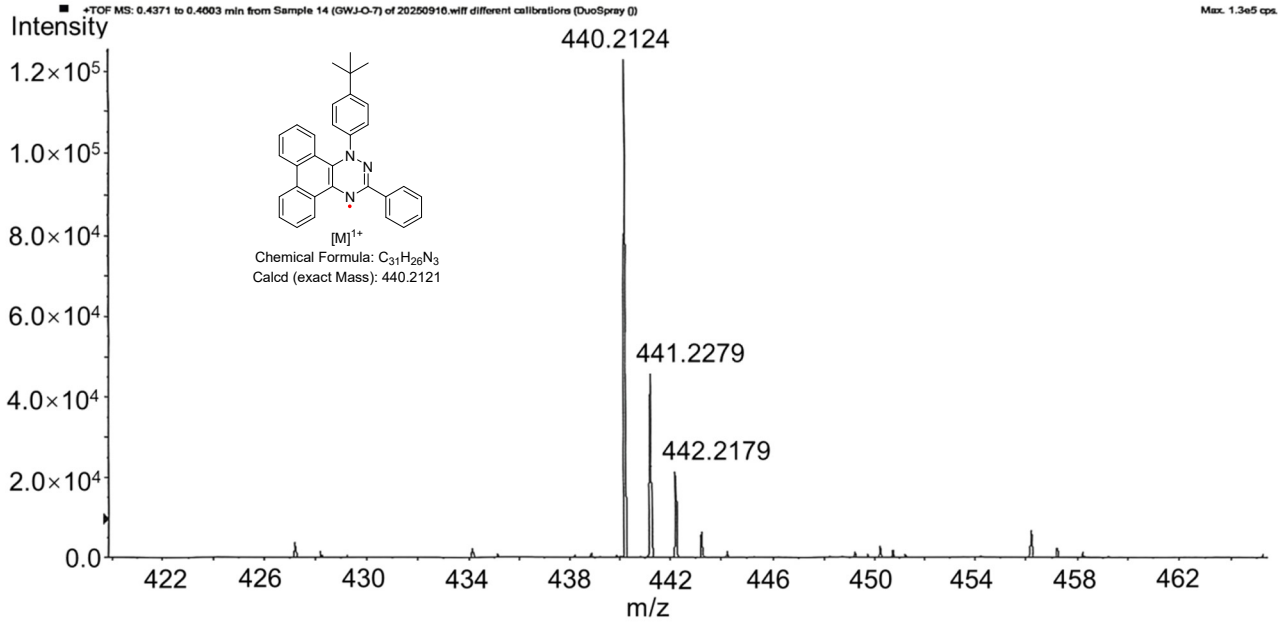

Fig. S50. HRMS (ESI−TOF) spectrum of molecular **1-*t*Bu** (sample label: 6–P101–O-7), obtained in the positive ion mode using methanol as the mobile flow phase. $[M]^{1+}$: Calcd: $C_{31}H_{26}N_3$ 440.2127, found 440.2124 (-0.681 ppm).

13. Optimized Geometries/Coordinate Outputs of DFT Calculations

Blatter (Neutral, in DCM):

Center Number	Atomic Number	Atomic Type	Coordinates (Angstroms) X	Y	Z
1	7	0	0.928448	-0.068939	0.032471
2	7	0	-0.332155	-0.541022	0.022892
3	7	0	-1.185446	1.668153	0.104798
4	6	0	-1.314351	0.350649	0.062185
5	6	0	-2.689308	-0.222969	0.064228
6	6	0	-3.790980	0.616185	-0.091632
7	6	0	-2.894107	-1.594267	0.218429
8	6	0	-4.179329	-2.114748	0.215054
9	6	0	-5.075763	0.092238	-0.097318
10	6	0	-5.274071	-1.273803	0.056354
11	6	0	1.932140	-1.084329	0.012861
12	6	0	1.812292	-2.115205	-0.911051
13	6	0	2.755510	-3.130443	-0.924513
14	6	0	3.811474	-3.115974	-0.021567
15	6	0	3.917207	-2.085078	0.903468
16	6	0	2.975928	-1.065661	0.929309
17	1	0	-3.631982	1.679234	-0.211545
18	1	0	-5.923815	0.753636	-0.223367
19	1	0	-6.277160	-1.681738	0.052487
20	1	0	-4.326905	-3.180420	0.338524
21	1	0	-2.043656	-2.250265	0.345197
22	1	0	3.039673	-0.272226	1.663112
23	1	0	4.729497	-2.077562	1.619161
24	1	0	4.547479	-3.909883	-0.034752
25	1	0	2.665847	-3.932030	-1.646569
26	1	0	0.983337	-2.112575	-1.606409
27	6	0	0.311293	3.537252	-0.001380
28	6	0	1.587132	4.043505	-0.123780
29	6	0	2.677446	3.175031	-0.227655
30	6	0	0.091458	2.153216	0.035248
31	6	0	1.207644	1.287856	-0.028721
32	6	0	2.496554	1.806365	-0.184856
33	1	0	3.344478	1.144158	-0.280940
34	1	0	3.676503	3.573498	-0.347129
35	1	0	1.745363	5.113719	-0.153080
36	1	0	-0.553609	4.186190	0.056194

Blatter (Neutral, Gas Phase):

Center Number	Atomic Number	Atomic Type	Coordinates (Angstroms) X	Y	Z
1	7	0	0.925218	-0.077964	-0.023202
2	7	0	-0.333771	-0.555746	-0.039626
3	7	0	-1.186136	1.650363	0.145759
4	6	0	-1.315700	0.335706	0.050049
5	6	0	-2.690470	-0.232901	0.054312
6	6	0	-3.789242	0.622715	0.062136
7	6	0	-2.896352	-1.611317	0.050449
8	6	0	-4.183598	-2.124214	0.051640
9	6	0	-5.075665	0.105830	0.063356
10	6	0	-5.276761	-1.267654	0.057492
11	6	0	1.935023	-1.081463	0.002465
12	6	0	1.817370	-2.178866	-0.840996
13	6	0	2.777342	-3.176957	-0.797514
14	6	0	3.846157	-3.085628	0.084166
15	6	0	3.947439	-1.992617	0.933932
16	6	0	2.991092	-0.989940	0.901117
17	1	0	-3.617516	1.690005	0.067760
18	1	0	-5.924398	0.777588	0.068598
19	1	0	-6.281965	-1.669479	0.058903
20	1	0	-4.334831	-3.195980	0.050391
21	1	0	-2.040653	-2.272016	0.051315
22	1	0	3.048076	-0.148664	1.579231
23	1	0	4.766134	-1.924854	1.638261
24	1	0	4.592807	-3.868092	0.115816
25	1	0	2.689931	-4.029864	-1.457797
26	1	0	0.971230	-2.237582	-1.511499
27	6	0	0.298979	3.524795	0.031685
28	6	0	1.565679	4.038504	-0.133725
29	6	0	2.652518	3.177988	-0.307257
30	6	0	0.083178	2.139162	0.044752
31	6	0	1.199140	1.281275	-0.078771
32	6	0	2.477262	1.808484	-0.284492
33	1	0	3.318952	1.149573	-0.438767
34	1	0	3.643172	3.582732	-0.466220
35	1	0	1.719141	5.109346	-0.145542
36	1	0	-0.567592	4.163296	0.140264

Blatter (Cation, Gas Phase):

Center Number	Atomic Number	Atomic Type	Coordinates (Angstroms) X	Y	Z
1	7	0	0.890663	-0.066883	-0.029106
2	7	0	-0.309444	-0.534462	0.005030
3	7	0	-1.173402	1.652740	0.069341
4	6	0	-1.341947	0.339196	0.030898
5	6	0	-2.691310	-0.236377	0.045416
6	6	0	-3.797391	0.615562	0.052943
7	6	0	-2.875017	-1.620921	0.052610
8	6	0	-4.155769	-2.143996	0.066438
9	6	0	-5.074200	0.083475	0.066630
10	6	0	-5.254744	-1.294217	0.073365
11	6	0	1.932744	-1.078681	-0.003787
12	6	0	1.909697	-2.069819	-0.969385
13	6	0	2.888918	-3.049710	-0.924122
14	6	0	3.846510	-3.033559	0.081721
15	6	0	3.835688	-2.038432	1.050857
16	6	0	2.872897	-1.042872	1.013424
17	1	0	-3.647990	1.686104	0.048905
18	1	0	-5.931470	0.742875	0.072555
19	1	0	-6.255267	-1.706423	0.085283
20	1	0	-4.298710	-3.215974	0.074069
21	1	0	-2.019202	-2.281148	0.053007
22	1	0	2.836953	-0.269781	1.770608
23	1	0	4.570837	-2.041044	1.844052
24	1	0	4.602730	-3.806532	0.115604
25	1	0	2.899831	-3.828719	-1.674289
26	1	0	1.145281	-2.067396	-1.735249
27	6	0	0.288138	3.536449	0.008480
28	6	0	1.556014	4.008784	-0.113270
29	6	0	2.660166	3.120400	-0.253737
30	6	0	0.063235	2.133736	0.006665
31	6	0	1.187209	1.258288	-0.080485
32	6	0	2.497315	1.768589	-0.237519
33	1	0	3.336240	1.100325	-0.359336
34	1	0	3.651788	3.533084	-0.383835
35	1	0	1.738873	5.075093	-0.122131
36	1	0	-0.573530	4.184405	0.091051

Blatter (Anion, Gas Phase):

Center Number	Atomic Number	Atomic Type	Coordinates (Angstroms) X	Y	Z
1	7	0	-0.970046	-0.108384	0.150035
2	7	0	0.351264	-0.547724	0.377806
3	7	0	1.088705	1.519192	-0.573704
4	6	0	1.247815	0.279857	-0.092477
5	6	0	2.655341	-0.231406	-0.034414
6	6	0	3.709441	0.587471	-0.430304
7	6	0	2.936767	-1.525691	0.400748
8	6	0	4.243759	-1.986096	0.448312
9	6	0	5.017880	0.123486	-0.390969
10	6	0	5.291939	-1.163184	0.051561
11	6	0	-1.924958	-1.077076	0.005435
12	6	0	-1.624389	-2.423058	0.304888
13	6	0	-2.576811	-3.413129	0.141469
14	6	0	-3.852797	-3.127839	-0.329950
15	6	0	-4.146871	-1.806703	-0.653449
16	6	0	-3.215941	-0.797875	-0.492857
17	1	0	3.470198	1.587655	-0.765320
18	1	0	5.828084	0.771447	-0.704489
19	1	0	6.312888	-1.524634	0.085536
20	1	0	4.446995	-2.993465	0.792304
21	1	0	2.109844	-2.156550	0.697649
22	1	0	-3.468924	0.209872	-0.786936
23	1	0	-5.123304	-1.552471	-1.050727
24	1	0	-4.591011	-3.909127	-0.454415
25	1	0	-2.311156	-4.434850	0.390369
26	1	0	-0.634321	-2.658066	0.662119
27	6	0	-0.331398	3.458554	-0.338817
28	6	0	-1.517382	4.037706	0.096570
29	6	0	-2.517721	3.253279	0.649378
30	6	0	-0.124784	2.076547	-0.264271
31	6	0	-1.196453	1.282187	0.209530
32	6	0	-2.341251	1.869929	0.720485
33	1	0	-3.114646	1.245115	1.147882
34	1	0	-3.433236	3.699061	1.017109
35	1	0	-1.651275	5.110607	0.017368
36	1	0	0.477286	4.062079	-0.732613

1 (Neutral, in DCM):

Center	Atomic	Atomic	Coordinates (Angstroms)

1 (Neutral, Gas Phase):

Center	Atomic	Atomic	Coordinates (Angstroms)

Number	Number	Type	X	Y	Z
1	6	0	2.634277	-4.473441	0.783938
2	6	0	3.173759	-3.268500	0.392642
3	6	0	1.249146	-4.619541	0.911093
4	6	0	0.425596	-3.547508	0.658516
5	6	0	0.963616	-2.308978	0.273874
6	6	0	2.354507	-2.159662	0.117622
7	6	0	2.890328	-0.890024	-0.365983
8	6	0	2.030234	0.219489	-0.536434
9	6	0	0.641313	0.079723	-0.161838
10	6	0	0.085293	-1.167050	0.090276
11	6	0	4.239387	-0.753260	-0.732603
12	6	0	2.535161	1.391025	-1.135724
13	7	0	-0.236115	1.151686	-0.097992
14	7	0	-1.576421	0.960493	-0.202336
15	7	0	-1.250512	-1.346029	0.191466
16	6	0	-2.006135	-0.274348	-0.068400
17	6	0	-3.477356	-0.469426	-0.185094
18	6	0	-4.007224	-1.757805	-0.211319
19	6	0	-4.338870	0.624807	-0.268358
20	6	0	-5.706838	0.430244	-0.376561
21	6	0	-5.377211	-1.949597	-0.321584
22	6	0	-6.230543	-0.857258	-0.403703
23	6	0	0.128152	2.464905	0.315672
24	6	0	1.079050	2.634572	1.315597
25	6	0	1.421153	3.917019	1.716734
26	6	0	0.814179	5.021604	1.132242
27	6	0	-0.147577	4.838432	0.145393
28	6	0	-0.496384	3.561495	-0.267318
29	1	0	-3.338403	-2.605559	-0.149153
30	1	0	-5.778265	-2.955065	-0.343670
31	1	0	-7.299713	-1.007711	-0.487442
32	1	0	-6.367568	1.286054	-0.435760
33	1	0	-3.932021	1.626690	-0.241790
34	1	0	-1.239734	3.406297	-1.037646
35	1	0	-0.626838	5.694610	-0.312091
36	1	0	1.084959	6.020796	1.448206
37	1	0	2.160336	4.050145	2.496346
38	1	0	1.541075	1.771095	1.776952
39	6	0	3.856723	1.487914	-1.500225
40	6	0	4.723108	0.414466	-1.276810
41	1	0	4.247709	-3.187399	0.304013
42	1	0	3.288504	-5.310434	0.993420
43	1	0	0.828460	-5.569471	1.215638
44	1	0	-0.646733	-3.635962	0.765178
45	1	0	5.766451	0.488484	-1.555716
46	1	0	4.917122	-1.585882	-0.612159
47	1	0	4.219546	2.393890	-1.968676
48	1	0	1.875379	2.220588	-1.343473

Number	Number	Type	X	Y	Z
1	6	0	2.633269	-4.462899	0.808824
2	6	0	3.171043	-3.264384	0.399139
3	6	0	1.250028	-4.604195	0.952678
4	6	0	0.426723	-3.533383	0.698807
5	6	0	0.964931	-2.302492	0.295374
6	6	0	2.352385	-2.157223	0.120375
7	6	0	2.883224	-0.893749	-0.382424
8	6	0	2.024100	0.218221	-0.541065
9	6	0	0.642015	0.084652	-0.143467
10	6	0	0.084831	-1.161238	0.113310
11	6	0	4.222461	-0.764170	-0.781221
12	6	0	2.521095	1.383225	-1.158085
13	7	0	-0.236659	1.157421	-0.072916
14	7	0	-1.576019	0.965513	-0.183895
15	7	0	-1.246744	-1.341452	0.217487
16	6	0	-2.002923	-0.271076	-0.052088
17	6	0	-3.469326	-0.472538	-0.184115
18	6	0	-3.989226	-1.763705	-0.210758
19	6	0	-4.333730	0.616048	-0.286189
20	6	0	-5.697604	0.412698	-0.415246
21	6	0	-5.355090	-1.963892	-0.342264
22	6	0	-6.212244	-0.877450	-0.445099
23	6	0	0.129369	2.468705	0.332947
24	6	0	1.138028	2.650368	1.273282
25	6	0	1.478929	3.933794	1.667457
26	6	0	0.814858	5.032244	1.138430
27	6	0	-0.203560	4.839025	0.213971
28	6	0	-0.552718	3.560909	-0.191366
29	1	0	-3.309670	-2.600729	-0.129779
30	1	0	-5.750726	-2.971094	-0.365096
31	1	0	-7.278593	-1.034552	-0.546459
32	1	0	-6.363158	1.263087	-0.489688
33	1	0	-3.926218	1.617163	-0.256850
34	1	0	-1.344838	3.393706	-0.907253
35	1	0	-0.729661	5.689707	-0.199296
36	1	0	1.084103	6.032464	1.450425
37	1	0	2.261545	4.072957	2.401670
38	1	0	1.646768	1.791611	1.690693
39	6	0	3.834041	1.472793	-1.551378
40	6	0	4.699766	0.397089	-1.342951
41	1	0	4.244116	-3.184763	0.303013
42	1	0	3.287677	-5.298606	1.021041
43	1	0	0.831264	-5.549475	1.272391
44	1	0	-0.645227	-3.606665	0.817355
45	1	0	5.735960	0.463888	-1.647347
46	1	0	4.895744	-1.602188	-0.677409
47	1	0	4.189498	2.374445	-2.032551
48	1	0	1.859324	2.214406	-1.350860

1 (Cation, Gas Phase):

Center Number	Atomic Number	Atomic Type	Coordinates (Angstroms) X	Y	Z
1	6	0	2.503992	-4.538510	0.761103
2	6	0	3.075289	-3.323650	0.439102
3	6	0	1.118197	-4.692945	0.777933
4	6	0	0.312678	-3.613057	0.497313
5	6	0	0.885507	-2.374248	0.187945
6	6	0	2.279512	-2.216598	0.127541
7	6	0	2.850916	-0.936620	-0.314214
8	6	0	2.038169	0.209254	-0.471227
9	6	0	0.628986	0.078188	-0.146154
10	6	0	0.030332	-1.218241	-0.001962
11	6	0	4.202208	-0.838352	-0.661491
12	6	0	2.584020	1.375180	-1.037224
13	7	0	-0.224507	1.095839	0.046519
14	7	0	-1.533958	0.970737	0.067292
15	7	0	-1.273764	-1.351388	0.029848
16	6	0	-2.037822	-0.253177	-0.034046
17	6	0	-3.495123	-0.386650	-0.145088
18	6	0	-4.060475	-1.654596	-0.283691
19	6	0	-4.314285	0.744254	-0.121940
20	6	0	-5.685221	0.602355	-0.235185
21	6	0	-5.433132	-1.787880	-0.399899
22	6	0	-6.245793	-0.661879	-0.374706
23	6	0	0.202607	2.452344	0.339450
24	6	0	1.083882	2.655092	1.387525
25	6	0	1.471594	3.952880	1.677221
26	6	0	0.982788	5.012001	0.922043
27	6	0	0.087879	4.782725	-0.115041
28	6	0	-0.320832	3.490843	-0.409384
29	1	0	-3.421589	-2.526437	-0.300119
30	1	0	-5.871041	-2.770856	-0.509570
31	1	0	-7.319122	-0.769213	-0.463227
32	1	0	-6.320019	1.477844	-0.213766
33	1	0	-3.875058	1.725639	-0.007367
34	1	0	-1.023326	3.287255	-1.206419
35	1	0	-0.298063	5.610360	-0.694464
36	1	0	1.293290	6.022831	1.150288
37	1	0	2.151680	4.136704	2.497692
38	1	0	1.455769	1.817817	1.963998
39	6	0	3.913029	1.433857	-1.383842
40	6	0	4.731632	0.326639	-1.173381
41	1	0	4.151802	-3.242919	0.441846
42	1	0	3.142013	-5.378689	1.001991
43	1	0	0.679635	-5.650361	1.023822

1 (Anion, Gas Phase):

Center Number	Atomic Number	Atomic Type	Coordinates (Angstroms) X	Y	Z
1	6	0	2.990432	-4.099942	1.102514
2	6	0	3.418794	-2.964632	0.456117
3	6	0	1.644979	-4.235853	1.469289
4	6	0	0.759285	-3.225574	1.184550
5	6	0	1.183243	-2.053650	0.534347
6	6	0	2.533633	-1.913126	0.147098
7	6	0	2.954947	-0.715263	-0.560542
8	6	0	2.014135	0.330882	-0.750625
9	6	0	0.697772	0.200762	-0.223643
10	6	0	0.228059	-0.987145	0.292089
11	6	0	4.249270	-0.555093	-1.082686
12	6	0	2.413514	1.487738	-1.460230
13	7	0	-0.259872	1.243004	-0.298240
14	7	0	-1.568090	0.830327	-0.653997
15	7	0	-1.094042	-1.202952	0.512836
16	6	0	-1.887940	-0.317646	-0.123946
17	6	0	-3.313563	-0.730533	-0.320930
18	6	0	-3.731592	-2.007191	0.043532
19	6	0	-4.246440	0.154722	-0.860009
20	6	0	-5.565422	-0.232270	-1.037645
21	6	0	-5.054155	-2.393230	-0.129352
22	6	0	-5.976294	-1.509166	-0.672134
23	6	0	-0.146677	2.439405	0.365166
24	6	0	1.025646	2.797269	1.058863
25	6	0	1.127727	4.032092	1.676732
26	6	0	0.087544	4.951942	1.637230
27	6	0	-1.078510	4.595072	0.967172
28	6	0	-1.206839	3.367609	0.344449
29	1	0	-2.995934	-2.681972	0.459837
30	1	0	-5.365268	-3.390062	0.159746
31	1	0	-7.007950	-1.810705	-0.808404
32	1	0	-6.278862	0.466089	-1.458961
33	1	0	-3.911247	1.144583	-1.138943
34	1	0	-2.119326	3.095086	-0.163290
35	1	0	-1.912706	5.286866	0.931262
36	1	0	0.178965	5.915194	2.121844
37	1	0	2.041863	4.272759	2.207407
38	1	0	1.845374	2.096769	1.124388
39	6	0	3.684110	1.605837	-1.963290
40	6	0	4.618486	0.578279	-1.770954
41	1	0	4.463769	-2.882484	0.190828
42	1	0	3.697764	-4.889068	1.327835
43	1	0	1.308064	-5.131924	1.976247

44	1	0	-0.764361	-3.698430	0.528551
45	1	0	5.779373	0.367016	-1.440650
46	1	0	4.846612	-1.698688	-0.566210
47	1	0	4.312815	2.334415	-1.829201
48	1	0	1.961984	2.234150	-1.235018

44	1	0	-0.286463	-3.289834	1.454541
45	1	0	5.622102	0.671163	-2.166306
46	1	0	4.977385	-1.345712	-0.961141
47	1	0	3.964101	2.496452	-2.513036
48	1	0	1.687523	2.276367	-1.607002

1-*t*Bu (Neutral, in DCM):

Center Number	Atomic Number	Atomic Type	Coordinates (Angstroms) X	Y	Z
1	6	0	-4.361832	-3.903460	1.193557
2	6	0	-3.113246	-4.076471	0.638995
3	6	0	-4.888284	-2.618824	1.362879
4	6	0	-4.144827	-1.523997	0.989116
5	6	0	-2.863197	-1.685538	0.437896
6	6	0	-2.337444	-2.975505	0.235419
7	6	0	-1.042074	-3.126938	-0.422482
8	6	0	-0.260551	-1.984391	-0.711122
9	6	0	-0.745272	-0.691591	-0.284680
10	6	0	-2.058754	-0.516837	0.128400
11	6	0	-0.574437	-4.382263	-0.845937
12	6	0	0.919347	-2.134223	-1.467340
13	7	0	0.028416	0.458048	-0.327342
14	7	0	-0.551052	1.685135	-0.377559
15	7	0	-2.603543	0.711304	0.271974
16	6	0	-1.834502	1.740411	-0.098981
17	6	0	-2.465189	3.086935	-0.174225
18	6	0	-3.830138	3.225516	0.068473
19	6	0	-1.710663	4.217397	-0.490428
20	6	0	-2.314142	5.463402	-0.559439
21	6	0	-4.431496	4.474234	-0.000513
22	6	0	-3.676163	5.596240	-0.314710
23	6	0	1.431082	0.486445	-0.086236
24	6	0	1.995185	-0.367527	0.848341
25	6	0	3.364646	-0.329780	1.076386
26	6	0	4.193539	0.557563	0.393318
27	6	0	3.591876	1.419215	-0.530964
28	6	0	2.230595	1.393331	-0.773701
29	1	0	-4.415244	2.349121	0.311365
30	1	0	-5.493061	4.570002	0.190466
31	1	0	-4.145641	6.570590	-0.370314
32	1	0	-1.719850	6.334483	-0.805716
33	1	0	-0.650335	4.115459	-0.678942
34	1	0	1.782862	2.063549	-1.495358
35	1	0	4.200205	2.125751	-1.082396
36	6	0	5.702230	0.623903	0.618800
37	1	0	3.774350	-1.007836	1.811949
38	1	0	1.371268	-1.059641	1.399871
39	6	0	1.343763	-3.375002	-1.879114
40	6	0	0.601879	-4.512548	-1.548169
41	1	0	-2.732577	-5.081468	0.526040
42	1	0	-4.937061	-4.769082	1.497422
43	1	0	-5.872449	-2.486876	1.794372
44	1	0	-4.528097	-0.522276	1.125276
45	1	0	0.935081	-5.491980	-1.866517
46	1	0	-1.156163	-5.269790	-0.642606
47	1	0	2.247806	-3.464565	-2.467873
48	1	0	1.490971	-1.263759	-1.754623
49	6	0	6.172778	-0.381763	1.668077
50	6	0	6.083143	2.033145	1.092975
51	6	0	6.425289	0.321928	-0.701034
52	1	0	5.951385	-1.409385	1.371496
53	1	0	5.710421	-0.197315	2.640205
54	1	0	7.254110	-0.294891	1.791184
55	1	0	5.570836	2.281128	2.025284
56	1	0	5.825041	2.790722	0.351176
57	1	0	7.159974	2.087753	1.269675
58	1	0	6.163860	1.042581	-1.477606
59	1	0	6.170003	-0.676551	-1.063087
60	1	0	7.506713	0.364829	-0.551617

2 (Neutral, in DCM):

Center Number	Atomic Number	Atomic Type	Coordinates (Angstroms) X	Y	Z
1	6	0	-6.467032	-1.255844	-0.032839
2	6	0	-5.466295	-2.202956	0.108482
3	6	0	-4.120348	-1.820410	0.111980
4	6	0	-3.791743	-0.449824	-0.027490
5	6	0	-4.822994	0.513257	-0.174641
6	6	0	-6.150761	0.090746	-0.174391
7	6	0	-3.056900	-2.772005	0.248395
8	6	0	-2.428311	-0.042097	-0.026153
9	6	0	-1.405557	-1.004132	0.104817
10	6	0	-1.759680	-2.384434	0.240168
11	6	0	-0.049317	-0.588226	0.090754
12	6	0	0.239435	0.796689	-0.010033
13	6	0	-0.774187	1.736562	-0.166385
14	6	0	-2.104570	1.335441	-0.174063
15	6	0	-3.169537	2.287524	-0.326202
16	6	0	-4.462365	1.897758	-0.324550
17	1	0	-5.258295	2.624550	-0.437974

2 (Neutral, Gas Phase):

Center Number	Atomic Number	Atomic Type	Coordinates (Angstroms) X	Y	Z
1	6	0	-6.467882	-1.243733	-0.013632
2	6	0	-5.466319	-2.189344	0.120739
3	6	0	-4.120743	-1.808598	0.115404
4	6	0	-3.793965	-0.438498	-0.026742
5	6	0	-4.825567	0.523548	-0.169311
6	6	0	-6.152615	0.101409	-0.158975
7	6	0	-3.056389	-2.758934	0.245038
8	6	0	-2.431050	-0.031265	-0.032554
9	6	0	-1.409395	-0.992701	0.094715
10	6	0	-1.759917	-2.371994	0.230608
11	6	0	-0.051569	-0.580996	0.079048
12	6	0	0.239942	0.803442	-0.023499
13	6	0	-0.773652	1.742042	-0.184960
14	6	0	-2.105657	1.344565	-0.186391
15	6	0	-3.170879	2.294261	-0.337870
16	6	0	-4.463451	1.905588	-0.326615
17	1	0	-5.257544	2.633925	-0.439610

18	1	0	-2.906399	3.332556	-0.440695
19	1	0	-3.316205	-3.818776	0.356973
20	1	0	-7.504605	-1.565981	-0.034847
21	1	0	-5.714794	-3.252314	0.216336
22	1	0	-6.937531	0.827314	-0.288338
23	1	0	-0.965314	-3.111145	0.341853
24	1	0	-0.541334	2.784669	-0.290520
25	7	0	0.943988	-1.509269	0.145025
26	7	0	1.582200	1.136469	0.029990
27	6	0	2.190789	-1.055127	0.051939
28	7	0	2.561015	0.213435	-0.004253
29	6	0	3.296601	-2.051145	0.007773
30	6	0	4.631263	-1.644318	-0.004765
31	6	0	3.000856	-3.412964	-0.026679
32	6	0	5.648905	-2.584640	-0.053278
33	1	0	4.867363	-0.589230	0.024677
34	6	0	4.021358	-4.351552	-0.075289
35	1	0	1.967159	-3.730624	-0.018168
36	6	0	5.347846	-3.941272	-0.088978
37	1	0	6.681153	-2.257270	-0.061775
38	1	0	3.778977	-5.406658	-0.102628
39	1	0	6.144198	-4.674316	-0.127505
40	6	0	2.042087	2.488083	0.056006
41	6	0	2.988486	2.897585	-0.873545
42	6	0	1.573845	3.359506	1.031873
43	6	0	3.458067	4.202236	-0.832713
44	1	0	3.346935	2.196065	-1.615552
45	6	0	2.046907	4.662687	1.060535
46	1	0	0.855473	3.013539	1.764400
47	6	0	2.986480	5.087020	0.129246
48	1	0	4.192094	4.529227	-1.558128
49	1	0	1.686784	5.344229	1.820549
50	1	0	3.353955	6.104845	0.156168

18	1	0	-2.910955	3.338979	-0.459835
19	1	0	-3.313934	-3.805720	0.354416
20	1	0	-7.504786	-1.554364	-0.007853
21	1	0	-5.715329	-3.237932	0.230984
22	1	0	-6.940672	0.836753	-0.268834
23	1	0	-0.957753	-3.090013	0.327420
24	1	0	-0.536430	2.787432	-0.321472
25	7	0	0.934677	-1.504647	0.136968
26	7	0	1.585973	1.136665	0.014968
27	6	0	2.183741	-1.057304	0.031781
28	7	0	2.561240	0.208735	-0.035223
29	6	0	3.280965	-2.059244	-0.002061
30	6	0	4.616978	-1.661328	-0.017899
31	6	0	2.973384	-3.417403	-0.017121
32	6	0	5.626353	-2.609689	-0.049772
33	1	0	4.853149	-0.606303	-0.000201
34	6	0	3.986003	-4.363579	-0.049069
35	1	0	1.934740	-3.717175	-0.004130
36	6	0	5.314715	-3.963369	-0.065908
37	1	0	6.661039	-2.291494	-0.059933
38	1	0	3.736861	-5.416936	-0.061115
39	1	0	6.105511	-4.702283	-0.091001
40	6	0	2.055029	2.481091	0.052939
41	6	0	3.057029	2.872190	-0.825103
42	6	0	1.551455	3.371428	0.993996
43	6	0	3.539138	4.170500	-0.773750
44	1	0	3.450125	2.152025	-1.529445
45	6	0	2.037875	4.668534	1.034257
46	1	0	0.795902	3.041309	1.694949
47	6	0	3.028699	5.072941	0.149938
48	1	0	4.316617	4.478508	-1.460502
49	1	0	1.649427	5.360869	1.769634
50	1	0	3.407244	6.085793	0.186154

2 (Cation, Gas Phase):

Center Number	Atomic Number	Atomic Type	Coordinates (Angstroms) X	Y	Z
1	6	0	-6.454694	-1.250305	-0.017382
2	6	0	-5.465218	-2.199723	0.084804
3	6	0	-4.107968	-1.823367	0.082395
4	6	0	-3.776951	-0.453299	-0.023957
5	6	0	-4.805363	0.516409	-0.133851
6	6	0	-6.127340	0.105071	-0.128363
7	6	0	-3.061838	-2.780189	0.180650
8	6	0	-2.416487	-0.055924	-0.025472
9	6	0	-1.415602	-1.029111	0.068776
10	6	0	-1.754771	-2.400202	0.170044
11	6	0	-0.039306	-0.604507	0.047062
12	6	0	0.251524	0.804083	-0.020899
13	6	0	-0.765410	1.757179	-0.135925
14	6	0	-2.082213	1.343437	-0.141655
15	6	0	-3.149321	2.297397	-0.261433
16	6	0	-4.438676	1.903527	-0.254149
17	1	0	-5.232532	2.635582	-0.342399
18	1	0	-2.891354	3.344379	-0.354508
19	1	0	-3.322978	-3.828089	0.263269
20	1	0	-7.494007	-1.550416	-0.014716
21	1	0	-5.718485	-3.249403	0.167683
22	1	0	-6.913833	0.844988	-0.213950
23	1	0	-0.959931	-3.128652	0.243254
24	1	0	-0.528926	2.805917	-0.234189
25	7	0	0.931282	-1.490149	0.072512
26	7	0	1.575013	1.110872	0.013161
27	6	0	2.197316	-1.065227	0.025320
28	7	0	2.530548	0.227688	0.014750
29	6	0	3.294423	-2.044422	0.005720
30	6	0	4.625369	-1.622977	0.007872
31	6	0	2.997848	-3.407254	-0.015490
32	6	0	5.644142	-2.559136	-0.011270
33	1	0	4.856423	-0.567021	0.029130
34	6	0	4.022459	-4.337547	-0.035021
35	1	0	1.966100	-3.729687	-0.017162
36	6	0	5.345473	-3.915926	-0.032940
37	1	0	6.674780	-2.230531	-0.007714
38	1	0	3.789592	-5.393756	-0.051653
39	1	0	6.145459	-4.644549	-0.047871
40	6	0	2.033960	2.485202	0.039423
41	6	0	2.901206	2.908282	-0.952466
42	6	0	1.628847	3.311486	1.075540
43	6	0	3.359229	4.216300	-0.913642
44	1	0	3.208052	2.225262	-1.733388
45	6	0	2.103455	4.612986	1.105386
46	1	0	0.969246	2.938609	1.848744
47	6	0	2.960717	5.065243	0.110347
48	1	0	4.030767	4.570199	-1.683944
49	1	0	1.809288	5.270143	1.912310
50	1	0	3.325579	6.083226	0.137581

2 (Anion, Gas Phase):

Center Number	Atomic Number	Atomic Type	Coordinates (Angstroms) X	Y	Z
1	6	0	-6.475866	-1.178341	0.109232
2	6	0	-5.478991	-2.077435	0.471708
3	6	0	-4.133890	-1.712135	0.408675
4	6	0	-3.791550	-0.401821	-0.026121
5	6	0	-4.817153	0.509594	-0.401279
6	6	0	-6.155139	0.094950	-0.323674
7	6	0	-3.072799	-2.614450	0.759881
8	6	0	-2.424662	-0.007949	-0.093130
9	6	0	-1.401661	-0.924936	0.260372
10	6	0	-1.774632	-2.237623	0.680126
11	6	0	-0.038675	-0.544557	0.196932
12	6	0	0.254186	0.814318	-0.133773
13	6	0	-0.732760	1.669647	-0.558392
14	6	0	-2.091911	1.291711	-0.533252
15	6	0	-3.135330	2.180365	-0.907487
16	6	0	-4.443869	1.813713	-0.847855
17	1	0	-5.226381	2.505151	-1.138156
18	1	0	-2.862846	3.175019	-1.245017
19	1	0	-3.338837	-3.613739	1.085691
20	1	0	-7.515215	-1.480914	0.163128
21	1	0	-5.738009	-3.076082	0.804122
22	1	0	-6.936716	0.789360	-0.610419
23	1	0	-0.973833	-2.918010	0.939640
24	1	0	-0.477599	2.671398	-0.880059
25	7	0	0.948319	-1.442194	0.399516
26	7	0	1.609241	1.169956	-0.001263
27	6	0	2.179863	-1.020711	0.040969
28	7	0	2.575628	0.183454	-0.239359
29	6	0	3.229703	-2.076581	-0.088232
30	6	0	4.573096	-1.738530	-0.247997
31	6	0	2.875529	-3.421804	-0.040270
32	6	0	5.538804	-2.725301	-0.365285
33	1	0	4.840720	-0.690548	-0.271958
34	6	0	3.843622	-4.410562	-0.159113
35	1	0	1.830330	-3.666839	0.090862
36	6	0	5.178063	-4.067506	-0.323176
37	1	0	6.578978	-2.448158	-0.487780
38	1	0	3.553120	-5.453834	-0.123541
39	1	0	5.933473	-4.838522	-0.416163
40	6	0	2.089593	2.457184	0.141577
41	6	0	3.395362	2.775924	-0.269042
42	6	0	1.329854	3.469119	0.756607
43	6	0	3.895044	4.055679	-0.096536
44	1	0	3.995792	2.001053	-0.719486
45	6	0	1.850170	4.739164	0.923737
46	1	0	0.340796	3.243483	1.128357
47	6	0	3.133901	5.056483	0.492520
48	1	0	4.902649	4.271672	-0.432976
49	1	0	1.241451	5.491429	1.411702
50	1	0	3.532415	6.053906	0.623467

3 (Neutral, in DCM):

Center Number	Atomic Number	Atomic Type	Coordinates (Angstroms) X	Y	Z

3 (Neutral, Gas Phase):

Center Number	Atomic Number	Atomic Type	Coordinates (Angstroms) X	Y	Z

1	7	0	2.005658	0.979623	0.029879
2	7	0	3.112610	0.220744	-0.023248
3	7	0	1.795943	-1.739137	0.158547
4	6	0	2.945847	-1.096494	0.045028
5	6	0	4.200396	-1.899450	0.012355
6	6	0	4.132625	-3.291550	0.011375
7	6	0	5.449166	-1.278472	-0.015825
8	6	0	6.608444	-2.039227	-0.044133
9	6	0	5.294138	-4.049900	-0.017893
10	6	0	6.535074	-3.426815	-0.045244
11	6	0	2.258134	2.386948	0.028261
12	6	0	3.081668	2.917351	-0.955513
13	6	0	3.361266	4.275612	-0.944520
14	6	0	2.823388	5.092787	0.042005
15	6	0	2.006682	4.548596	1.025347
16	6	0	1.722676	3.190643	1.025747
17	1	0	3.165140	-3.774313	0.033781
18	1	0	5.228944	-5.130791	-0.019346
19	1	0	7.441383	-4.019223	-0.066562
20	1	0	7.572482	-1.546358	-0.064295
21	1	0	5.508165	-0.198624	-0.011935
22	1	0	1.101757	2.753567	1.797588
23	1	0	1.597471	5.179447	1.803976
24	1	0	3.045204	6.152303	0.048108
25	1	0	4.001146	4.695276	-1.710118
26	1	0	3.494682	2.264655	-1.713523
27	6	0	-0.584674	-1.603631	0.166304
28	6	0	-1.736431	-0.835896	0.088031
29	6	0	-1.637952	0.566891	-0.042572
30	6	0	0.659533	-0.980183	0.129761
31	6	0	0.730831	0.441795	0.035339
32	6	0	-0.418194	1.220118	-0.072733
33	1	0	-0.361103	2.292746	-0.186399
34	16	0	-3.225294	1.238711	-0.154218
35	7	0	-3.023943	-1.325336	0.102245
36	1	0	-0.635839	-2.682069	0.240969
37	6	0	-3.895717	-0.381755	-0.013622
38	6	0	-5.347363	-0.606179	-0.035963
39	6	0	-6.248664	0.451629	-0.153182
40	6	0	-7.613523	0.207441	-0.171839
41	6	0	-8.089802	-1.093331	-0.074192
42	6	0	-7.195456	-2.151660	0.042356
43	6	0	-5.831889	-1.912701	0.061221
44	1	0	-5.893843	1.473188	-0.229208
45	1	0	-8.305552	1.034772	-0.262504
46	1	0	-9.155649	-1.282962	-0.088770
47	1	0	-7.563340	-3.167016	0.118035
48	1	0	-5.129436	-2.730641	0.150341

1	7	0	2.011128	0.983842	0.051295
2	7	0	3.117740	0.223143	-0.014565
3	7	0	1.795485	-1.731717	0.210851
4	6	0	2.945264	-1.094061	0.072069
5	6	0	4.191807	-1.903200	0.015734
6	6	0	4.108991	-3.293239	0.011257
7	6	0	5.443187	-1.291911	-0.034898
8	6	0	6.593505	-2.062837	-0.091519
9	6	0	5.261856	-4.060912	-0.045963
10	6	0	6.506603	-3.448755	-0.097647
11	6	0	2.264228	2.387315	0.044357
12	6	0	3.138441	2.906965	-0.900820
13	6	0	3.414679	4.264900	-0.897868
14	6	0	2.826435	5.097766	0.044364
15	6	0	1.964802	4.566465	0.994663
16	6	0	1.683434	3.208923	1.001863
17	1	0	3.133266	-3.756806	0.054293
18	1	0	5.187934	-5.140782	-0.050000
19	1	0	7.406491	-4.049116	-0.140455
20	1	0	7.561698	-1.580195	-0.129503
21	1	0	5.503978	-0.212471	-0.025457
22	1	0	1.029325	2.782367	1.751292
23	1	0	1.519121	5.207850	1.743574
24	1	0	3.045315	6.157333	0.044141
25	1	0	4.093299	4.673080	-1.635264
26	1	0	3.595637	2.238217	-1.617155
27	6	0	-0.583846	-1.592639	0.216453
28	6	0	-1.735649	-0.829732	0.111357
29	6	0	-1.636439	0.570077	-0.052436
30	6	0	0.662569	-0.972391	0.172329
31	6	0	0.733836	0.447443	0.053774
32	6	0	-0.414971	1.220727	-0.085886
33	1	0	-0.354203	2.289205	-0.228082
34	16	0	-3.221411	1.239078	-0.193841
35	7	0	-3.022747	-1.320095	0.127192
36	1	0	-0.632624	-2.668242	0.312387
37	6	0	-3.890794	-0.380856	-0.018851
38	6	0	-5.342200	-0.604964	-0.044675
39	6	0	-6.242032	0.445116	-0.214596
40	6	0	-7.606094	0.200624	-0.234000
41	6	0	-8.082308	-1.094136	-0.083739
42	6	0	-7.188846	-2.145046	0.085649
43	6	0	-5.826098	-1.905400	0.105394
44	1	0	-5.880322	1.459710	-0.332786
45	1	0	-8.297857	1.021928	-0.366625
46	1	0	-9.147578	-1.284510	-0.098807
47	1	0	-7.558005	-3.155616	0.202398
48	1	0	-5.116323	-2.710859	0.235908

3 (Cation, Gas Phase):

Center Number	Atomic Number	Atomic Type	Coordinates (Angstroms) X	Y	Z
1	7	0	1.992673	0.952121	0.031278
2	7	0	3.071652	0.242045	0.027031
3	7	0	1.787227	-1.724516	0.133512
4	6	0	2.951989	-1.102733	0.055058
5	6	0	4.201739	-1.876034	0.017283
6	6	0	4.141500	-3.269736	-0.006263
7	6	0	5.439740	-1.231444	0.001454
8	6	0	6.604190	-1.978754	-0.037804
9	6	0	5.310452	-4.009147	-0.046771
10	6	0	6.541585	-3.366060	-0.062287
11	6	0	2.224049	2.385872	0.033737
12	6	0	2.992115	2.923488	-0.984076
13	6	0	3.239064	4.287322	-0.970552
14	6	0	2.736548	5.077075	0.055065
15	6	0	1.983448	4.510946	1.075815
16	6	0	1.717355	3.150597	1.071753
17	1	0	3.179780	-3.763161	0.007266
18	1	0	5.262167	-5.089508	-0.066080
19	1	0	7.454004	-3.947148	-0.092296
20	1	0	7.563054	-1.478266	-0.047586
21	1	0	5.487735	-0.151740	0.024922
22	1	0	1.148279	2.688686	1.868669
23	1	0	1.611102	5.125625	1.883913
24	1	0	2.939359	6.139583	0.063787
25	1	0	3.828643	4.731354	-1.760990
26	1	0	3.384030	2.284859	-1.764402
27	6	0	-0.584591	-1.637746	0.162989
28	6	0	-1.716302	-0.872274	0.082553
29	6	0	-1.620501	0.565408	-0.057954
30	6	0	0.670729	-1.000460	0.115067
31	6	0	0.736991	0.434947	0.024727
32	6	0	-0.423694	1.224279	-0.086332
33	1	0	-0.361847	2.295575	-0.203631
34	16	0	-3.202146	1.227970	-0.177533
35	7	0	-2.995037	-1.354465	0.099002
36	1	0	-0.629941	-2.714677	0.240357
37	6	0	-3.868207	-0.413157	-0.023080
38	6	0	-5.309422	-0.622656	-0.037827
39	6	0	-6.197759	0.443371	-0.191051
40	6	0	-7.561608	0.212012	-0.198264
41	6	0	-8.044163	-1.082397	-0.052172
42	6	0	-7.163739	-2.147797	0.100275
43	6	0	-5.800032	-1.924078	0.107585
44	1	0	-5.831050	1.456721	-0.306092

3 (Anion, Gas Phase):

Center Number	Atomic Number	Atomic Type	Coordinates (Angstroms) X	Y	Z
1	7	0	2.025377	1.030156	0.015340
2	7	0	3.122280	0.189339	-0.260474
3	7	0	1.814667	-1.632656	0.561085
4	6	0	2.929579	-1.048007	0.110575
5	6	0	4.131271	-1.931557	-0.024831
6	6	0	4.015485	-3.299061	0.207907
7	6	0	5.376424	-1.410908	-0.373787
8	6	0	6.479073	-2.242331	-0.496077
9	6	0	5.120828	-4.131039	0.089659
10	6	0	6.356399	-3.607745	-0.265017
11	6	0	2.314358	2.378519	0.095774
12	6	0	3.524612	2.874430	-0.419365
13	6	0	3.836019	4.219469	-0.311976
14	6	0	2.977307	5.114032	0.313213
15	6	0	1.791753	4.622915	0.850263
16	6	0	1.459499	3.285019	0.749254
17	1	0	3.042091	-3.682636	0.482106
18	1	0	5.015861	-5.193592	0.274660
19	1	0	7.218900	-4.257014	-0.357443
20	1	0	7.440525	-1.824127	-0.769772
21	1	0	5.459121	-0.345420	-0.541497
22	1	0	0.549205	2.924874	1.206455
23	1	0	1.115259	5.290732	1.370905
24	1	0	3.228521	6.163530	0.392484
25	1	0	4.772705	4.573161	-0.727704
26	1	0	4.200387	2.180892	-0.894850
27	6	0	-0.579957	-1.492560	0.499803
28	6	0	-1.740672	-0.763897	0.207126
29	6	0	-1.632076	0.555105	-0.252768
30	6	0	0.671325	-0.906115	0.371509
31	6	0	0.741203	0.478248	-0.008130
32	6	0	-0.387918	1.180057	-0.381810
33	1	0	-0.311502	2.198118	-0.735155
34	16	0	-3.209691	1.185963	-0.555619
35	7	0	-3.031151	-1.232981	0.306964
36	1	0	-0.645909	-2.525123	0.814126
37	6	0	-3.896794	-0.343173	-0.054614
38	6	0	-5.345748	-0.572635	-0.051973
39	6	0	-6.250272	0.400769	-0.477845
40	6	0	-7.614130	0.153826	-0.461012
41	6	0	-8.098761	-1.069817	-0.018931
42	6	0	-7.203654	-2.044867	0.406656
43	6	0	-5.841046	-1.802148	0.391385
44	1	0	-5.883990	1.358789	-0.827356

45	1	0	-8.249085	1.038169	-0.317374
46	1	0	-9.111328	-1.261882	-0.057513
47	1	0	-7.545271	-3.153551	0.213245
48	1	0	-5.099749	-2.739531	0.225011

45	1	0	-8.300989	0.920824	-0.796572
46	1	0	-9.163969	-1.262392	-0.005909
47	1	0	-7.572031	-3.002128	0.754581
48	1	0	-5.132000	-2.550078	0.720498

4 (Neutral, in DCM):

Center Number	Atomic Number	Atomic Type	Coordinates (Angstroms) X	Y	Z
1	7	0	0.699965	-0.218721	0.001479
2	7	0	-0.576195	-0.624205	0.004584
3	7	0	-1.296334	1.646243	-0.011843
4	6	0	-1.499976	0.337901	-0.004265
5	6	0	-2.908497	-0.147427	-0.005625
6	6	0	-3.954227	0.765247	0.123670
7	6	0	-3.202213	-1.505430	-0.133750
8	6	0	-4.519029	-1.939999	-0.129994
9	6	0	-5.270284	0.327401	0.129435
10	6	0	-5.557154	-1.025815	0.003133
11	6	0	1.718125	-1.182059	0.013013
12	6	0	1.441818	-2.545357	0.029431
13	6	0	2.483199	-3.458380	0.040482
14	6	0	3.801244	-3.018934	0.035294
15	6	0	4.082110	-1.660358	0.019094
16	6	0	3.046396	-0.745090	0.008080
17	1	0	-3.727767	1.817997	0.221959
18	1	0	-6.073529	1.045996	0.234053
19	1	0	-6.584854	-1.367302	0.007627
20	1	0	-4.735133	-2.996222	-0.231645
21	1	0	-2.396542	-2.219154	-0.239996
22	1	0	5.099002	-1.289850	0.014894
23	1	0	4.615348	-3.731618	0.044078
24	1	0	2.261720	-4.517248	0.053271
25	1	0	0.411461	-2.869401	0.034302
26	6	0	0.350880	3.420018	-0.025645
27	6	0	1.679377	3.794648	-0.030930
28	6	0	2.706819	2.847511	-0.024560
29	6	0	0.008404	2.062078	-0.014358
30	6	0	1.045618	1.117903	-0.008234
31	6	0	2.383460	1.508334	-0.013230
32	8	0	3.385030	0.581324	-0.007965
33	1	0	3.748012	3.141043	-0.029068
34	1	0	1.938486	4.845586	-0.040220
35	1	0	-0.444924	4.153195	-0.031321

4 (Neutral, Gas Phase):

Center Number	Atomic Number	Atomic Type	Coordinates (Angstroms) X	Y	Z
1	7	0	-0.699825	-0.220344	0.000362
2	7	0	0.574222	-0.631335	0.000390
3	7	0	1.300021	1.639634	-0.000520
4	6	0	1.500779	0.331099	-0.000033
5	6	0	2.906965	-0.154276	0.000021
6	6	0	3.951182	0.767085	0.000343
7	6	0	3.198308	-1.517593	-0.000246
8	6	0	4.514602	-1.950039	-0.000168
9	6	0	5.266847	0.331072	0.000429
10	6	0	5.552459	-1.027523	0.000174
11	6	0	-1.721678	-1.178902	0.000160
12	6	0	-1.449236	-2.542297	-0.000378
13	6	0	-2.491880	-3.453375	-0.000632
14	6	0	-3.807989	-3.011517	-0.000398
15	6	0	-4.084977	-1.652401	0.000122
16	6	0	-3.048820	-0.738210	0.000437
17	1	0	3.714289	1.821727	0.000520
18	1	0	6.072447	1.053939	0.000715
19	1	0	6.580334	-1.367354	0.000233
20	1	0	4.731303	-3.010556	-0.000373
21	1	0	2.386605	-2.231395	-0.000530
22	1	0	-5.098970	-1.276039	0.000334
23	1	0	-4.623387	-3.721892	-0.000634
24	1	0	-2.273301	-4.512380	-0.001023
25	1	0	-0.417406	-2.859991	-0.000569
26	6	0	-0.339551	3.417075	-0.000741
27	6	0	-1.665056	3.796384	-0.000555
28	6	0	-2.696050	2.852641	0.000003
29	6	0	-0.000709	2.057138	-0.000388
30	6	0	-1.042363	1.118092	0.000136
31	6	0	-2.378671	1.512729	0.000386
32	8	0	-3.385478	0.588740	0.001186
33	1	0	-3.736533	3.146003	0.000183
34	1	0	-1.920328	4.847858	-0.000837
35	1	0	0.462860	4.141382	-0.001166

4 (Cation, Gas Phase):

Center Number	Atomic Number	Atomic Type	Coordinates (Angstroms) X	Y	Z
1	7	0	-0.682002	-0.196127	0.000022
2	7	0	0.537496	-0.593907	0.000006
3	7	0	1.275722	1.653636	-0.000186
4	6	0	1.515819	0.359736	-0.000084
5	6	0	2.896205	-0.138262	-0.000032
6	6	0	3.948726	0.779109	0.000119
7	6	0	3.166369	-1.508829	-0.000116
8	6	0	4.476746	-1.952811	-0.000031
9	6	0	5.255601	0.327035	0.000201
10	6	0	5.521069	-1.037224	0.000112
11	6	0	-1.712187	-1.182029	0.000018
12	6	0	-1.404255	-2.540682	-0.000118
13	6	0	-2.431001	-3.457535	-0.000143
14	6	0	-3.758864	-3.023886	-0.000040
15	6	0	-4.066264	-1.678025	0.000097
16	6	0	-3.037792	-0.748578	0.000124
17	1	0	3.732960	1.838207	0.000179
18	1	0	6.070645	1.037949	0.000343
19	1	0	6.544869	-1.387817	0.000190
20	1	0	4.685010	-3.014122	-0.000080
21	1	0	2.354519	-2.222059	-0.000260
22	1	0	-5.086727	-1.320364	0.000182
23	1	0	-4.561449	-3.749305	-0.000074
24	1	0	-2.205572	-4.514448	-0.000247
25	1	0	-0.369599	-2.849126	-0.000199
26	6	0	-0.344520	3.432122	-0.000183
27	6	0	-1.669830	3.782029	-0.000096
28	6	0	-2.708035	2.827355	0.000044
29	6	0	0.001492	2.069945	-0.000130
30	6	0	-1.045140	1.109984	0.000009
31	6	0	-2.402840	1.495548	0.000098
32	8	0	-3.381499	0.565083	0.000286
33	1	0	-3.746051	3.130267	0.000119
34	1	0	-1.941873	4.829478	-0.000135
35	1	0	0.448958	4.165461	-0.000297

4 (Anion, Gas Phase):

Center Number	Atomic Number	Atomic Type	Coordinates (Angstroms) X	Y	Z
1	7	0	-0.721664	-0.241309	0.269074
2	7	0	0.610932	-0.659774	0.164880
3	7	0	1.308804	1.639577	0.039430
4	6	0	1.483807	0.310595	0.086340
5	6	0	2.905724	-0.158587	0.031733
6	6	0	3.934282	0.769948	-0.104311
7	6	0	3.229660	-1.512632	0.114813
8	6	0	4.551475	-1.926507	0.058836
9	6	0	5.258567	0.355159	-0.159431
10	6	0	5.573980	-0.994043	-0.079271
11	6	0	-1.706117	-1.173059	0.099101
12	6	0	-1.453571	-2.540837	-0.037011
13	6	0	-2.503003	-3.442731	-0.185267
14	6	0	-3.815485	-3.009162	-0.221441
15	6	0	-4.078092	-1.640268	-0.104802
16	6	0	-3.050918	-0.742500	0.060895
17	1	0	3.662319	1.814953	-0.164439
18	1	0	6.047931	1.089971	-0.266642
19	1	0	6.606788	-1.319181	-0.122428
20	1	0	4.786974	-2.982355	0.123723
21	1	0	2.425214	-2.226884	0.226812
22	1	0	-5.088684	-1.252148	-0.130295
23	1	0	-4.631209	-3.709807	-0.339524
24	1	0	-2.278503	-4.498569	-0.278423
25	1	0	-0.424647	-2.866598	-0.018303
26	6	0	-0.358927	3.392882	-0.130304
27	6	0	-1.693959	3.784968	-0.159685
28	6	0	-2.714733	2.852683	-0.062984
29	6	0	-0.001990	2.047263	0.005319
30	6	0	-1.050918	1.117161	0.106355
31	6	0	-2.368048	1.511795	0.075845
32	8	0	-3.385466	0.585669	0.229000
33	1	0	-3.760088	3.129592	-0.074883
34	1	0	-1.940092	4.835101	-0.261921
35	1	0	0.440826	4.118345	-0.207737

5 (Neutral, in DCM):

Center	Atomic	Atomic	Coordinates (Angstroms)

5 (Neutral, in Gas Phase):

Center	Atomic	Atomic	Coordinates (Angstroms)

Number	Number	Type	X	Y	Z
1	7	0	-0.573597	-0.197744	0.051863
2	7	0	0.717466	-0.568206	0.094131
3	7	0	1.420139	1.674892	-0.202691
4	6	0	1.636432	0.382894	-0.024006
5	6	0	3.047649	-0.090848	0.041442
6	6	0	4.090302	0.820377	-0.116892
7	6	0	3.345243	-1.436654	0.256731
8	6	0	4.664258	-1.861432	0.308859
9	6	0	5.408814	0.392243	-0.065507
10	6	0	5.700026	-0.949167	0.146504
11	6	0	-1.504024	-1.259956	-0.054041
12	6	0	-1.042390	-2.546983	-0.335691
13	6	0	-1.928635	-3.604737	-0.430718
14	6	0	-3.290952	-3.395770	-0.259692
15	6	0	-3.757030	-2.118560	-0.002344
16	6	0	-2.875493	-1.047686	0.106879
17	1	0	3.860083	1.863760	-0.282850
18	1	0	6.210219	1.109313	-0.192020
19	1	0	6.729469	-1.283151	0.185820
20	1	0	4.884107	-2.908235	0.477457
21	1	0	2.540971	-2.148262	0.385859
22	1	0	-4.818428	-1.938839	0.121055
23	1	0	-3.990106	-4.218117	-0.335013
24	1	0	-1.549740	-4.595082	-0.646571
25	1	0	0.014894	-2.705108	-0.480575
26	6	0	-0.198071	3.436771	-0.288702
27	6	0	-1.506565	3.858422	-0.220249
28	6	0	-2.536304	2.939913	-0.020503
29	6	0	0.114495	2.075204	-0.174204
30	6	0	-0.933581	1.144216	-0.004688
31	6	0	-2.254986	1.589738	0.104051
32	16	0	-3.576003	0.510590	0.502793
33	1	0	-3.562315	3.278850	0.050463
34	1	0	-1.744208	4.910345	-0.312390
35	1	0	0.617938	4.134579	-0.422424

Number	Number	Type	X	Y	Z
1	7	0	-0.572716	-0.202668	0.085255
2	7	0	0.717665	-0.576235	0.122211
3	7	0	1.418136	1.663373	-0.226771
4	6	0	1.635675	0.375209	-0.020951
5	6	0	3.045220	-0.093991	0.044996
6	6	0	4.077737	0.783075	-0.276835
7	6	0	3.349334	-1.398194	0.430422
8	6	0	4.668646	-1.817456	0.491728
9	6	0	5.396123	0.358392	-0.220180
10	6	0	5.695238	-0.941296	0.164674
11	6	0	-1.505376	-1.257461	-0.057865
12	6	0	-1.047961	-2.532891	-0.388939
13	6	0	-1.939300	-3.580672	-0.531299
14	6	0	-3.300674	-3.370624	-0.361641
15	6	0	-3.761110	-2.102736	-0.052943
16	6	0	-2.875567	-1.043190	0.109403
17	1	0	3.830420	1.794198	-0.568791
18	1	0	6.193112	1.044863	-0.475211
19	1	0	6.725362	-1.270928	0.211375
20	1	0	4.896897	-2.830748	0.796397
21	1	0	2.545298	-2.073842	0.687556
22	1	0	-4.821239	-1.919083	0.070030
23	1	0	-4.003304	-4.184604	-0.477548
24	1	0	-1.565460	-4.563373	-0.785139
25	1	0	0.011156	-2.681894	-0.529272
26	6	0	-0.200388	3.424050	-0.316864
27	6	0	-1.506892	3.845744	-0.234362
28	6	0	-2.534131	2.930894	-0.003313
29	6	0	0.115818	2.063947	-0.185571
30	6	0	-0.931194	1.139522	0.016272
31	6	0	-2.250884	1.583900	0.140216
32	16	0	-3.552955	0.501263	0.591383
33	1	0	-3.559725	3.267005	0.076925
34	1	0	-1.745698	4.895628	-0.340741
35	1	0	0.616971	4.113953	-0.474266

5 (Cation, in Gas Phase):

Center Number	Atomic Number	Atomic Type	Coordinates (Angstroms) X	Y	Z
1	7	0	-0.553191	-0.173141	-0.009073
2	7	0	0.684184	-0.536307	-0.001091
3	7	0	1.406379	1.698592	-0.066764
4	6	0	1.654873	0.408541	-0.015397
5	6	0	3.039217	-0.080373	0.016642
6	6	0	4.084952	0.833163	-0.125237
7	6	0	3.318626	-1.437011	0.192446
8	6	0	4.631738	-1.872085	0.224333
9	6	0	5.394945	0.389819	-0.096703
10	6	0	5.669925	-0.960997	0.077564
11	6	0	-1.496119	-1.265604	-0.048629
12	6	0	-0.996648	-2.563775	-0.186311
13	6	0	-1.861746	-3.633085	-0.211944
14	6	0	-3.235556	-3.423870	-0.098215
15	6	0	-3.731754	-2.145315	0.025978
16	6	0	-2.869178	-1.046148	0.046893
17	1	0	3.862449	1.882364	-0.259723
18	1	0	6.204046	1.098393	-0.210648
19	1	0	6.695814	-1.304635	0.100597
20	1	0	4.846983	-2.922590	0.365434
21	1	0	2.512409	-2.146431	0.314171
22	1	0	-4.798365	-1.975187	0.102801
23	1	0	-3.918009	-4.262925	-0.115230
24	1	0	-1.468261	-4.633690	-0.322621
25	1	0	0.066127	-2.717488	-0.276920
26	6	0	-0.175796	3.467626	-0.092841
27	6	0	-1.481936	3.865291	-0.064395
28	6	0	-2.528637	2.929654	0.007338
29	6	0	0.129612	2.094395	-0.056049
30	6	0	-0.934345	1.136846	-0.003027
31	6	0	-2.282644	1.577457	0.044366
32	16	0	-3.631782	0.503029	0.200631
33	1	0	-3.553110	3.278512	0.038955
34	1	0	-1.728266	4.918609	-0.091910
35	1	0	0.647926	4.165421	-0.137369

5 (Anion, in Gas Phase):

Center Number	Atomic Number	Atomic Type	Coordinates (Angstroms) X	Y	Z
1	7	0	-0.599456	-0.227301	0.334132
2	7	0	0.761076	-0.581189	0.386792
3	7	0	1.380624	1.615673	-0.347170
4	6	0	1.601622	0.351753	0.029580
5	6	0	3.037627	-0.076799	0.070445
6	6	0	4.036755	0.811445	-0.317644
7	6	0	3.400255	-1.356886	0.487639
8	6	0	4.732934	-1.738326	0.516341
9	6	0	5.371401	0.428041	-0.291793
10	6	0	5.726118	-0.847203	0.125955
11	6	0	-1.468332	-1.247862	0.024140
12	6	0	-1.008863	-2.511087	-0.379992
13	6	0	-1.905316	-3.517857	-0.700029
14	6	0	-3.275949	-3.302155	-0.654112
15	6	0	-3.741482	-2.053334	-0.254938
16	6	0	-2.861647	-1.050326	0.113256
17	1	0	3.735229	1.800289	-0.635191
18	1	0	6.138460	1.129418	-0.598781
19	1	0	6.767548	-1.146051	0.148059
20	1	0	4.999938	-2.735860	0.844754
21	1	0	2.616436	-2.037401	0.792158
22	1	0	-4.805544	-1.855552	-0.196761
23	1	0	-3.972898	-4.087288	-0.916004
24	1	0	-1.520584	-4.484012	-1.005054
25	1	0	0.057195	-2.670406	-0.431079
26	6	0	-0.292805	3.340213	-0.524077
27	6	0	-1.613567	3.765600	-0.424223
28	6	0	-2.608713	2.885355	-0.043348
29	6	0	0.073266	2.016542	-0.260880
30	6	0	-0.955571	1.124551	0.122555
31	6	0	-2.258078	1.562418	0.250616
32	16	0	-3.483702	0.432419	0.842017
33	1	0	-3.642098	3.195764	0.037670
34	1	0	-1.863801	4.796368	-0.646922
35	1	0	0.495705	4.021250	-0.818346

6 (Neutral, in DCM):

Center Number	Atomic Number	Atomic Type	Coordinates (Angstroms) X	Y	Z
1	7	0	-0.217141	0.754509	-0.050943
2	7	0	-1.554045	0.620161	-0.001393
3	7	0	-1.343578	-1.733832	-0.183509
4	6	0	-2.043022	-0.611377	-0.074651
5	6	0	-3.527656	-0.710501	-0.032275
6	6	0	-4.137807	-1.963243	-0.008093
7	6	0	-4.322396	0.436572	-0.016328
8	6	0	-5.703799	0.328656	0.024320
9	6	0	-5.520475	-2.067597	0.033405

6 (Neutral, Gas Phase):

Center Number	Atomic Number	Atomic Type	Coordinates (Angstroms) X	Y	Z
1	7	0	-0.218557	0.761680	-0.060564
2	7	0	-1.556257	0.629579	0.004692
3	7	0	-1.347465	-1.722773	-0.227406
4	6	0	-2.045166	-0.602692	-0.086195
5	6	0	-3.526543	-0.705354	-0.031823
6	6	0	-4.127608	-1.961057	0.001160
7	6	0	-4.324221	0.437918	-0.012331
8	6	0	-5.703700	0.322967	0.041380
9	6	0	-5.508161	-2.071625	0.056415

10	6	0	-6.307327	-0.922954	0.049369
11	6	0	0.242508	2.107412	-0.048306
12	6	0	-0.257845	2.980009	0.909425
13	6	0	0.156775	4.302903	0.901571
14	6	0	1.060939	4.747350	-0.055307
15	6	0	1.547241	3.866697	-1.013411
16	6	0	1.136927	2.541435	-1.017726
17	1	0	-3.522358	-2.852287	-0.019576
18	1	0	-5.984238	-3.045878	0.054221
19	1	0	-7.386673	-1.005456	0.080980
20	1	0	-6.311329	1.224928	0.034050
21	1	0	-3.853993	1.411130	-0.040108
22	1	0	1.495452	1.852156	-1.771927
23	1	0	2.240445	4.212996	-1.769188
24	1	0	1.382347	5.781052	-0.057908
25	1	0	-0.226687	4.987550	1.647167
26	1	0	-0.963153	2.616343	1.645217
27	6	0	0.824314	-2.751899	-0.170131
28	6	0	2.191426	-2.646162	-0.082357
29	6	0	2.778446	-1.383100	0.049084
30	6	0	0.012555	-1.606012	-0.142335
31	6	0	0.630715	-0.339157	-0.050035
32	6	0	2.018107	-0.232390	0.069945
33	1	0	2.488342	0.732150	0.190253
34	6	0	4.271511	-1.303629	0.156900
35	1	0	2.813469	-3.532442	-0.101810
36	1	0	0.338349	-3.715281	-0.253150
37	9	0	4.710374	-0.062565	0.388834
38	9	0	4.876589	-1.725476	-0.966825
39	9	0	4.744876	-2.077616	1.146249

10	6	0	-6.299396	-0.931136	0.076892
11	6	0	0.244136	2.110132	-0.057064
12	6	0	-0.301766	3.004147	0.854814
13	6	0	0.123112	4.322782	0.850674
14	6	0	1.082493	4.747972	-0.058476
15	6	0	1.610719	3.850377	-0.976348
16	6	0	1.190090	2.529499	-0.983961
17	1	0	-3.499671	-2.840811	-0.016452
18	1	0	-5.967779	-3.051145	0.084768
19	1	0	-7.377594	-1.018948	0.119067
20	1	0	-6.316713	1.214979	0.052804
21	1	0	-3.854018	1.410969	-0.045483
22	1	0	1.579832	1.830180	-1.712311
23	1	0	2.344803	4.180500	-1.699424
24	1	0	1.412946	5.778185	-0.056848
25	1	0	-0.295562	5.020498	1.563956
26	1	0	-1.054329	2.654967	1.548224
27	6	0	0.816628	-2.743743	-0.222466
28	6	0	2.182140	-2.644360	-0.115963
29	6	0	2.773658	-1.388532	0.052611
30	6	0	0.005923	-1.596886	-0.180506
31	6	0	0.628761	-0.334574	-0.061334
32	6	0	2.014524	-0.237668	0.086228
33	1	0	2.489484	0.719518	0.239278
34	6	0	4.267157	-1.315039	0.180467
35	1	0	2.803391	-3.530206	-0.144255
36	1	0	0.322387	-3.699763	-0.328392
37	9	0	4.695515	-0.083418	0.473087
38	9	0	4.876287	-1.683965	-0.956335
39	9	0	4.722874	-2.133406	1.138023

6 (Cation, Gas Phase):

Center Number	Atomic Number	Atomic Type	Coordinates (Angstroms) X	Y	Z
1	7	0	-0.231210	0.730828	-0.055193
2	7	0	-1.513475	0.621984	-0.050538
3	7	0	-1.332344	-1.721755	-0.178880
4	6	0	-2.059378	-0.618435	-0.082878
5	6	0	-3.521104	-0.693507	-0.032672
6	6	0	-4.137717	-1.945923	0.006283
7	6	0	-4.296264	0.469512	-0.019126
8	6	0	-5.675146	0.374027	0.033145
9	6	0	-5.516773	-2.031089	0.060836
10	6	0	-6.285678	-0.873263	0.074097
11	6	0	0.258281	2.098169	-0.051718
12	6	0	-0.215843	2.952405	0.929863
13	6	0	0.227729	4.264721	0.925855
14	6	0	1.108112	4.700354	-0.056185
15	6	0	1.552884	3.829124	-1.042798
16	6	0	1.130809	2.509233	-1.047341
17	1	0	-3.532652	-2.841584	-0.004586
18	1	0	-5.995017	-3.000600	0.094297
19	1	0	-7.364805	-0.943684	0.116009
20	1	0	-6.276313	1.273067	0.039806
21	1	0	-3.820517	1.439489	-0.057172
22	1	0	1.452907	1.823677	-1.821010
23	1	0	2.223124	4.177439	-1.816659
24	1	0	1.445863	5.728060	-0.057021
25	1	0	-0.118195	4.947460	1.689766
26	1	0	-0.909232	2.591527	1.677792
27	6	0	0.811219	-2.769215	-0.215928
28	6	0	2.158618	-2.641089	-0.127309
29	6	0	2.755480	-1.357209	0.036026
30	6	0	-0.008693	-1.608422	-0.157057
31	6	0	0.615748	-0.332755	-0.053143
32	6	0	2.020405	-0.215400	0.075010
33	1	0	2.491497	0.745300	0.219077
34	6	0	4.260639	-1.301641	0.174675
35	1	0	2.798577	-3.514148	-0.159606
36	1	0	0.322260	-3.728441	-0.314828
37	9	0	4.694263	-0.056279	0.344206
38	9	0	4.840224	-1.801082	-0.915524
39	9	0	4.656818	-2.028478	1.216719

6 (Anion, Gas Phase):

Center Number	Atomic Number	Atomic Type	Coordinates (Angstroms) X	Y	Z
1	7	0	-0.181858	0.834252	-0.014883
2	7	0	-1.534523	0.603296	0.301394
3	7	0	-1.313876	-1.526578	-0.762227
4	6	0	-1.988148	-0.522694	-0.168795
5	6	0	-3.457236	-0.738011	0.021263
6	6	0	-4.047650	-1.919092	-0.419552
7	6	0	-4.258540	0.229515	0.626502
8	6	0	-5.617524	0.015095	0.794398
9	6	0	-5.410777	-2.130198	-0.258353
10	6	0	-6.201382	-1.166645	0.351626
11	6	0	0.212928	2.148444	-0.100587
12	6	0	-0.639178	3.174417	0.350788
13	6	0	-0.266160	4.502202	0.236850
14	6	0	0.947350	4.870136	-0.330257
15	6	0	1.783006	3.861860	-0.798246
16	6	0	1.435205	2.528344	-0.689806
17	1	0	-3.410582	-2.658101	-0.885905
18	1	0	-5.856144	-3.053756	-0.609107
19	1	0	-7.264153	-1.332713	0.481464
20	1	0	-6.226473	0.774334	1.270636
21	1	0	-3.793450	1.146609	0.962161
22	1	0	2.096134	1.775138	-1.092589
23	1	0	2.726378	4.114794	-1.268253
24	1	0	1.231026	5.910847	-0.414398
25	1	0	-0.944417	5.265283	0.601883
26	1	0	-1.589174	2.899862	0.781148
27	6	0	0.849999	-2.580091	-0.826973
28	6	0	2.203843	-2.564121	-0.525645
29	6	0	2.768861	-1.442471	0.056932
30	6	0	0.031188	-1.468508	-0.583830
31	6	0	0.659214	-0.289956	-0.090099
32	6	0	1.982048	-0.305396	0.292933
33	1	0	2.428081	0.573081	0.741180
34	6	0	4.208772	-1.390417	0.412878
35	1	0	2.816607	-3.431767	-0.732296
36	1	0	0.382756	-3.462003	-1.245534
37	9	0	4.888621	-0.438306	-0.266996
38	9	0	4.852958	-2.546245	0.176434
39	9	0	4.418456	-1.101326	1.715836

7 (Neutral, in DCM):

Center Number	Atomic Number	Atomic Type	Coordinates (Angstroms) X	Y	Z
1	7	0	-0.893569	-0.869853	-0.011320
2	7	0	-1.253692	0.412275	-0.163380
3	7	0	-3.525327	-0.143331	0.283735
4	6	0	-2.543118	0.700783	0.010073
5	6	0	-2.878787	2.145987	-0.128849
6	6	0	-4.178477	2.581777	0.123013
7	6	0	-1.911586	3.074917	-0.514176
8	6	0	-2.242279	4.415503	-0.644496
9	6	0	-4.504750	3.924072	-0.003165
10	6	0	-3.538727	4.844719	-0.388121
11	6	0	0.464285	-1.242300	-0.054281
12	6	0	1.551856	-0.332418	0.119987

7 (Neutral, Gas Phase):

Center Number	Atomic Number	Atomic Type	Coordinates (Angstroms) X	Y	Z
1	7	0	-0.892887	-0.867625	-0.017070
2	7	0	-1.254802	0.414393	-0.161144
3	7	0	-3.532350	-0.148472	0.258886
4	6	0	-2.549373	0.697699	-0.001651
5	6	0	-2.886047	2.140441	-0.130550
6	6	0	-4.176812	2.572769	0.163214
7	6	0	-1.930203	3.067677	-0.543020
8	6	0	-2.264487	4.407688	-0.658870
9	6	0	-4.505403	3.914615	0.051492
10	6	0	-3.551338	4.835376	-0.359684
11	6	0	0.466766	-1.237330	-0.052847
12	6	0	1.553934	-0.325024	0.115133

13	6	0	2.870551	-0.797578	-0.120690
14	6	0	3.078662	-2.156482	-0.419965
15	6	0	2.035952	-3.041135	-0.459131
16	6	0	0.734047	-2.587810	-0.272276
17	1	0	-4.929709	1.862251	0.418695
18	1	0	-5.517329	4.250762	0.198532
19	1	0	-3.794458	5.892246	-0.488855
20	1	0	-1.484716	5.126756	-0.949295
21	1	0	-0.902206	2.742865	-0.718764
22	1	0	2.190563	-4.095385	-0.647101
23	1	0	4.075621	-2.535245	-0.586628
24	6	0	3.993072	0.123026	-0.018438
25	6	0	1.382013	1.008994	0.611580
26	6	0	-4.163452	-2.472771	0.399548
27	6	0	-3.801267	-3.801447	0.310215
28	6	0	-2.477434	-4.182329	0.077093
29	6	0	-3.193074	-1.470621	0.266647
30	6	0	-1.859638	-1.861682	0.077312
31	6	0	-1.516951	-3.202693	-0.046627
32	8	0	-0.231285	-3.553604	-0.328483
33	1	0	-2.192681	-5.221335	-0.019275
34	1	0	-4.556976	-4.570021	0.409375
35	1	0	-5.192334	-2.175042	0.552545
36	6	0	3.764874	1.442584	0.422397
37	6	0	2.436542	1.838412	0.767147
38	6	0	5.314981	-0.243555	-0.347352
39	6	0	6.349307	0.655036	-0.236825
40	6	0	6.114880	1.963531	0.212011
41	6	0	4.838411	2.347555	0.535773
42	1	0	0.400376	1.349532	0.889881
43	1	0	2.284625	2.835417	1.164419
44	1	0	5.535125	-1.238547	-0.706890
45	1	0	7.353349	0.349063	-0.502842
46	1	0	6.936336	2.663531	0.298020
47	1	0	4.633456	3.353899	0.882382

13	6	0	2.874480	-0.793731	-0.107420
14	6	0	3.084340	-2.156300	-0.381168
15	6	0	2.042203	-3.040588	-0.419812
16	6	0	0.738629	-2.585247	-0.254838
17	1	0	-4.910562	1.843972	0.478406
18	1	0	-5.510010	4.242511	0.285650
19	1	0	-3.809654	5.882835	-0.449250
20	1	0	-1.518572	5.120208	-0.987047
21	1	0	-0.931216	2.729360	-0.783662
22	1	0	2.193166	-4.097644	-0.590079
23	1	0	4.083923	-2.535999	-0.524887
24	6	0	3.997028	0.125999	-0.013545
25	6	0	1.383181	1.025978	0.578643
26	6	0	-4.163839	-2.476087	0.373692
27	6	0	-3.800059	-3.803044	0.292112
28	6	0	-2.473387	-4.182396	0.072716
29	6	0	-3.194181	-1.471422	0.246848
30	6	0	-1.858757	-1.861920	0.069082
31	6	0	-1.513213	-3.202725	-0.046205
32	8	0	-0.224046	-3.554693	-0.315092
33	1	0	-2.182111	-5.219264	-0.017796
34	1	0	-4.555208	-4.572025	0.387516
35	1	0	-5.191428	-2.172635	0.516531
36	6	0	3.769459	1.450432	0.408932
37	6	0	2.439011	1.852681	0.733181
38	6	0	5.318571	-0.244490	-0.334235
39	6	0	6.354441	0.651415	-0.230974
40	6	0	6.121091	1.963667	0.203567
41	6	0	4.844584	2.352423	0.516672
42	1	0	0.398334	1.374909	0.831144
43	1	0	2.282897	2.856378	1.110712
44	1	0	5.537208	-1.241616	-0.687321
45	1	0	7.357903	0.340891	-0.491653
46	1	0	6.942827	2.662919	0.285432
47	1	0	4.641425	3.363355	0.849553

7 (Cation, Gas Phase):

Center Number	Atomic Number	Atomic Type	Coordinates (Angstroms) X	Y	Z
1	7	0	-0.940377	-0.864513	-0.000548
2	7	0	-1.242245	0.381950	-0.072142
3	7	0	-3.551106	-0.102319	0.124431
4	6	0	-2.559686	0.741646	-0.022702
5	6	0	-2.817249	2.184947	-0.122795
6	6	0	-4.091988	2.670265	0.171350
7	6	0	-1.808290	3.066126	-0.516766
8	6	0	-2.077249	4.420798	-0.613023
9	6	0	-4.349405	4.026370	0.081880
10	6	0	-3.344059	4.902127	-0.309952
11	6	0	0.429947	-1.249653	0.003124
12	6	0	1.520861	-0.324894	0.142536
13	6	0	2.828813	-0.823944	-0.088763
14	6	0	3.010575	-2.199696	-0.335792
15	6	0	1.972719	-3.086483	-0.345223
16	6	0	0.678085	-2.611082	-0.173270
17	1	0	-4.867936	1.980095	0.472233
18	1	0	-5.335776	4.403073	0.316698
19	1	0	-3.549820	5.962067	-0.382676
20	1	0	-1.298878	5.102226	-0.929014
21	1	0	-0.824941	2.689931	-0.765503
22	1	0	2.117442	-4.147406	-0.491453
23	1	0	4.006093	-2.589017	-0.484279
24	6	0	3.975103	0.061132	-0.026787
25	6	0	1.384054	1.031380	0.577660
26	6	0	-4.252076	-2.397538	0.246606
27	6	0	-3.896702	-3.722835	0.216843
28	6	0	-2.560596	-4.138146	0.077285
29	6	0	-3.255178	-1.414651	0.145273
30	6	0	-1.904445	-1.832754	0.048243
31	6	0	-1.572697	-3.195689	-0.010068
32	8	0	-0.288797	-3.558327	-0.198518
33	1	0	-2.297685	-5.185511	0.025996
34	1	0	-4.665038	-4.481301	0.289280
35	1	0	-5.280209	-2.075827	0.329205
36	6	0	3.781985	1.400000	0.373515
37	6	0	2.470176	1.832504	0.704346
38	6	0	5.284706	-0.348560	-0.351275
39	6	0	6.336285	0.529002	-0.272851
40	6	0	6.137424	1.856159	0.139546
41	6	0	4.876485	2.282947	0.457164
42	1	0	0.422870	1.424593	0.848396
43	1	0	2.339895	2.844435	1.069345
44	1	0	5.486253	-1.354560	-0.687832
45	1	0	7.330623	0.193375	-0.535846
46	1	0	6.977808	2.534420	0.200425
47	1	0	4.700188	3.303335	0.774354

7 (Anion, Gas Phase):

Center Number	Atomic Number	Atomic Type	Coordinates (Angstroms) X	Y	Z
1	7	0	0.815429	-0.028420	-0.310271
2	7	0	-0.481233	-0.476215	0.024035
3	7	0	-1.294822	1.731454	-0.443085
4	6	0	-1.410438	0.426118	-0.155453
5	6	0	-2.803333	-0.092509	0.027160
6	6	0	-3.887771	0.768387	-0.116618
7	6	0	-3.042308	-1.434050	0.326447
8	6	0	-4.338648	-1.899957	0.482771
9	6	0	-5.186327	0.298759	0.032198
10	6	0	-5.417809	-1.036052	0.334466
11	6	0	1.873331	-0.899633	-0.196545
12	6	0	1.775798	-2.301478	-0.454945
13	6	0	2.893366	-3.151874	-0.228151
14	6	0	4.111852	-2.589119	0.162682
15	6	0	4.224209	-1.223480	0.316430
16	6	0	3.134156	-0.389676	0.141610
17	1	0	-3.680274	1.804732	-0.346530
18	1	0	-6.020688	0.980044	-0.086057
19	1	0	-6.430351	-1.402760	0.453565
20	1	0	-4.509498	-2.943514	0.719236
21	1	0	-2.195114	-2.098031	0.439245
22	1	0	5.163039	-0.764129	0.598873
23	1	0	4.985713	-3.203106	0.317925
24	6	0	2.750077	-4.586959	-0.440556
25	6	0	0.587955	-2.870853	-1.028224
26	6	0	0.234953	3.595075	-0.170450
27	6	0	1.518023	4.061786	0.080739
28	6	0	2.579349	3.185159	0.260406
29	6	0	-0.026966	2.221521	-0.265040
30	6	0	1.064489	1.350576	-0.112382
31	6	0	2.323335	1.822276	0.169567
32	8	0	3.381386	0.951294	0.327369
33	1	0	3.587532	3.523053	0.456468
34	1	0	1.696217	5.128713	0.142100
35	1	0	-0.597931	4.276016	-0.288634
36	6	0	1.547057	-5.097338	-0.973940
37	6	0	0.486192	-4.191838	-1.290742
38	6	0	3.771842	-5.505768	-0.133076
39	6	0	3.619308	-6.855767	-0.349450
40	6	0	2.426530	-7.353568	-0.889742
41	6	0	1.410563	-6.481050	-1.192538
42	1	0	-0.231116	-2.209175	-1.259338
43	1	0	-0.415567	-4.589742	-1.741499
44	1	0	4.697922	-5.153782	0.299062
45	1	0	4.424267	-7.534538	-0.096321
46	1	0	2.306490	-8.416095	-1.061065
47	1	0	0.476810	-6.847091	-1.604903

8 (Neutral, in DCM):

Center Number	Atomic Number	Atomic Type	Coordinates (Angstroms) X	Y	Z

8 (Neutral, Gas Phase):

Center Number	Atomic Number	Atomic Type	Coordinates (Angstroms) X	Y	Z

1	7	0	-2.614119	0.935256	0.193039
2	7	0	-3.897627	0.528655	0.164248
3	7	0	-3.261344	-1.463603	-0.951620
4	6	0	-4.149082	-0.642034	-0.404992
5	6	0	-5.582858	-1.044907	-0.426944
6	6	0	-5.939402	-2.313602	-0.880440
7	6	0	-6.581088	-0.170357	0.004062
8	6	0	-7.911148	-0.561355	-0.017917
9	6	0	-7.271107	-2.702659	-0.899595
10	6	0	-8.260780	-1.828489	-0.469100
11	6	0	-2.417787	2.235925	0.746140
12	6	0	-3.042994	2.554120	1.945071
13	6	0	-2.885136	3.825098	2.476929
14	6	0	-2.108450	4.769413	1.817252
15	6	0	-1.494552	4.443396	0.614536
16	6	0	-1.651333	3.177284	0.069326
17	1	0	-5.166287	-2.992198	-1.214214
18	1	0	-7.536399	-3.692249	-1.250093
19	1	0	-9.300122	-2.132603	-0.484643
20	1	0	-8.677537	0.126157	0.317866
21	1	0	-6.310483	0.817313	0.351949
22	1	0	-1.193161	2.925292	-0.878857
23	1	0	-0.898826	5.178607	0.088692
24	1	0	-1.985943	5.759421	2.237620
25	1	0	-3.369153	4.075103	3.412366
26	1	0	-3.644441	1.807328	2.446467
27	6	0	-0.939557	-1.930960	-1.336177
28	6	0	0.385520	-1.594346	-1.190065
29	6	0	0.760095	-0.413139	-0.525911
30	6	0	-1.953411	-1.094977	-0.844209
31	6	0	-1.575823	0.121122	-0.230344
32	6	0	-0.229594	0.439837	-0.057558
33	1	0	0.051786	1.349455	0.453754
34	6	0	2.189540	-0.034956	-0.367556
35	1	0	1.153172	-2.245719	-1.587661
36	1	0	-1.234889	-2.846041	-1.833889
37	6	0	3.135808	-0.912555	0.033826
38	6	0	4.591581	-0.603388	-0.013868
39	6	0	2.797222	-2.263172	0.562686
40	6	0	5.179254	-0.053830	-1.154719
41	6	0	6.540529	0.210821	-1.192409
42	6	0	7.337876	-0.066562	-0.088464
43	6	0	6.765986	-0.624594	1.048079
44	6	0	5.406690	-0.901176	1.079895
45	6	0	3.457026	-3.393738	0.078256
46	6	0	1.840793	-2.424150	1.566271
47	6	0	1.532091	-3.685973	2.053626
48	6	0	3.138250	-4.657320	0.554052
49	6	0	2.172049	-4.807952	1.541883
50	6	0	2.493268	1.390524	-0.680472
51	6	0	2.016293	1.967038	-1.859212
52	6	0	2.277363	3.297450	-2.154403
53	6	0	3.001154	4.080240	-1.262871
54	6	0	3.461413	3.522213	-0.076679
55	6	0	3.210289	2.187799	0.211440
56	1	0	4.563877	0.163307	-2.019602
57	1	0	6.979841	0.631856	-2.088318
58	1	0	8.399742	0.143563	-0.116773
59	1	0	7.379701	-0.850808	1.911325
60	1	0	4.967768	-1.345606	1.965801
61	1	0	4.216925	-3.279882	-0.686483
62	1	0	1.338342	-1.551557	1.966834
63	1	0	0.789609	-3.793084	2.834708
64	1	0	3.646083	-5.526317	0.154313
65	1	0	1.926125	-5.793533	1.916994
66	1	0	1.441836	1.363465	-2.552956
67	1	0	1.911458	3.723432	-3.080596
68	1	0	3.200542	5.120342	-1.488858
69	1	0	4.015681	4.128069	0.629437
70	1	0	3.570473	1.758195	1.138603

1	7	0	-2.613050	0.953634	0.171333
2	7	0	-3.895966	0.541738	0.167829
3	7	0	-3.267600	-1.455167	-0.950081
4	6	0	-4.149421	-0.634062	-0.392324
5	6	0	-5.578939	-1.044254	-0.391627
6	6	0	-5.930382	-2.313854	-0.842778
7	6	0	-6.574630	-0.177179	0.055328
8	6	0	-7.901051	-0.577826	0.051832
9	6	0	-7.258489	-2.711836	-0.843196
10	6	0	-8.247124	-1.846048	-0.396286
11	6	0	-2.413642	2.267984	0.680573
12	6	0	-3.120650	2.664062	1.809619
13	6	0	-2.955333	3.948199	2.302469
14	6	0	-2.091808	4.836150	1.675136
15	6	0	-1.400265	4.437522	0.539520
16	6	0	-1.563071	3.157498	0.032914
17	1	0	-5.150414	-2.976825	-1.190496
18	1	0	-7.522614	-3.701444	-1.193241
19	1	0	-9.284066	-2.157445	-0.397916
20	1	0	-8.668022	0.102877	0.398573
21	1	0	-6.298619	0.810341	0.398138
22	1	0	-1.038556	2.853886	-0.863846
23	1	0	-0.733263	5.124908	0.035848
24	1	0	-1.962710	5.836412	2.066775
25	1	0	-3.502893	4.253797	3.184498
26	1	0	-3.795476	1.962156	2.279181
27	6	0	-0.950332	-1.935097	-1.330304
28	6	0	0.376000	-1.610133	-1.179845
29	6	0	0.756805	-0.432905	-0.513167
30	6	0	-1.961988	-1.091232	-0.844272
31	6	0	-1.577137	0.124931	-0.234647
32	6	0	-0.229554	0.425645	-0.048243
33	1	0	0.059663	1.330026	0.466672
34	6	0	2.184327	-0.055328	-0.348323
35	1	0	1.142014	-2.268499	-1.568136
36	1	0	-1.257713	-2.847633	-1.823385
37	6	0	3.138730	-0.934399	0.031117
38	6	0	4.590698	-0.613744	-0.019782
39	6	0	2.811974	-2.294664	0.538760
40	6	0	5.162801	-0.021850	-1.146120
41	6	0	6.520465	0.253737	-1.188303
42	6	0	7.330302	-0.055450	-0.103408
43	6	0	6.774612	-0.655655	1.018307
44	6	0	5.418653	-0.942735	1.054393
45	6	0	3.505346	-3.408739	0.065380
46	6	0	1.833324	-2.481415	1.515373
47	6	0	1.536703	-3.750683	1.986199
48	6	0	3.200465	-4.680378	0.526388
49	6	0	2.213248	-4.855614	1.487156
50	6	0	2.476270	1.379889	-0.624769
51	6	0	1.972101	1.989511	-1.774859
52	6	0	2.212196	3.331036	-2.030696
53	6	0	2.942865	4.092150	-1.127327
54	6	0	3.431714	3.500863	0.029594
55	6	0	3.201695	2.155743	0.277719
56	1	0	4.534254	0.221811	-1.993612
57	1	0	6.947865	0.708167	-2.072865
58	1	0	8.390013	0.162240	-0.135601
59	1	0	7.399049	-0.906997	1.866071
60	1	0	4.989481	-1.424837	1.924733
61	1	0	4.283695	-3.272334	-0.676045
62	1	0	1.301652	-1.620614	1.902018
63	1	0	0.775603	-3.877449	2.745332
64	1	0	3.736831	-5.536325	0.137194
65	1	0	1.978364	-5.847419	1.851142
66	1	0	1.390095	1.400017	-2.473970
67	1	0	1.826972	3.782560	-2.936251
68	1	0	3.127134	5.140695	-1.322649
69	1	0	3.993262	4.088905	0.744048
70	1	0	3.586154	1.696683	1.180084

8 (Cation, Gas Phase):

Center Number	Atomic Number	Atomic Type	Coordinates (Angstroms) X	Y	Z
1	7	0	-2.618797	0.897057	0.160661
2	7	0	-3.866586	0.531171	0.104858
3	7	0	-3.225656	-1.542343	-0.801658
4	6	0	-4.152899	-0.692401	-0.353647
5	6	0	-5.570321	-1.084014	-0.377315
6	6	0	-5.920319	-2.362812	-0.810721
7	6	0	-6.563108	-0.190944	0.029769
8	6	0	-7.891150	-0.578408	0.002311
9	6	0	-7.251176	-2.742978	-0.834107
10	6	0	-8.237069	-1.853081	-0.428571
11	6	0	-2.413563	2.253564	0.626340
12	6	0	-3.036742	2.641584	1.800553
13	6	0	-2.863219	3.943663	2.241194
14	6	0	-2.089336	4.832160	1.506058
15	6	0	-1.486129	4.426177	0.322865
16	6	0	-1.645600	3.126412	-0.129772
17	1	0	-5.147610	-3.049234	-1.127217
18	1	0	-7.520674	-3.735338	-1.169547
19	1	0	-9.276868	-2.152588	-0.448560
20	1	0	-8.659529	0.115219	0.316360
21	1	0	-6.293054	0.802535	0.359474

8 (Anion, Gas Phase):

Center Number	Atomic Number	Atomic Type	Coordinates (Angstroms) X	Y	Z
1	7	0	-2.646694	1.070872	0.039748
2	7	0	-3.873984	0.451185	0.331713
3	7	0	-3.254012	-1.288617	-1.186340
4	6	0	-4.091267	-0.628565	-0.361362
5	6	0	-5.447791	-1.233148	-0.178163
6	6	0	-5.771059	-2.419376	-0.830965
7	6	0	-6.408486	-0.625703	0.629762
8	6	0	-7.661203	-1.197860	0.786940
9	6	0	-7.028739	-2.988712	-0.678444
10	6	0	-7.977925	-2.383073	0.132468
11	6	0	-2.564374	2.418041	0.310156
12	6	0	-3.567526	3.050594	1.068954
13	6	0	-3.507712	4.409651	1.323830
14	6	0	-2.470214	5.195342	0.838324
15	6	0	-1.489273	4.580676	0.067421
16	6	0	-1.526777	3.224460	-0.197787
17	1	0	-5.014028	-2.875427	-1.454184
18	1	0	-7.266825	-3.911164	-1.194590
19	1	0	-8.958119	-2.828523	0.254407
20	1	0	-8.396521	-0.716845	1.420932
21	1	0	-6.151474	0.299334	1.127988

22	1	0	-1.190116	2.802708	-1.057277
23	1	0	-0.892445	5.120524	-0.255869
24	1	0	-1.959447	5.847645	1.855457
25	1	0	-3.333926	4.263158	3.160991
26	1	0	-3.641027	1.934450	2.352567
27	6	0	-0.923638	-2.053168	-1.163842
28	6	0	0.371961	-1.691164	-1.017264
29	6	0	0.752179	-0.440932	-0.407604
30	6	0	-1.959391	-1.183625	-0.716035
31	6	0	-1.581815	0.088676	-0.173989
32	6	0	-0.231239	0.432699	-0.006783
33	1	0	0.041016	1.376714	0.439767
34	6	0	2.166871	-0.039703	-0.302014
35	1	0	1.155001	-2.344256	-1.377551
36	1	0	-1.216664	-2.990564	-1.616174
37	6	0	3.156420	-0.919253	0.007692
38	6	0	4.592802	-0.570773	-0.092148
39	6	0	2.860011	-2.281659	0.510139
40	6	0	5.098845	0.108887	-1.201921
41	6	0	6.448465	0.405884	-1.287480
42	6	0	7.309581	0.041598	-0.259740
43	6	0	6.818221	-0.639414	0.845240
44	6	0	5.471417	-0.957227	0.921972
45	6	0	3.525473	-3.387627	-0.024561
46	6	0	1.928414	-2.481246	1.530529
47	6	0	1.642832	-3.760292	1.984034
48	6	0	3.223385	-4.666074	0.413910
49	6	0	2.279806	-4.855494	1.417792
50	6	0	2.419843	1.413779	-0.519286
51	6	0	1.936455	2.050408	-1.663532
52	6	0	2.157277	3.404162	-1.866286
53	6	0	2.848586	4.145451	-0.915867
54	6	0	3.318318	3.524506	0.233103
55	6	0	3.107574	2.167156	0.429303
56	1	0	4.431325	0.394342	-2.004933
57	1	0	6.830590	0.920670	-2.159130
58	1	0	8.362929	0.280748	-0.325001
59	1	0	7.485407	-0.930474	1.645681
60	1	0	5.092211	-1.500998	1.778804
61	1	0	4.272414	-3.237030	-0.794640
62	1	0	1.444206	-1.623856	1.982514
63	1	0	0.929790	-3.901561	2.785645
64	1	0	3.730265	-5.517406	-0.020981
65	1	0	2.055617	-5.854409	1.768245
66	1	0	1.402459	1.473518	-2.410890
67	1	0	1.800371	3.878468	-2.771712
68	1	0	3.025209	5.201303	-1.074012
69	1	0	3.855395	4.096043	0.978622
70	1	0	3.486279	1.681612	1.320434

22	1	0	-0.761236	2.790036	-0.823687
23	1	0	-0.673125	5.164811	-0.342692
24	1	0	-2.429809	6.256278	1.046842
25	1	0	-4.293232	4.862165	1.918660
26	1	0	-4.382093	2.451500	1.444057
27	6	0	-0.916863	-1.716132	-1.583189
28	6	0	0.412587	-1.421477	-1.341095
29	6	0	0.775877	-0.340358	-0.538217
30	6	0	-1.953224	-0.929951	-1.053170
31	6	0	-1.575058	0.236452	-0.331538
32	6	0	-0.252824	0.479762	-0.032082
33	1	0	0.006410	1.331348	0.583167
34	6	0	2.182380	-0.018098	-0.255356
35	1	0	1.187573	-2.043017	-1.774371
36	1	0	-1.198376	-2.569572	-2.187029
37	6	0	3.128316	-0.954130	0.029433
38	6	0	4.582365	-0.643976	0.028876
39	6	0	2.785263	-2.360748	0.371293
40	6	0	5.169126	0.094323	-1.001632
41	6	0	6.525878	0.379215	-0.995337
42	6	0	7.332584	-0.073410	0.040182
43	6	0	6.767643	-0.823797	1.063602
44	6	0	5.411620	-1.111308	1.052443
45	6	0	3.538424	-3.421755	-0.133634
46	6	0	1.735841	-2.656975	1.246415
47	6	0	1.443058	-3.965713	1.588828
48	6	0	3.241916	-4.735395	0.203574
49	6	0	2.191917	-5.014068	1.065799
50	6	0	2.513772	1.436154	-0.287878
51	6	0	2.037680	2.241355	-1.323521
52	6	0	2.314652	3.599727	-1.354071
53	6	0	3.058197	4.183012	-0.336280
54	6	0	3.519753	3.396398	0.710332
55	6	0	3.250298	2.036466	0.732756
56	1	0	4.545277	0.448433	-1.812769
57	1	0	6.955465	0.954839	-1.805957
58	1	0	8.392041	0.149754	0.046118
59	1	0	7.386129	-1.185900	1.875684
60	1	0	4.977695	-1.703004	1.849928
61	1	0	4.364068	-3.210661	-0.803118
62	1	0	1.137149	-1.846626	1.642955
63	1	0	0.620876	-4.168841	2.263287
64	1	0	3.832885	-5.542194	-0.212514
65	1	0	1.956842	-6.037795	1.328842
66	1	0	1.438853	1.786948	-2.104368
67	1	0	1.938639	4.206278	-2.168749
68	1	0	3.263901	5.245887	-0.351584
69	1	0	4.084230	3.845282	1.518119
70	1	0	3.606659	1.425201	1.552784

14. References

[S1] Gubaidullin, A. T.; Buzykin, B. I.; Litvinov, I. A.; Gazetdinova N. G. Molecular and Crystal Structure of a Superstable Free Radical, 1,3-Diphenyl-1,4-dihydro-1,2,4-benzotriazin-4-yl. *Russ. J. Gen. Chem.,* **2004***, 74* (6), 939–943.

[S2] Zheng, Y.; Miao, M. s.; Kemei, M. C.; Seshadri, R.; Wudl, F. The Pyreno-Triazinyl Radical – Magnetic and Sensor Properties. *Isr. J. Chem.* **2014**, *54* (5-6), 774–778.

[S3] Berezin, A. A.; Constantinides, C. P.; Drouza, C.; Manoli, M.; Koutentis, P. A. From Blatter Radical to 7-Substituted 1,3-Diphenyl-1,4-dihydrothiazolo[5′,4′:4,5] benzo[1,2-e][1,2,4]triazin-4-yls: Toward Multifunctional Materials. *Org. Lett.* **2012**, *14* (21), 5586–5589.

[S4] Kaszyński, P.; Constantinides, C. P.; Young, V. G. The Planar Blatter Radical: Structural Chemistry of 1,4-Dihydrobenzo[e][1,2,4]triazin -4-yls. *Agnew. Chem. Int. Ed.* **2016**, *55* (37), 11149–11152.

[S5] Constantinides, C. P.; Koutentis, P. A.; Krassos, H.; Rawson, J. M.; Tasiopoulos, A. J. Characterization and Magnetic Properties of a “Super Stable” Radical 1,3-Diphenyl-7-trifluoromethyl-1,4-dihydro-1,2,4-benzotriazin-4-yl. *J. Org. Chem.* **2011**, *76* (8), 2798–2806.

[S6] Zissimou, G. A.; Bartos, P.; Pietrzak, A.; Kaszyński, P. “Upper” Ring Expansion of the Planar Blatter Radical

via Photocyclization: Limitations and Impact on the Electronic Structure. *J. Org. Chem.* **2022**, *87* (7), 4829–4837.

[S7] Hu, X.; Chen, H.; Zhao, L.; Miao, M.; Zheng, Y. Observation of a Solid-State-Induced Thermally Populated Spin-Triplet State in Radical Regioisomers. *Chem. Mater.* **2019**, *31* (24), 10256–10262.

[S8] Ciccullo, F.; Gallagher, N. M.; Geladari, O.; Chassé, T.; Rajca, A.; Casu, M. B. A Derivative of the Blatter Radical as a Potential Metal-Free Magnet for Stable Thin Films and Interfaces. *ACS Appl. Mater. Interfaces* **2016**, *8* (3), 1805–1812.

[S9] Savva, A. C.; Mirallai, S. I.; Zissimou, G. A.; Berezin, A. A.; Demetriades, M.; Kourtellaris, A.; Constantinides, C. P.; Nicolaides, C.; Trypiniotis, T.; Koutentis, P. A. Preparation of Blatter Radicals via Aza-Wittig Chemistry: The Reaction of N-Aryliminophosphoranes with 1-(Het)aroyl-2-aryldiazenes. *J. Org. Chem.* **2017**, *82* (14), 7564−7575.

[S10] Constantinides, C. P.; Obijalska, E.; Kaszyński, P. Access to 1,4-Dihydrobenzo[e][1,2,4]triazin-4-yl Derivatives. *Org. Lett.* **2016**, *18* (5), 916−919.

[S11] Jasiński, M.; Szczytko, J.; Pociecha, D.; Monobe, H.; Kaszyński, P. Substituent-Dependent Magnetic Behavior of Discotic Benzo[e][1,2,4]triazinyls. *J. Am. Chem. Soc.* **2016**, *138* (30), 9421−9424.

[S12] Hutchison, K. A.; Srdanov, G.; Menon, R.; Gabriel, J.-C. P.; Knight, B.; Wudl, F. A Pressure Sensitive Two-Dimensional Tetracyanoquinodimethane (TCNQ) Salt of a Stable Free Radical. *J. Am. Chem. Soc.* **1996**, *118* (51), 13081-13082.

[S13] Bartos, P.; Anand, B.; Pietrzak, A.; Kaszyński, P. Functional Planar Blatter Radical through Pschorr-Type Cyclization. *Org. Lett.* **2020**, *22* (1), 180-184.

[S14] Hande, A. A.; Darrigan, C.; Bartos, P.; Baylère, P.; Pietrzak, A.; Kaszyński, P.; Chrostowska, A. UV-photoelectron spectroscopy of stable radicals: the electronic structure of planar Blatter radicals as materials for organic electronics. *Phys. Chem. Chem. Phys.* **2020***, 22,* (41), 23637-23644.

[S15] Dąbrowski, M.; Wyrębek, P.; Trzybiński, D.; Woźniak, K.; Grela, K. In a Quest for Selectivity Paired with Activity: A Ruthenium Olefin Metathesis Catalyst Bearing an Unsymmetrical Phenanthrene-Based N-Heterocyclic Carbene. *Chem. Eur. J.* **2020**, *26* (17), 3782–3794.

[S16] Hisler, K.; Commeureuc, A. G. J.; Zhou, S.-z.; Murphy, J. A. Synthesis of indoles via alkylidenation of acyl hydrazides. *Tetrahedron Letters* **2009**, *50* (26), 3290–3293.

[S17] Kauffman, J. M.; Moyna, G. Diarylamino Groups as Photostable Auxofluors in 2-Benzoxazolylfluorene, 2,5-Diphenyloxazoles, 1,3,5-Hexatrienes, 1,4-Distyrylbenzenes, and 2,7-Distyrylfluorenes. *J. Org. Chem.* **2003**, *68* (3), 839–853.

[S18] Stuparu, M. C. Efficient preparation and properties of triazole-linked corannulene derivatives. *Tetrahedron* **2012**, *68* (18), 3527–3531.

[S19] Berezin, A. A.; Zissimou, G.; Constantinides, C. P.; Beldjoudi, Y.; Rawson, J. M.; Koutentis, P. A. Route to Benzo- and Pyrido-Fused 1,2,4-Triazinyl Radicals via N′-(Het)aryl-N′-[2-nitro(het)aryl] hydrazides. *J. Org. Chem.* **2014**, *79* (1), 314–327.

[S20] Wang, W.-j.; Zhang, T.; Duan, L.-j.; Zhang, X.-j.; Yan, M. KOt-Bu promoted homocoupling and decomposition of N′-aryl acylhydrazines: Synthesis of unsymmetric N′,N′-diaryl acylhydrazines. *Tetrahedron* **2015**, *71* (48), 9073–9080.

[S21] Dolomanov, O. V.; Bourhis, L. J.; Gildea, R. J.; Howard, J. A. K.; Puschmann, H. OLEX2: a complete structure

solution, refinement and analysis program. *J. Appl. Crystallogr.* **2009**, *42* (2), 339–341.

[S22] Sheldrick, G. M. SHELXT– Integrated space-group and crystal-structure determination. *Acta Cryst.* **2015**, *71* (1), 3–8.

[S23] Sze, S. M.; Ng: K. K.; Physics of Semiconductor Devices (**2006**), John Wiley & Sons, Hoboken, New Jersey.

[S24] (a) Tauc, J.; Grigorovici, R.; Vancu, A. Optical Properties And Electronic Structure of Amorphous Germanium. *Phys. Status Solidi B* **1966**, *15* (2), 627−637. (b) Davis, E.; Mott, N. Conduction in non-crystalline systems V. Conductivity, optical absorption and photoconductivity in amorphous semiconductors. *Philos. Mag.* **1970**, *22* (179), 0903−0922. (c) Mott, N. F.; Davis, E. A. Electronic Processes in Non-Crystalline Materials; OUP Oxford, **2012**. (d) Makuła, P.; Pacia, M.; Macyk, W. How To Correctly Determine the Band Gap Energy of Modified Semiconductor Photocatalysts Based on UV–Vis Spectra. *J. Phys. Chem. Lett.* **2018**, *9* (23), 6814–6817.

[S25] Connelly, N. G.; Geiger, W. E. Chemical Redox Agents for Organometallic Chemistry. *Chem. Rev.* **1996**, *96* (2), 877-910.

[S26] M. J. Frisch, G. W. Trucks, H. B. Schlegel, G. E. Scuseria, M. A. Robb, J. Cheeseman, G. Scalmani, V. Barone, B. Mennucci, G. A. Petersson, H. Nakatsuji, M. Caricato, X. Li, H. P. Hratchian, A. F. Izmaylov, J. Bloino, G. Zheng, J. L. Sonnenberg, M. Hada, M. Ehara, K. Toyota, R. Fukuda, J. Hasegawa, M. Ishida, T. Nakajima, Y. Honda, O. Kitao, H. Nakai, T. Vreven, J. A. Montgomery, Jr. J. E. Peralta, F. Ogliaro, M. Bearpark, J. J. Heyd, E. Brothers, K. N. Kudin, V. N. Staroverov, T. Keith, R. Kobayashi, J. Normand, K. Raghavachari, A. Rendell, J. C. Burant, S. S. Iyengar, J. Tomasi, M. Cossi, N. Rega, J. M. Millam, M. Klene, J. E. Knox, J. B. Cross, V. Bakken, C. Adamo, J. Jaramillo, R. Gomperts, R. E. Stratmann, O. Yazyev, A. J. Austin, R. Cammi, C. Pomelli, J. W. Ochterski, R. L. Martin, K. Morokuma, V. G. Zakrzewski, G. A. Voth, P. Salvador, J. J. Dannenberg, S. Dapprich, A. D. Daniels, O. Farkas, J. B. Foresman, J. V. Ortiz, J. ioslowski and D. J. Fox, Gaussian 09, Revision D.01; Gaussian, Inc., Wallingford CT. 2013.

[S 27] Zhao, Y.; Truhlar, D. G. The M06 suite of density functionals for main group thermochemistry, thermochemical kinetics, noncovalent interactions, excited states, and transition elements: two new functionals and systematic testing of four M06-class functionals and 12 other functionals. *Theor. Chem. Acc.* **2007**, *120* (1-3), 215–241.

[S28] Marenich, A. V.; Cramer, C. J.; Truhlar, D. G. Universal Solvation Model Based on Solute Electron Density and on a Continuum Model of the Solvent Defined by the Bulk Dielectric Constant and Atomic Surface Tensions. *J. Phys. Chem. B* **2009**, *113* (18), 6378–6396.

[S29] Grimme, S.; Antony, J.; Ehrlich, S.; Krieg, H. A consistent and accurateab initioparametrization of density functional dispersion correction (DFT-D) for the 94 elements H-Pu. *J. Chem. Phys.* **2010**, *132* (15), 154104−154118.

[S30] Lu, T.; Chen, F. Multiwfn: A multifunctional wavefunction analyzer. *J. Comput. Chem.* **2011**, *33* (5), 580−592.

[S31] (a) Konezny, S. J.; Doherty, M. D.; Luca, O. R.; Crabtree, R. H.; Soloveichik, G. L.; Batista, V. S. Reduction of Systematic Uncertainty in DFT Redox Potentials of Transition-Metal Complexes. *J. Phys. Chem. C* **2012**, *116* (10), 6349−6356; (b) Wang, D.; Huang, S.; Wang, C.; Yue, Y.; Zhang, Q. Computational prediction for oxidation and reduction potentials of organic molecules used in organic light-emitting diodes. *Org. Electron.* **2019**, *64*, 216−222; (c) Ortiz-Rodríguez, J. C.; Santana, J. A.; Méndez-Hernández, D. D. Linear correlation

models for the redox potential of organic molecules in aqueous solutions. *J. Mol. Model.* **2020**, *26* (4), 70; (d) Wang, X.; Li, F.; Zhang, J. Theoretical prediction for redox potentials of oxygen-centered organic anions in aprotic solvents. *Theor. Chem. Acc.* **2023**, *142* (7), 62.